Investigation of Microbial Fuel Cell Performance and Microbial Community Dynamics During Acclimation and Carbon Source Pulse Tests

by

Victor Laine Beaumont

A thesis presented to the
University of Waterloo
in fulfillment of the thesis requirement
for the degree of

Master of Applied Science
in
Chemical Engineering

Waterloo, Ontario, Canada, 2007

I hereby declare that I am the sole author of this thesis.

This is a true copy of the thesis, including any required final revisions, as accepted by my examiners.

I understand that my thesis may be made electronically available to the public.

Vic Beaumont

Abstract

Microbial fuel cells were designed and operated using waste activated sludge as a substrate and as a source of microorganisms for the anodic chamber. Waste activated sludge provided a bacterial consortium predisposed to the solubilization of particulate matter and utilization of substrates commonly found in wastewater. Dissolved oxygen and ferricyanide were used as the electron acceptors in the catholytes. Microbial fuel cell comparisons were made while operating under identical conditions but using the two different electron acceptors. Comparisons were based on the electricity production observed during MFC operation, wastewater quality of the waste activated sludge anolytes and the community level physiological profiling of the microbial communities in the anolytes. Electrons liberated during substrate utilization in the anodic chamber traveled to the cathodic chamber where they reduced the electron acceptors. The anode and cathode chambers were connected by a Nafion® proton exchange membrane to allow for cation migration. Various soluble carbon sources were dosed to the microbial fuel cells at measured intervals during operation via direct injection to the anolyte.

During bovine serum albumin dosing, average power production levels reached 0.062 mW and 0.122 mW for the dissolved oxygen microbial fuel cell and the ferricyanide microbial fuel cell, respectively. These were 100% and 25% greater than the power production levels observed throughout the rest of the study. Increases in current production were observed following the dosing of sodium acetate, glucose and bovine serum albumin. No increase in current was observed following glycerol dosing. Sodium acetate dosing triggered an immediate response, while glucose and bovine serum albumin responded in approximately 2 minutes. A chemical oxygen demand mass balance was calculated for both microbial fuel cells. The lack of balance closure was attributed to unmeasured methane production. An accumulation of particulate waste activated sludge components was observed for both microbial fuel cells. The anolyte pH during operation was typically less than waste activated sludge pH, which was attributed to volatile fatty acid accumulation in the anolytes during fermentation processes.

Community level physiological profiling was accomplished through the analysis of ecological

data obtained with BIOLOG® ECOplates. Samples were plated and analyzed under anaerobic conditions, mimicking the environment in the anode chamber of the MFCs. ECOplate data were transformed by a logarithmic function prior to principle component analysis. The community level physiological profiling indicated that shifts in the microbial community profile, as measured through the carbon source utilization patterns, occurred throughout acclimation and following the dosing of various carbon source substrates. Shifts due to glycerol dosing differed from shifts due to the dosing of sodium acetate, glucose and bovine serum albumin.

Acknowledgments

I would like to thank my supervisors, Dr. Raymond Legge and Dr. Wayne Parker. The help and guidance you have provided has enabled me to forge on through enormous amounts of design, construction, operation, analysis, and writing. I would also like to thank Dr. Mark Pritzker for his unofficial supervisory status, all of his support throughout the project and the generous lab space for my apparatus. Having 'three' supervisors seemed daunting at first, but your encouragement, kind nature, and exemplary supervision has left me so grateful to have had all of you work on this project with me.

I would like to thank the Natural Sciences and Engineering Research Council (NSERC) and the University of Waterloo for their financial support throughout the duration of my Masters studies.

I would like to thank Wolfgang Haselrieder and Thomas Engenhorst who pioneered many aspects of this project before and during my studies. Wolfgang's efforts in design and initial testing of the MFC system and Thomas' help and support with the second MFC and rigorous analysis procedures have helped make this thesis possible. I would also like to thank Forogh Askari for her dedication and assistance throughout the Winter 2007 term. Without her help, it would have been impossible to finish so much in one term.

I would like to thank all of my fellow graduate students in the Chemical Engineering department and the Civil and Environmental Engineering department for the assistance, training, and company they provided throughout my studies. I will avoid names, since that would require an entire page, and this thesis is long enough already.

Finally, I want to thank my family, including my lovely wife, Hilary, my father for always helping me, my mother for her everlasting love, and my brothers and sisters-in-law, including the Group of Seven, for a lifetime of fun and memories in only 26 years.

To my wife, Hilary Beaumont-Brown, little Rose, who will more than likely have arrived by the time this thesis is finalized, and the siblings that I hope will arrive over the coming years... just to be fair

Contents

List of Tables

List of Figures

1. Introduction

Environmentally friendly and sustainable energy production is coming to the forefront of both research and world issues. Water and wastewater treatment are also a top priority in the developing global community. Microbial fuel cells (MFCs) are an alternative energy technology that have the capacity to simultaneously treat wastewater. They have seen a recent surge in popularity within research circles due to their potential to address both of these continuing world concerns. With the eventual goal of scaling up MFC technology for use with commercial and industrial applications, further research is needed in many areas pertaining to design, configuration, integration into existing technologies, operation and system stability (Du, Li, & Gu, 2007).

In this chapter, the theory behind MFCs is presented along with principles of wastewater treatment as they pertain to MFCs. The research objectives and thesis organization follow. Finally, a short literature review is provided. The literature review focuses on several key studies in the evolution of MFCs as well as some of the more recent, promising discoveries. The references presented at the end of this chapter include MFC-related materials not cited but collected by the author throughout this study.

1.1. Microbial Fuel Cell (MFC) Theory

The MFC theory is presented in two sub-sections. The principles and basic designs are presented first, followed by wastewater principles applicable to MFC operation.

1.1.1. Microbial Fuel Cell (MFC) Design Principles

Figure 1.1 presents the basic design of a two-chamber MFC similar to that used in this study. In order for electricity generation to occur, bacteria in the anode chamber utilize substrates in the anolyte to liberate electrons. Electrons that reach the anode surface, travel through the anode and the circuit to the cathode. Electrons at the cathode surface reduce electron

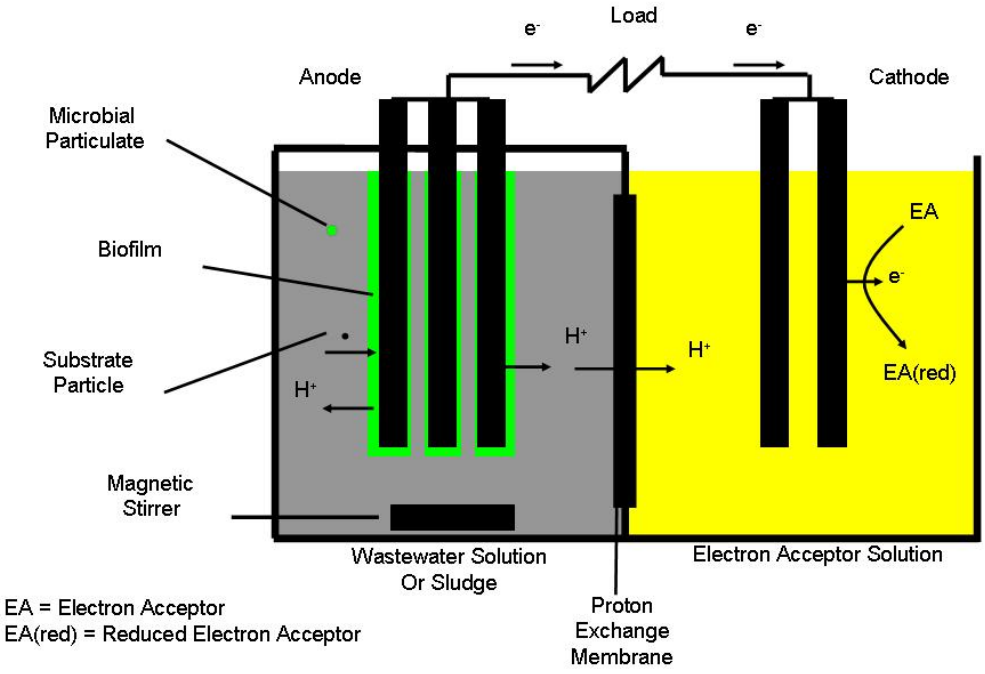

Figure 1.1.: *Basic Two-Chamber Microbial Fuel Cell*

acceptors. The electrical circuit is closed by means of proton migration from the anolyte, through the proton exchange membrane and to the catholyte where the electron acceptor is present.

The anolyte consists of a substrate and the microbial community active in the substrate. In this study, the anolyte consisted of waste activated sludge as a substrate, and the bacterial consortium was that which was naturally present in the waste activated sludge. For successful operation, particulate matter in the anolyte would need to be solubilized before microbes could utilize it. The anolyte requires mixing throughout MFC operation to keep particulate components in suspension and to assist in mass transfer of substrates to the anode surface. This is accomplished in the MFC illustrated in Figure 1.1 by the magnetic stirrer in the anode chamber.

The anode consists of an electrically conductive, non-toxic material, ideally conducive to bacterial attachment. In this study, the anodes were graphite plates. Most substrate utilization reactions resulting in electricity generation take place at or near the anode surface. This allows liberated electrons to travel through the anode and the rest of the electrical circuit. When bacteria attach themselves to the anodes and form a biofilm, the electrons liberated during substrate utilization have a higher probability of traveling through the anode and electrical circuit as compared to being involved in competing electron acceptor reactions within the anolyte. Alternatively, electrons may reach the anode surface from the anolyte solution if they are transported via electron mediators. Electron mediators are chemicals in the anolyte that shuttle electrons liberated during substrate utilization reactions in the anolyte to the anode surface. Theoretically, with each liberated electron, there is a corresponding proton liberated to the anolyte.

The electrical circuit placed between the anodes and the cathodes consists of a load to introduce a resistance to the system. In this study, a potentiostat controlled the voltage between the anodes and cathodes by varying the effective resistance of the circuit load. If the MFC were powering a device, the device would represent the load and associated resistance in the circuit.

Electrons pass through the circuit to the cathode that consists of an electrically conductive material. In this study, the cathodes and anodes were made of graphite plates. Reduction reactions for the electron acceptors take place at the cathode surface where the electron moves from the cathode to the electron acceptor.

The catholyte consists of an electron acceptor solution. In this study, two different electron acceptors were compared, dissolved oxygen and ferricyanide. Higher electron acceptor concentrations in the catholyte result in higher concentrations at the cathode surface to aid in electron transfer.

The proton exchange membrane provides a physical/chemical barrier between the anolyte and catholyte and defines the physical barrier between the effective anode and cathode chambers. Protons in the anolyte selectively migrate through the proton exchange membrane to the catholyte to maintain electroneutrality within the system.

A head space gas exists in the anode chamber, and measurement of the gas composition and quantity allows for the determination of any off-gas properties during MFC operation.

1.1.2. MFC and Wastewater Theoretical Principles and Variables

The two electrical variables of concern in any electrochemical system are the voltage and the current. By definition, the product of these two variables is the power. The flow of electrons from the anode to the cathode is driven by the voltage difference between the two electrodes and the concentrations of readily available electron donors and acceptors at the anode and cathode surfaces, respectively. The voltage between the electrodes was controlled in this study through automatic resistance adjustments made by the potentiostat. The current was measured and power calculated during MFC operation. The electron donor reaction at the anode is represented by Equation 1.1:

$$Organics\ in\ Wastewater\ +\ H_2O\ \rightarrow\ CO_2\ +\ NH_4^+\ +\ HCO_3^-\ +\ H^+ +\ e^-\quad (1.1)$$

This reaction is carried out by the bacteria in the anolyte or at the anode surface. Liberated electrons travel through the anode to the cathode via the electrical circuit where they react with the electron acceptors at the cathode, as described by Equation 1.2:

$$EA\ +\ e^-\ \rightarrow\ EA^- \quad (1.2)$$

where,
EA = oxidized electron acceptor
EA^- = reduced electron acceptor

Alternatively, sources of electrons in the anolyte can be oxidized by competing electron acceptors in the anolyte, negating their electron capacity for electricity production. Since oxygen is such an electron acceptor, the anode chamber was kept under anaerobic conditions to eliminate the presence of oxygen in the anolyte. However, oxygen is not eliminated from the anolyte, as it is present in some of the substrates. A poor seal on the anode chamber would allow oxygen into the anolyte as well. Under anaerobic conditions, some nitrogen

species such as nitrate and nitrite as well as carbon can act as electron acceptors. Thus, competing electron acceptor reactions may exist in the anolyte, as represented in Equations 1.3 through 1.5:

$$O_2 + 4H^+ + 4e^- \rightarrow 2H_2O \tag{1.3}$$

$$\begin{aligned} 2NO_3^- + 12H^+ + 10e^- &\rightarrow N_2(g) + 6H_2O \\ 2NO_2^- + 8H^+ + 6e^- &\rightarrow N_2(g) + 4H_2O \end{aligned} \tag{1.4}$$

$$HCO_3^- + 9H^+ + 8e^- \rightarrow CH_4(g) + 3H_2O \tag{1.5}$$

The wastewater characteristics measured in this study were chemical oxygen demand (COD), soluble and total Kjeldahl nitrogen (TKN) and pH. COD is a measure of the amount of oxidizable material in the MFC anolytes, while the TKN is a measure of the amount of nitrogen in the MFC anolytes. The COD is indicative of the amount of energy that the anolyte could supply as electrons to the anode. TKN and free and saline ammonia (FSA) measurements allowed the tracking of the nitrogen components in the anolytes in the form of particulate and FSA. When increased levels of FSA were observed, particulate components in the anolyte containing nitrogen had been solubilized. Under anaerobic conditions, carbon can act as an electron acceptor, as illustrated in Equation 1.5. This leads to methane production, which is measured as an off-gas in the head space of the anode chamber. Also, under anaerobic conditions, fermentation processes can lead to the production of volatile fatty acids, that tend to lower the pH in the anolyte.

A more thorough description of the design, principles, associated equations, procedures and methods used in this study are presented in Chapters 2 through 4 and Appendicies B and C.

1.2. Research Objectives

The research objectives established for this study are:

- to compare the impact of using dissolved oxygen and ferricyanide as electron acceptors on the generation of electrical power from two MFCs, operated identically with a waste activated sludge feed
- to compare the impact of electron acceptor type on the wastewater quality variables and any off-gases produced during operation
- to evaluate the destination of COD fed to the system by calculating a chemical oxygen demand (COD) mass balance on each MFC
- to perform community level physiological profiling (CLPP) of the MFC anolyte microbial communities to determine if these change as a result of system establishment or the pulsing of different carbon feeds
- to evaluate the use of data transforms of ecological data before performing principal component analysis (PCA) for CLPP of the MFC anolyte microbial communities
- to evaluate the effects of an acclimation period and the dosing of simple carbon sources to the anolytes on electricity production, anolyte wastewater quality, and microbial community profiles for the purpose of gaining a better understanding of MFC start-up periods and which types of carbon sources were responsible for electricity production

1.3. Thesis Organization

This thesis is organized into several chapters, with the associated references listed at the end of each chapter. Chapter 1 presents theoretical principles applicable to MFCs, the research objectives and a brief literature review. Chapter 2 presents the design parameters for the MFCs and the associated apparatus. Chapter 2 also presents and evaluates the MFC system operation and overall performance in addition to the full COD mass balance. Chapter 3 introduces the use of BIOLOG® ECOplates to collect ecological data from the MFC anolytes. This included the materials, anaerobic sampling and ECOplate analytical methods, data treatment, data transforms and principal component analysis for interpretation of results. Transforms of data from all ECOplates are evaluated, while the microbial

ecology is presented for the first experiment. Chapter 4 presents the full comparison of the two MFCs with respect to electricity production, wastewater quality and microbial ecology. The analysis is presented in five sections that describe the acclimation period and each of the four CSPTs in the carbon dosing period. Chapter 5 presents the principle conclusions from Chapters 2 through 4 and establishes a set of recommendations for future work.

There are five appendicies included with this thesis. Appendix A lists the nomenclature used throughout the study. Appendix B presents the sampling and feeding procedures during the study. Appendix C contains complete analytical techniques and the associated reagent chemistries used throughout this study. Appendices D and E include the raw and analytical data files and collected literature to date, respectively, and are provided as compact discs.

1.4. MFC Literature Review

While MFCs are a relatively new technology, the concept of utilizing microorganisms to generate electricity was first recognized in the 18th century. Potter was the first person to demonstrate a half cell using microorganisms to generate electricity in 1912. The results of these experiments were not reported for almost 20 years. Some studies on microbial and bio-fuel cells were reported between the 1950s and the 1980s, though little attention was paid to this technology until recently (Bullen, Arnot, Lakeman, & C., 2006).

The vast majority of the advances made in MFC research have occurred over the last 5 to 10 years. With renewed interest in alternative fuels and water treatment, MFC research has benefited from a surge in popularity and applicable research. Bennetto *et al* were one of the first groups to consistently pursue MFC research in the 1980s and 1990s (Allen & Bennetto, 1993). It was only more recently that the use of wastewater or other waste streams as an anolyte/substrate became more widely studied (Moon, Chang, & Kim, 2006; Min, Kim, Oh, Regan, & Logan, 2005; He, Minteer, & Angenent, 2005; Aelterman, Rabaey, Clauwaert, & Verstraete, 2006; S. J. You, Zhao, Jiang, & Zhang, 2006). Some studies have also investigated the production of hydrogen gas from wastewater under fermentation conditions in MFCs (Logan, Oh, Kim, & Van Ginkel, 2002; Liu, Grot, & Logan, 2005).

Early MFC designs utilized two separate chambers, one for the anode side and one for the cathode side (Bullen et al., 2006). Recently, an alternative design was proposed by Liu *et al*

(Liu & Logan, 2004; Liu, Ramnarayanan, & Logan, 2004). The single chamber design was annular in nature, consisting of a central, hollow cathode, separated from the anolyte by the proton exchange membrane. Multiple anode rods existed in the anode chamber, while the whole structure was encapsulated in an acrylic glass cylinder. The electron acceptor was oxygen that passed through the centre of the hollow cathode. The greatest advantage of this design is the exploitation of the relatively large concentration of oxygen in air as opposed to water. Subsequent studies of MFCs by this particular research group involved the single chamber MFC.

A subject of earlier studies in MFCs was the requirement for electron mediators that were involved in the transport of electrons to the anode surface (Bullen et al., 2006). Gil *et al* (2003) amongst other groups found that electron transfer to the anodes could be self-mediated or unnecessary if biofilms form on the anode surface (Zhang, Xu, Diao, & Shuang, 2006; Prasad et al., 2007). A very recent study utilized some of the accepted electron mediators from earlier studies to examine the effects the mediators have on electricity production and fermentation within the anolyte (Sund, McMasters, Crittenden, Harrell, & Sumner, 2007). One particular electron mediator, resazurin, was found to increase electricity production while having little effect on fermentation rates.

A large number of recent studies on MFCs have focused on electrode materials and surface area impacts. The effects of electrode materials have been tested by a few research groups, focusing on the use or addition of metals such as manganese, copper and gold (Park & Zeikus, 2002; Crittenden, Sund, & Sumner, 2006; Kargi & Eker, 2007). The impact of electrode surface area, spacing and relative size to the proton exchange membrane on electricity generation have also been investigated (Oh & Logan, 2006; Ghangrekar & Shinde, 2007). When the proton exchange membrane surface area was considerably smaller than the electrode surface areas, current production was found to be greatly limited. This was attributed to a greater internal resistance in the cell design. The use of platinum catalysts for the cathode have also been investigated (Zhao et al., 2005; Cheng, Liu, & Logan, 2006b). Relatively small loadings of platinum on the cathode surface were observed to increase current densities over that of a non-catalysed carbon cathode.

A few review papers that describe the state of MFC research have been published recently

(Bullen et al., 2006; Du et al., 2007; Davis & Higson, 2007). For a thorough review of MFC research and the state of the art, Appendix E provides a collection of MFC-related literature.

References

References marked with an asterisk indicate studies included in the meta-analysis.

Aelterman, P., Rabaey, K., Clauwaert, P., & Verstraete, W. (2006). Microbial fuel cells for wastewater treatment. *Water Science & Technology*, *54*(8), 9-15.

*Aelterman, P., Rabaey, K., Pham, H. T., Boon, N., & Verstraete, W. (2006). Continuous electricity generation at high voltages and currents using stacked microbial fuel cells. *Environmental Science and Technology*, *40*, 3388-3394.

Allen, R. M., & Bennetto, H. P. (1993). Microbial fuel-cells: electricity production from carbohydrates. *Applied Biochemistry & Biotechnology*, *39*, 27-40.

*Bennetto, H. P., Stirling, J. L., Tanaka, K., & Vega, C. A. (1983). Anodic reactions in microbial fuel cells. *Biotechnology and Bioengineering*, *25*(2), 559-568.

*Biffinger, J. C., Ray, R., Little, B., & Ringeisen, B. R. (2007). Diversifying biological fuel cell designs by use of nanoporous filters. *Environmental Science and Technology*, *41*, 1444-1449.

Bullen, R. A., Arnot, T. C., Lakeman, J. B., & C., W. F. (2006). Biofuel cells and their development. *Biosensors and Bioelectronics*, *21*, 2015-2045.

*Cheng, S., Liu, H., & Logan, B. E. (2006a). Increased power generation in a continuous flow mfc with advective flow through the porous anode and reduced electrode spacing. *Environmental Science and Technology*, *40*, 2426-2432.

Cheng, S., Liu, H., & Logan, B. E. (2006b). Power densities using different cathode catalysts (pt and cotmpp) and polymer binders (nafion and ptfe) in single chamber microbial fuel cells. *Environmental Science and Technology*, *40*(1), 364-369.

*Clauwaert, P., Rabaey, K., Aelterman, P., DeSchamphelaire, L., Pham, T. H., Boeckx, P., et al. (2007). Biological denitrification in microbial fuel cells. *Environmental Science and Technology*, *41*, 3354-3360.

Crittenden, S. R., Sund, C. J., & Sumner, J. J. (2006). Mediating electron transfer from bacteria to a gold electrode via a self-assembled monolayer. *Langmuir*, *22*, 9473-9476.

Davis, F., & Higson, S. P. J. (2007). Biofuel cells—recent advances and applications. *Biosensors and Bioelectronics*, *22*, 1224-1235.

Du, Z., Li, H., & Gu, T. (2007). A state of the art review on microbial fuel cells: A promising technology for wastewater treatment and bioenergy. *Biotechnology Advances*, *25*, 464-482.

References

*Finkelstein, D. A., Tender, L. M., & Zeikus, J. G. (2006). Effect of electrode potential on electrode-reducing microbiota. *Environmental Science and Technology*, *40*, 6990-6995.

*Freguia, S., Rabaey, K., Yuan, Z., & Keller, J. (2007). Electron and carbon balances in microbial fuel cells reveal temporary bacterial storage behaviour during electricity generation. *Environmental Science and Technology*, *41*, 2915-2921.

Ghangrekar, M. M., & Shinde, V. B. (2007). Performance of membrane-less microbial fuel cell treating wastewater and effect of electrode distance and area on electricity production. *Bioresource Technology*, *98*, 2879-2885.

Gil, G. C., Chang, I. S., Kim, B. H., Kim, M., Jang, J. K., Park, H. S., et al. (2003). Operational parameters affecting the performance of a mediator-less microbial fuel cell. *Biosensors and Bioelectronics*, *18*, 327-334.

He, Z., Minteer, S. D., & Angenent, L. T. (2005). Electricity generation from artificial wastewater using an upflow microbial fuel cell. *Environmental Science and Technology*, *39*, 5262-5267.

*He, Z., Wagner, N., Minteer, S. D., & Angenent, L. T. (2006). An upflow microbial fuel cell with an interior cathode: Assessment of the internal resistance by impedance spectroscopy. *Environmental Science and Technology*, *40*(17), 5212-5217.

*Heilmann, J., & Logan, B. E. (2006). Production of electricity from proteins using a microbial fuel cell. *Water Environment Research*, *78*(5), 531-537.

*Hobson, P. N., & Wheatley, A. D. (Eds.). (1993). *Anaerobic digestion* (1st ed.). Elsevier Applied Science, London and New York.

Kargi, F., & Eker, S. (2007). Electricity generation with simultaneous wastewater treatment by a microbial fuel cell (mfc) with cu and cu-au electrodes. *Journal of Chemical Technology and Biotechnology*, *82*, 658-662.

*Kim, B. H., Chang, I. S., & Gadd, G. M. (2007). Challenges in microbial fuel cell development and operation. *Applied Microbial Biotechnology*, *76*, 485-494.

*Kim, B. H., Park, H. S., Kim, H. J., Kim, G. T., Chang, I. S., Lee, J., et al. (2004). Enrichment of microbial community generating electricity using a fuel-cell-type electrochemical cell. *Applied Microbiology and Biotechnology*, *63*, 672-681.

*Kim, J. R., Cheng, S., Oh, S.-E., & Logan, B. E. (2007). Power generation using different cation, anion, and ultrafiltration membranes in microbial fuel cells. *Environmental Science and Technology*, *41*, 1004-1009.

*Kim, J. R., Jung, S. H., Regan, J. M., & Logan, B. E. (2007). Electricity generation

and microbial community analysis of alcohol powered microbial fuel cells. *Bioresource Technology*, *98*, 2568-2577.

Liu, H., Grot, S., & Logan, B. E. (2005). Electrochemically assisted microbial production of hydrogen from acetate. *Environmental Science and Technology*, *39*, 4317-4320.

Liu, H., & Logan, B. E. (2004). Electricity generation using an air-cathode single chamber microbial fuel cell in the presence and absence of a proton exchange membrane. *Environmental Science & Technology*, *38*(14), 4040-4046.

Liu, H., Ramnarayanan, R., & Logan, B. E. (2004). Production of electricity during wastewater treatment using a single chamber microbial fuel cell. *Environmental Science and Technology*, *38*, 2281-2285.

*Logan, B. E. (2005). Simultaneous wastewater treatment and biological electricity generation. *Water Science & Technology*, *52*(1-2), 31-37.

Logan, B. E., Oh, S. E., Kim, I., & Van Ginkel, S. (2002). Biological hydrogen production measured in batch anaerobic respirometers. *Enironmental Science & Technology*, *36*, 2530-2535.

*Lovely, D. R. (2006). Microbial fuel cells: novel microbial physiologies and engineering approaches. *Current Opinon in Biotechnology*, *17*, 327-332.

*Menicucci, J., Beyenal, H., Marsili, E., Veluchamy, R. A., Demir, G., & Lewandowski, Z. (2006). Procedure for determining maximum sustainable power generated by microbial fuel cells. *Environmental Science and Technology*, *40*, 1062-1068.

*Milliken, C. E., & May, H. D. (2007). Sustained generation of electricity by the spore-forming, gram-positive *Desulfitobacterium hafniense* strain dcb2. *Applied Microbial and Cell Physiology*, *73*, 1180-1189.

Min, B., Kim, J. R., Oh, S. E., Regan, J. M., & Logan, B. E. (2005). Electricity generation from swine wastewater using microbial fuel cells. *Water Research*, *39*, 4961-4968.

*Moon, H., Chang, I. S., Jang, J. K., & Kim, B. H. (2005). Residence time distribution in microbial fuel cell and its influence on cod removal with electricity generation. *Biochemical Engineering Journal*, *27*, 59-65.

Moon, H., Chang, I. S., & Kim, B. H. (2006). Continuous electricity production from artificial wastewater using a mediator-less microbial fuel cell. *Bioresource Technology*, *97*, 621-627.

*Morris, J. M., Jin, S., Wang, J., Zhu, C., & Urynowicz, M. A. (2007). Lead dioxide as an alternative catalyst to platinum in microbial fuel cells. *Electrochemisry Communica-*

tions, *9*, 1730-1734.

Oh, S.-E., & Logan, B. E. (2006). Proton exchange membrane and electrode surface areas as factors that affect power generation in microbial fuel cells. *Applied Microbiology and Biotechnology*, *70*(2), 162-169.

Park, D. H., & Zeikus, J. G. (2002). Impact of electrode composition on electricity generation in a single-compartment fuel cell using *Shewanella putrefaciens*. *Applied Microbiology and Biotechnology*, *59*, 58-61.

*Pham, T. H., Rabaey, K., Aelterman, P., Clauwaert, P., DeSchamphelaire, L., Boon, N., et al. (2006). Microbial fuel cells in relation to conventional anaerobic digestion technology. *Engineering Life Sciences*, *6*(3), 285-292.

Prasad, D., Arun, S., Murugesan, M., Padmanaban, S., Satyanarayanan, R. S., Berchmans, S., et al. (2007). Direct electron transfer with yeast cells and construction of a mediatorless microbial fuel cell. *Biosensors and Bioelectronics*, *22*, 2604-2610.

*Prasad, D., Sivaram, T. K., Berchmans, S., & Yegnaraman, V. (2006). Microbial fuel cell constructed with a micro-organism isolated from sugar industry effluent. *Journal of Power Sources*, *160*, 991-996.

*Rabaey, K., Clauwaert, P., Aelterman, P., & Verstraete, W. (2005). Tubular microbial fuel cells for efficient electricity generation. *Environmental Science and Technology*, *39*, 8077-8082.

*Rabaey, K., VanDeSompel, K., Maignien, L., Boon, N., Aelterman, P., Clauwaert, P., et al. (2006). Microbial fuel cells for sulfide removal. *Environmental Science and Technology*, *40*(17), 5218-5224.

*Rabaey, K., & Verstraete, W. (2005). Microbial fuel cells: novel biotechnology for energy generation. *Trends in Biotechnology*, *23*, 291-298.

*Reguera, G., Nevin, K. P., Nicoll, J. S., Covalla, S. F., Woodard, T. L., & Lovely, D. R. (2006). Biofilm and nanowire production leads to increased current in *Geobacter sulfurreducens* fuel cells. *Applied and Environmental Microbiology*, *72*(11), 7345-7348.

*Ringeisen, B. R., Henderson, E., Wu, P. K., Pietron, J., Ray, R., Little, B., et al. (2006). High power density form a miniature microbial fuel cell using *Shewanella oneidensis* dsp10. *Environmental Science and Technology*, *40*, 2629-2634.

*Ringeisen, B. R., Ray, R., & Little, B. (2007). A miniature microbial fuel cell operating with an aerobic anode chamber. *Journal of Power Sources*, *165*, 591-597.

*Roller, S. D., Bennetto, H. P., & Delaney, G. M. (1994). Electron-transfer coupling in

microbial fuel-cells: Comparison of redox-mediator reduction rates and respiratory rates of bacteria. *Journal of chemical technology and biotechnology*, *34*(1), 3-12.

*Rozendal, R. A., Hamelers, H. V. M., & Buisman, C. J. N. (2006). Effects of membrane cation transport on ph and microbial fuel cell performance. *Environmental Science and Technology*, *40*(17), 5206-5211.

*Scott, K., & Murano, C. (2007). Microbial fuel cells utilising carbohydrates. *Journal of Chemical Technology and Biotechnology*, *82*, 92-100.

*Shin, S.-H., Choi, Y., Na, S.-H., Jung, S., & Kim, S. (2006). Development of bipolar plate stack type microbial fuel cells. *Bulletin Korean Chemistry Society*, *27*(2), 281-285.

Sund, C. J., McMasters, S., Crittenden, S. R., Harrell, L. E., & Sumner, J. J. (2007). Effect of electron mediators on current generation and fermentation in a microbial fuel cell. *Applied Microbial Biotechnology*, *76*, 561-568.

*Tartakovsky, B., & Guiot, S. R. (2006). A comparison of air and hydrogen peroxide oxygenated microbial fuel cell reactors. *Biotechnology Progress*, *22*, 241-246.

*TerHeijne, A., Hamelers, H. V. M., & Buisman, C. J. N. (2007). Microbial fuel cell operation with continuous biological ferrous iron oxidation of the catholyte. *Environmental Science and Technology*, *41*, 4130-4134.

*TerHeijne, A., Hamelers, H. V. M., DeWilde, V., Rozendal, R. A., & Buisman, C. J. N. (2006). A bipolar membrane combined with ferric iron reduction as an efficient cathode system in microbial fuel cells. *Environmental Science and Technology*, *40*(17), 5200-5205.

*You, S., Zhao, Q., Zhang, J., Jiang, J., & Zhao, S. (2006). A microbial fuel cell using permanganate as the cathodic electron acceptor. *Journal of Power Sources*, *162*, 1409-1415.

You, S. J., Zhao, Q. L., Jiang, J. Q., & Zhang, J. N. (2006). Treatment of domestic wastewater with simultaneous electricity generation in microbial fuel cell under continuous operation. *Chemical and Biochemical Engineering Q.*, *20*(4), 407-412.

*Young, T. G., Hadjipetrou, L., & Lilly, M. D. (1966). The theoretical aspects of biochemical fuel cells. *Biotechnology and Bioengineering*, *3*, 581-593.

Zhang, E., Xu, W., Diao, G., & Shuang, C. (2006). Electricity generation from acetate and glucose by sedimentary bacterium attached to electrode in microbial-anode fuel cells. *Journal of Power Sources*, *161*, 820-825.

Zhao, F., Harnisch, F., Schröder, U., Scholz, F., Bogdanoff, P., & Herrmann, I. (2005).

Application of pyrolysed iron(ii) phthalocyanine and cotmpp based oxygen reduction catalysts as cathode materials in microbial fuel cells. *Electrochemistry Communications*, *7*, 1405-1410.

*Zhao, F., Harnisch, F., Schröder, U., Scholz, F., Bogdanoff, P., & Herrmann, I. (2006). Challenges and constraints of using oxygen cathodes in microbial fuel cells. *Environmental Science and Technology*, *40*(17), 5193-5199.

2. Microbial Fuel Cell Design, Construction, Operation and Performance

Abstract

Microbial fuel cells (MFCs) are a relatively new alternative energy technology. Though in the early stages of research, their potential for electricity production and simultaneous wastewater treatment is very encouraging. MFCs are very complex systems that embody biological, chemical and electrochemical processes. If they are to reach commercial scale in the future, a better understanding of their behaviour is needed. This study focused on the design and operation of a two-MFC system under a parallel electrical configuration that uses waste activated sludge as the anolyte and biodegradable substrate. Electrical, wastewater and operational variables were measured throughout the study. In addition, several model carbon sources were introduced into the anolyte at regular intervals to obtain information on performance impacts and the biochemical processes taking place in the MFCs. An overall chemical oxygen demand (COD) balance was performed on each MFC to determine the portion of the chemical energy that was converted to electrical energy. The head space gas of each MFC was analyzed to determine methane production since the anodic chambers were operated under anaerobic conditions. The first MFC, MFC#1, was operated with a dissolved oxygen catholyte, while the second MFC, MFC#2, was operated with a ferricyanide catholyte. Power densities of up to 167 mW/m^2 were observed from MFC#2 assuming that the effective surface area was equal to the surface area of the proton exchange membrane. The power densities were reduced by a factor of 40 if a surface area equal to that of the total cathode surface area was used. The COD balance revealed most of the particulate COD added was not consumed or removed via sampling. Following the measure of a COD accumulation term for each MFC, COD balance discrepancies of 46.8% and 43.8% of the total mass of COD fed to the MFCs were observed for MFC#1 and MFC#2, respectively. It

is suggested that these discrepancies were mainly due to unmeasured methane production. Head space gas volumes were considered very small, but leakage of the gas collection system is suspected.

Keywords: Alternative Energy, Chemical Oxygen Demand, Microbial Fuel Cell, Wastewater Treatment

2.1. Introduction

Sustainable electricity production is becoming one of the largest concerns of the twenty-first century. While nuclear power is a readily available alternative to fossil fuels, it is far from sustainable. More natural sources such as hydroelectric systems, windmills, and solar energy have been identified as some of the more promising sustainable alternatives. However, many regions do not lend themselves well to some or all of these options.

As a new technology, microbial fuel cells (MFCs) have quickly gained attention by researchers in sustainable energy production. A number of recent studies have investigated these systems operating with wastewater as a fuel or energy source (Moon, Chang, & Kim, 2006; Min, Kim, Oh, Regan, & Logan, 2005; He, Minteer, & Angenent, 2005; Aelterman, Rabaey, Clauwaert, & Verstraete, 2006; You, Zhao, Jiang, & Zhang, 2006). Typical wastewater treatment systems utilize biological treatment under aerobic conditions to biodegrade the organic components in the wastewater. Similarly, MFCs utilize microorganisms to biodegrade organic components under anaerobic conditions. Through this process, electrons are liberated and provide the current produced by the MFCs.

MFC research has evolved over the last few decades. Early MFC studies concentrated on simple systems with single microorganisms and simple substrates (Kim, Choi, Jung, & Kim, 2000). Several microorganisms were found to behave ideally under anaerobic conditions, readily freeing electrons during biodegradation of the substrate, including some *Shewanella* and *Geobacter* species (Bond & Lovley, 2003; Ringeisen, Ray, & Little, 2007). The use of electron mediators was accepted in early research, but the concept of mediatorless MFCs became prominent only in the late 1990's and continues to be more widely researched over MFCs operated with mediators (Gil et al., 2003; Moon et al., 2006). Over the past decade, many advances have been made with respect to system design and materials, including the development of the single chamber microbial fuel cell (SCMFC), which eliminates much of the problem associated with the low solubility of oxygen in water by directly contacting air with the cathode (Park & Zeikus, 2002; Liu & Logan, 2004; Cheng, Liu, & Logan, 2006b, 2006a). Further studies have begun to focus on naturally diverse microbial systems and substrates, such as those provided in wastewater. Further research is needed in many areas, including the use of multiple MFC reactor systems, the influence of various operational parameters, overall MFC performance and system responses to disturbance and upset.

The objective of this study was to develop and test two MFCs using different electron acceptors, while being operated in parallel and utilizing waste activated sludge as the anolyte and the substrate for biological activity. System acclimation, operation, performance and microbial community ecology were studied throughout start up and a series of carbon source pulse tests (CSPTs). In this chapter, the MFC systems and experimental methodology used throughout this research are described in detail. The materials required to build the MFCs are listed and the system design is outlined. The design and operation of the experiments is detailed with supporting documentation in Appendix B and C. The full data analysis methodology is referenced and analytical methods are provided in Appendix C. Results are presented and discussed in brief, as it is the focus of this chapter to fully describe the research methodology. Conclusions are drawn based on the system design and overall performance. Chapter 3 provides microbial community ecology evaluation, while chapter 4 presents a detailed comparison of MFC performance and system response results.

2.2. Materials and System Design

This section is divided into four major sub-sections: (i) the construction and operation of the microbial fuel cells themselves, (ii) the electrical system for parameter measurement and system control, (iii) the ancillary equipment for system operation and some system variable measurement, and (iv) the electrolytes. The overall system design and operation is described in Section 2.3.

2.2.1. Microbial Fuel Cells (MFCs)

The first MFC was constructed in May 2005 and a second MFC in May 2006. The only difference between the two MFCs was the use of sintered glass in the first MFC and Nafion® in the second MFC as a proton exchange medium. However, the sintered glass centerpiece in the first MFC was subsequently replaced with an identical Nafion® membrane in October 2006. For the purpose of this research, the two MFCs were considered to be structurally identical. Table 2.1 lists the materials required to build the MFCs.

The Nafion® membranes were soaked at room temperature in sulphuric acid before rinsing and MFC construction. The MFC centre plates were constructed first to ensure that the

Nafion® was installed properly. Once the MFC body was constructed, silicone was used to seal the chambers except the lids. The graphite anodes were sealed along with one set of graphite cathodes using silicone. The lids were sealed with a rubber gasket and the rest of the MFC fittings and wires were installed following silicone sealing.

Table 2.1.: *Microbial Fuel Cell Components*

Component	Materials and Specifications
Graphite electrodes (10 pieces, 5 for each fuel cell)	• dimensions (l*w*d): (100 x 90 x 5)mm • effective surface area, A = 141 cm^2 • surface sanded with grit 120 paper for roughness • boreholes at top (diam = 1 mm, depth = 20 mm) for wire connections (1 per electrode) • boreholes through face 15 mm from top (diam = 5 mm) to suspend electrodes from lid (3 per electrode)
Acrylic glass lids (2 identical)	• clear cast acrylic glass, Central Plastic Sales, Cambridge, Ontario, Canada • dimensions (l*w*d): (168 x 127 x 8.8)mm • 5 electrode ports in each lid: 3 on anode and 2 on cathode side • multi-functional port on anode side of each lid (1/2 inch NPT) allows for standard adapters, third electrode or sensors (pH, temperature, oxygen) • 1/4 inch NPT on anode side of each lid for process gas evacuation nozzle • sampling port on cathode side of each lid (boreholes for 1/2 inch NPT left untapped) • 14 boreholes (diam = 0.205in) arranged around each lid in a symmetrical rectangular pattern; additional 2 holes along the length of centreline, to connect to front, back, side wall, and centre plates
Front and back plates (2 front and 2 back, identical, lengthwise symmetrical)	• clear cast acrylic glass (see above) • dimensions (l*w*d): (127 x 90 x 8.8)mm • 4 threads (10/32in) from top on each for connection to lids • 6 boreholes (diam = 0.205in) on each, to connect plates with bottom plate and side wall plates • 2 threads (7/16-20) in each front and each back plate for adapter fittings, located to allow possible central flow access to and from resulting chambers • centred trench (depth = 4 mm, width = 8.9 mm): extended to 4.75 mm from the bottom edge of each, allows tighter centre plate construction
Side wall plates (4 identical)	• clear cast acrylic glass (see above) • dimensions (l*w*d): (150 x 81 x 8.8)mm • 3 threads (10/32in) at top of each for lid connection, matching lid dimensions • 2 threads (10/32in) one at either side of each to connect with front and back plates
Bottom plates (2 identical, symmetrical in transverse and length direction)	• clear cast acrylic glass (see above) • dimensions (l*w*d): (150 x 127 x 8.8)mm • centred transverse trench (depth = 3.8 mm, width = 8.9 mm) on centreline of each, allows tighter centre plate construction • 8 threads (10/32in) four at either end of each to connect with front and back plates

Table 2.1.: *continued*

Component	Materials and Specifications
Centre walls (2 identical)	• clear cast acrylic glass (see above) • dimensions (l*w*d): (158 x 85 x 85)mm • 2 threads (10/32 in) from top of each, to connect lid to centre wall • boreholes (inner diam = 30 mm, bored through) with a 15.1 mm shoulder (outer diam = 60.2 mm, depth = 4.5 mm) to support the membrane and circular membrane cap • 6 boreholes (diam = 0.173in, at diam = 49 mm, 1,3,5,7,9,11 o'clock arrangement) in 4.5 mm depth shoulder to connect membrane cap to centre wall
Circular membrane cap (2 identical)	• clear cast acrylic glass (see above) • dimensions: outer diam = 60 mm, depth = 8.8 mm, boreholes (diam = 30 mm, bored through) • 6 threads (8/32in, at diam = 49 mm, 1,3,5,7,9,11 o'clock arrangement) to connect membrane cap to centre wall • circular groove for O-Ring (depth = 0.1in, central diam = 1 7/16in, width = 3.375 mm), seals membrane connection
Nafion® impregnated open weave polyester cloth (2 identical)	• Ion Power Inc. • dimensions: diam = 42.6 mm • rough weave side pressed against O-Ring • additional sealing with silicone • after assembly with sealant permeable diam ≙ 29 mm
O-Ring (2 identical)	• butadiene-acrylonitrile rubber • dimension: inside diam = 1 5/16in, width = 1/8in) • volume swelling in contact with ferricyanide tolerable in this application
12 Acrylic rods (6 for each fuel cell)	• 3 rods fixing each set of anode graphite plates, dimensions: diam = 4.5 mm, length = 50 mm • 3 rods fixing each set of cathode graphite plates, dimensions: diam = 4.5 mm, length = 35 mm
Flat rubber gasket (2 identical)	• cut to fit outer dimensions of lid, allows better lid seal with front, back, side wall, and centre plates
Shoulder bolts	• 28 stainless steel bolts for each MFC body (10/32in, length = 3/4in), connects all the plates • 6 stainless steel bolts for each membrane cap (8/32in, length = 1/2in), connects membrane caps to centre plates
Silicone sealant	• allows sealing of MFC chambers and electrode slots as applicable following construction • GE Sealants & Adhesives, Huntersville, NC, USA

Table 2.1.: *continued*

Component	Materials and Specifications
Adapter fittings (8 identical, four per fuel cell)	• Swagelok • tube outer diam = 1/4in, thread size = 7/16-20, stainless steel, flow diameter = 0.19in, O-Ring used for sealing • attached at threads in front and back plates to allow inlet and outlet flows, continuous flow operation possible
Process gas evacuation nozzle (2 identical)	• dimension: 1/4 inch NPT, brass • attached to acrylic glass lids to allow controlled gas venting as needed, sealed with teflon tape
Copper wire (10 pieces)	• diameter = 1 mm • external wiring, tight fit in graphite electrodes ensuring good contact
Wire connector	• parallel connection of copper wires on each anode and each cathode (groups of 3 and 2 respectively)
Plastic adapter with rubber stopper	• seals multi-functional port on anode side (1/2 inch NPT) • easy access for gas samples • sealed with teflon tape
Butyl rubber stopper	• seals sampling port on cathode side (untapped boreholes for 1/2 inch NPT) • prevents environmental contact of cathodic liquid if desired
Tedlar bags	• 500 mL volume, attached via rubber tubing to the process gas evacuation nozzle • provides container to capture head space gas • provides a volumetric displacement method during sampling and feeding

The identical MFCs consisted of an anodic and cathodic chamber, each with approximately 500 mL working volume. The working volume represents the amount of anolyte or catholyte in the system. The remaining volume in the chambers allowed for a small head space volume of approximately 10 mL between the surface of the electrolyte and the MFC lid and the volume occupied by the electrodes. Figure 2.1 shows a fully constructed MFC. The ports described in Table 2.1 can be seen in the picture.

The Tedlar bags were attached to the process gas evacuation nozzles in the lid of each MFC. Prior to connection, the bags were completely evacuated, so no air or residual gases would be introduced into the system. The bags provided a collection system for any gases produced during MFC operation, since positive pressure in the head space would force system gas into the Tedlar bags. The two MFCs in this study are labeled MFC#1 and MFC#2. MFC#1 was the original prototype, later modified with a Nafion® centerpiece, and operated with a dissolved oxygen (DO) saline catholyte. MFC#2 was modeled after MFC#1 and incorporated Nafion® from its inception. MFC#2 operated with a ferricyanide catholyte. The electrolytes are described further in Section 2.2.4.

2.2.2. Electrical System

The electrical system was designed to meet two major objectives. Firstly, the cell voltage of both MFCs was to be controlled at a set value during operation and secondly, automated collection of voltage and current measurements was required. Table 2.2 lists the components of the electrical system designed to meet these objectives. The MFCs were connected to the potentiostat in parallel to ensure the same cell voltage for both MFCs. The multimeter was connected into the circuit of the MFC#1, allowing the the current in MFC#1 to be directly measured. Since the potentiostat measured the total current generated by both MFCs, the current flowing through the second MFC could be determined from the difference between the two measurements. Output signals from the multimeter and potentiostat were passed through a data collection unit and sent to a lab computer for automated voltage and current data recording. Figure 2.2 provides a basic wiring diagram to illustrate how the MFC system was controlled and monitored while data were recorded.

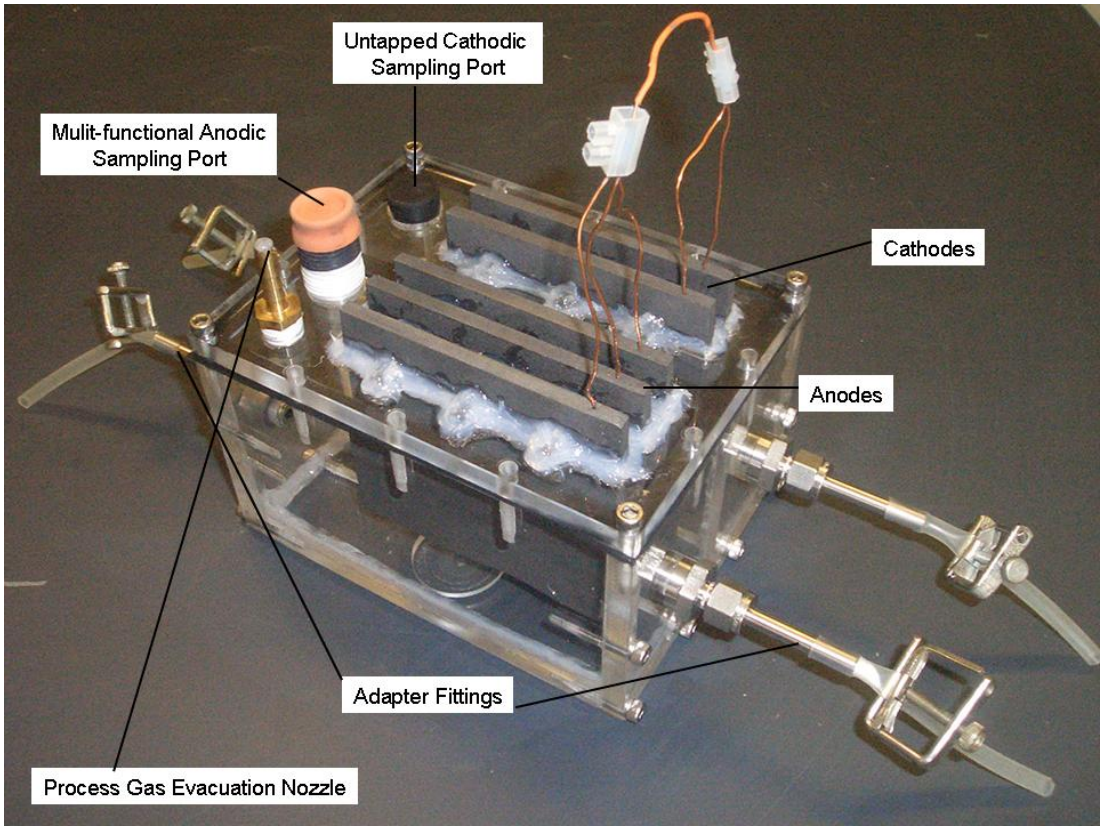

Figure 2.1.: *Constructed MFC (MFC#2)*

Table 2.2.: *Electrical System Components*

Component	Specifications
Potentiostat/Galvanostat	• EG&G PAR 173, dual channel, BNC voltage output • current range from 10 µampere to 1 ampere • control voltage ±2 volts • EG&G PAR 179 Digital Coulometer installed for signal output, BNC cable connections • signal input and system control: two cable sets with alligator clips, attach to electrode wires
Digital Multimeter	• Keithley 160B • standard banana plug input and output • signal input: two banana plug to alligator clip cables • signal output: one banana plug to BNC cable
eDAQ e-corder	• Model 401 • signal input: up to four BNC connections, three used (system voltage, total current, MFC#1 current) • signal output: USB 2.0 A/B for connection to lab computer
Lab Computer	• department standard: 1Ghz processor, 256 MB RAM, network data storage under user allocated space • Windows XP Professional OS • USB port for signal input • associated software: eDAQ Chart 5.0 software for continuous voltage and current signal recording, allows calculation of individual MFC currents, coulombs, and power

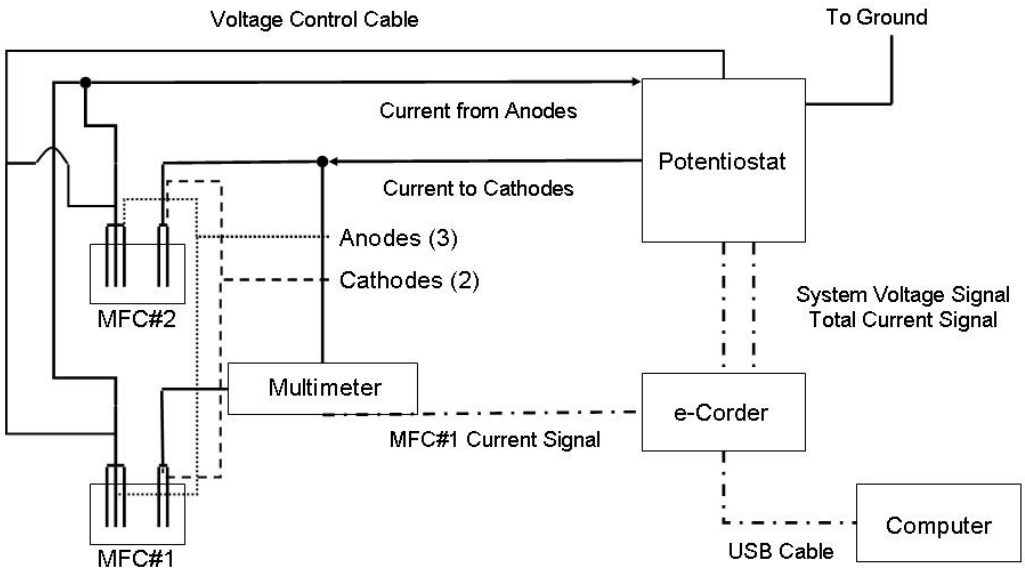

Figure 2.2.: *Electrical Layout Diagram*

2.2.3. Ancillary Equipment

Several other pieces of equipment were required: an incubator, two stirrer plates, an air pump, and a dissolved oxygen (DO) meter and probe. Table 2.3 lists these additional components with their associated specifications. The system operated with both MFCs, stirrer plates, air pump, and DO probe inside the incubator. The incubator was used to control the housed system at 37°C. Both MFCs were placed on stirrer plates to agitate the waste activated sludge in the anode compartments via magnetic stir-bars. The air pump was used to bubble air through the catholyte of MFC#1. The air was pumped through ports on the front and back of MFC#1 into the cathode chamber, which was left open to the atmosphere via the untapped sampling port in the MFC lid. A DO probe and meter was employed to measure dissolved oxygen in the catholyte of MFC#1 in order to ensure that DO concentrations remained relatively constant throughout MFC operation. Figure 2.3 illustrates the overall system layout.

Table 2.3.: *Ancillary System Components*

Component	Specifications
Incubator	• Thelco GCA Precision Scientific Model 6M • interior glass doors for system viewing with minimal temperature disturbance • metal shelving for multiple levels • ceiling vent used as wiring access between external electrical components and system power supply
Magnetic Stirrer Plates	• one Corning PC351, one Cole-Parmer Instrument Company Model 4658 • standard dial control for stirrer speed
Air Pump	• Tetratec Deep Water DW12 (used for fish tank aeration) • standard fish tank tubing connecting pump to plastic manifold • two output from the plastic manifold, standard fish tank tubing connecting plastic manifold to MFC#1 cathode chamber
Dissolved Oxygen (DO) Meter and Probe	• VWR SympHony SP70D • probe kept immersed in DI water when measurements not taken • probe placed in catholyte through untapped sampling port in cathode side of the MFC lid

Figure 2.3.: *Potentiostat and Multimeter with Data Collection System beside Incubator*

2.2.4. Electrolytes

In MFC#1, air was bubbled through a phosphate-buffered, saline catholyte to provide a source of dissolved oxygen. Dissolved oxygen concentrations as close to saturation as possible were maintained. In MFC#2, a phosphate-buffered, 0.05 M ferricyanide solution was used. In this cell, ferricyanide served as the electron acceptor through its redux reaction to form ferrocyanide.

The anolyte was the same for both MFCs. Waste activated sludge from the Waterloo region wastewater treatment plant was used as an initial anolyte and biological inocculent. Both the ferricyanide catholyte solution and the wastewater anolyte were subject to the same sampling and feeding system. This required weekly batches of waste activated sludge and a new batch of ferricyanide solution about every twenty days. The liquid level of MFC#1 was maintained with deionized water to make up for evaporation losses, while the air provided a constant supply of oxygen.

2.3. Experimental Design and Operation

The discussion of the experimental design and procedures is separated into four sub-sections: (i) overall system operation, (ii) sampling and feeding regimen, (iii) electrical measurements and (iv) wastewater and operational measurements. Analytical methods are described in Section 2.4.

2.3.1. System Operation

In the Section 2.2, the components of the microbial fuel cells, electrical equipment and ancillary equipment were listed. Two continuous experimental runs were carried out during this project; the first experiment lasted 28 days, while the second was 182 days in duration. The first experiment tested the entire setup and the various analytical techniques. Most of the results related to MFC performance and presented in this thesis were obtained from the second experiment.

Figure 2.2 illustrates the wiring setup for system operation. The potentiostat, multimeter, e-corder and lab computer were located outside the incubator, while the MFCs, stirrer plates, DO probe and air pump were kept inside the incubator. The incubator was operated at

37°C and the MFCs were operated under a controlled voltage of 0.3V between the anodes and cathodes for the duration of the experiments. This controlled voltage was chosen for comparison to previous studies and as an operational midpoint between MFC short circuit (V=0) and an average of the open circuit potential of the two MFCs (average V≈0.6).

2.3.2. Sampling and Feed System

The MFCs were designed with ports on the front and back to allow for continuous and fed-batch operation. The MFCs were operated under fed-batch conditions throughout both experiments. The use of a continuous flow system for the wastewater anolyte and catholyte solutions is a recommendation for future studies. However, these ports were used for sampling and feeding the wastewater anolyte in both MFCs via syringes and tubing. This ensured that the anode chamber remained anaerobic during operation. Ferricyanide catholyte sampling and feeding was accomplished via syringe and tubing at the untapped sampling port on the cathode side of the MFC#2 lid. The catholyte in MFC#1 was not subject to the same sampling and feeding system as the other electrolytes. Air was bubbled through this electrolyte and the untapped sampling port on the cathode side of the MFC#1 lid was left open. This made it necessary to top up the electrolyte levels every 48±3 hours with deionized water to replace water that evaporated during operation.

Sampling and feeding of both MFCs was scheduled every 48±3 hours throughout both experiments and for both MFCs. During the first experiment, the sampling and feeding for the two MFCs was staggered due to constraints with chemical oxygen demand and total Kjeldahl nitrogen analytical equipment. Throughout the second experiment, this constraint was removed and the sampling and feeding for the two MFCs was aligned to minimize analysis times. The sample and feed volumes were 100 mL, taken and delivered in two 50 mL portions.

The feed wastewater anolyte was stored in a refrigerator, while the feed ferricyanide catholyte was stored at room temperature. The sample wastewater anolyte was fractionated and preserved in Nalgene® bottles in a refrigerator until analysis. Wastewater fractionation involved the splitting of the sample into a 'total' sample, which represented a fraction of the original sample, and a 'soluble' sample, obtained through centrifugation and filtering. Total samples were stored without modification and preserved through refrigeration. Soluble samples were prepared by centrifuging (Beckman Model TJ-6 Centrifuge) a portion of the

original sample at a speed of 7000 RPM for 25-30 minutes and then passing the resulting liquid through a 1.5 μm glass microfibre filter (Whatman Grade 934-AH). The filtrate was preserved by adding concentrated sulphuric acid until the sample pH was approximately 2, and finally refrigerated. Ferricyanide catholyte samples were 100 mL in volume to maintain a similar hydraulic residence time to the anolyte in each MFC. Duplicate 1 mL portions of the ferricyanide catholyte samples were removed and placed in 1.5 mL sample vials before discarding the remainder. The 1 mL ferricyanide catholyte sample duplicates were stored at room temperature until analysis. Detailed fractionation and preservation methods can be found in Appendix B along with the overall sampling and feeding procedure.

2.3.3. Electrical Variables

Three electrical variables were measured throughout the second experiment, the cell voltage, total current and MFC#1 current. From these variables, the current for MFC#2 could be calculated along with the total coulombs of electricity and power produced by each MFC. Calculation of the electrical quantities from measurements is covered in Section 2.4.

2.3.4. Operational and Wastewater Variables

Throughout both experiments, a variety of operational and wastewater variables were measured. The associated analytical methods are discussed in Section 2.4. These variables included several parameters to monitor the system environment in addition to the parameters directly related to system evaluation.

The chemical oxygen demand (COD) is a measure of the amount of oxidizable material in a given sample. It is a standard wastewater variable that is a measure of the potential chemical energy in the wastewater anolyte. Throughout this study, the COD levels of both the total samples and the soluble portions were determined. The ratio of soluble COD to total COD was monitored, since some biological activity can result in the solubilization of the particulate matter that comprised a large percentage of the total COD. Therefore, after some treatment, total COD may decrease while soluble COD may increase.

Total Kjeldahl nitrogen (TKN) and free and saline ammonia (FSA) are nitrogen-specific wastewater quality measurements. These concentrations were monitored in the wastewater anolyte to characterize the behaviour of the nitrogen-containing species. TKN was fraction-

ated in the same manner as COD to determine the soluble portion of the TKN. The ratio of soluble TKN to total TKN was also monitored. FSA, by its very nature, is a soluble nitrogen-containing species, and is a portion of the soluble TKN. This provided another fractionation of the total TKN that is of interest, since ammonia is often the prevalent nitrogen-containing product in wastewater treatment processes.

In addition to these wastewater components, the pH of the wastewater anolyte samples was also measured. The pH was monitored to ensure no large fluctuations in anolyte acid-base chemistry. The wastewater pH was measured directly from the soluble portions of wastewater anolyte and feed, and no further analysis was required.

Ferricyanide ions in MFC#2 functioned as the electron acceptors. The change in ferricyanide concentration throughout MFC#2 operation was indicative of the electricity production. As electrons passed through the circuit to the cathode, the ferricyanide was reduced to ferrocyanide. The average concentration found in duplicate analytical ferricyanide samples was compared to the system current and coulombs of electricity produced during operation.

Measurements of dissolved oxygen concentration were made throughout the operation of MFC#1 to ensure that the oxygen levels did not fluctuate to any great degree. No direct analysis was required. The dissolved oxygen concentration was measured directly as mg/L and % saturation, and no further analysis was required.

Samples of the head space gas were taken throughout the operation of both MFCs. It was expected that the gas would mainly consist of nitrogen, carbon dioxide, and possibly methane. Gas chromatography was used to determine the percentages of each of these gases in 1 mL samples. Duplicate 1 mL samples were taken from each MFC, but due to the low volume of the head space, it was not possible to take a greater number of samples, which may have reduced the high variability in methane concentration measurements.

2.4. Analysis

The description of the analytical methods is divided into several sub-sections. The electrical parameter analysis is described first, followed by the analysis of the following wastewater measurements: COD, TKN and FSA and anolyte pH. The analysis of the catholyte

measurements, ferricyanide concentration for MFC#2 and DO concentration for MFC#1, follows the wastewater measurement analysis. The analytical methods for the head space gas are described in the final sub-section. Specific analysis methods are described in detail in Appendix C.

2.4.1. Electrical Parameters

The electrical data were collected using the eDAQ e-corder 401 unit, lab computer and Chart 5.0 software and then analyzed using the Chart 5.0 software, provided with the e-corder 401 unit. The results were exported to Microsoft Excel for general analysis and time plots. As described earlier, three electrical variables were directly measured, the cell voltage (V), total current (I), and MFC#1 current (I_1). The current resulting from MFC#2 (I_2) was calculated from Equation 2.1. The amount of electricity in coulombs (Q(t)) produced by the entire system or by an individual MFC was calculated using Equation 2.2. Finally, the power (P) produced by the entire system or by an individual MFC was calculated using Equation 2.3. With these equations, the current, voltage, power, and coulombs were monitored and recorded for each MFC.

$$I_2 = I - I_1 \tag{2.1}$$

$$Q(t) = \int_0^t I \cdot dt \tag{2.2}$$

$$P = I \times V \tag{2.3}$$

Normally, current and power are reported in the literature normalized to the anode or cathode surface area, where they are usually equal. However, the area of interest is only the effective, or utilized surface area. Since there were only two cathodes, an effective electrode surface area (EESA) of 282 cm^2 was used to normalize the current and power values. With increased internal resistance due to the MFC design, it is likely that only a small fraction of this area, that which would be approximately equal to the proton exchange membrane

surface area, was primarily utilized. This would provide a path of least resistance for proton shuttling to complete the electrical circuit. As such, an effective membrane surface area (EMSA) of 7 cm^2 was used to normalize the current and power values as well. These two effective surface areas likely bound the actual effective surface area utilized during the experiments.

2.4.2. Chemical Oxygen Demand (COD)

Following sample fractionation and preservation, the samples collected for COD analysis were stored at 4°C. The steps for the analysis of the COD wastewater anolyte and feed samples are listed below:

1. **Sample dilutions:** total 1:20 or 1:10, soluble 1:2 or none
2. **Digestion preparation:** triplicate total and soluble samples, calibration standards, digestive reagents
3. **Digestion:** 3.0 hours at 150°C
4. **Optical Density (OD) measurements:** $\lambda = 600$ nm, calibration curve generated, sample values recorded

During the first step, preserved samples were diluted with deionized water. Following dilution, triplicate 2.5 mL volumes of each wastewater sample was added to 10 mL COD digestion vials. A set of COD calibration standards were prepared at 0, 25, 50, 100, 200, 300, 400, 600, 800, and 1000 mg COD/L, and 2.5 mL of each standard was added to 10 mL COD digestion vials. If the previous COD digestion had used the exact same batch of reagents, only a 0 and a 1000 COD calibration standard were prepared to confirm the previous calibration curve. If confirmed, the previous calibration curve was re-used. After sample and standard addition, 3.5 mL of the sulphuric reagent and 1.5 mL of the chromatic reagent were added to each digestion vial. Recipes for these reagents are provided along with the overall procedure in Appendix C. Once the reagents were added, the vials were capped, shaken and placed in a block heater to be digested for 3 hours at 150 °C. Following digestion, the vials were allowed to cool before being cleaned with ethanol and tissues. Optical density measurements at a wavelength of 600 nm were recorded for each sample and standard using a spectrophotometer (Hach DR/2010 Portable Datalogging Spectrophotometer). The COD values were obtained by reading off the calibration curve. Refer to the standard method

for water and wastewater analysis, 5220D Colorimetric Method, as published by the American Public Health Association - American Water Works Association - Water Environment Foundation.

A cumulative COD balance applied to each MFC for the duration of the second experiment yielded performance characteristics with respect to the amount utilized in electricity production and the total amount of COD reduced. The total accumulation of COD (COD_{Acc}) for each MFC was calculated using Equation 2.4:

$$COD_{Acc} = COD_{Feed} + COD_{CSP} - COD_{Smpl} - COD_{Elec} - COD_{Gas} \quad (2.4)$$

where,
COD_{Acc} = cumulative COD accumulation in MFC (mg)
COD_{Feed} = cumulative COD of feed wastewater anolyte to MFC (mg)
COD_{CSP} = cumulative COD of carbon source pulses injected into MFC (mg)
COD_{Smpl} = cumulative COD of sample wastewater anolyte from MFC (mg)
COD_{Elec} = equivalent cumulative COD of electricity produced during MFC operation (mg)
COD_{Gas} = equivalent cumulative COD of methane gas produced during MFC operation (mg)

The COD_{Feed} and COD_{Smpl} values were obtained from measured sample results and known volumes. COD_{CSP} and COD_{Gas} were calculated from theoretical values for the substances, while COD_{Elec} was calculated from the coulombs of electricity (Q) produced during MFC operation. The theoretical COD values were calculated from the mass of oxygen required to oxidize the mass of the substance added. Calculation of COD_{Gas} is described further in Section 2.4.7. From the coulombs of electricity produced, the moles of electrons were calculated. This was related to the moles of oxygen required to oxidize enough organic matter to generate the same amount of electrons. The moles of oxygen was converted to the corresponding mass in each case (COD_{CSP}, COD_{Gas}, COD_{Elec}).

2.4.3. Total Kjeldahl Nitrogen (TKN) and Free and Saline Ammonia (FSA)

Nitrogen sources and ammonia are wastewater contaminants of concern in most treatment systems and also nutrients for biological growth. Similarly to COD analysis, several steps followed sample partitioning and preservation, as listed below:

1. **Sample dilutions:** total 1:2 or none, no soluble sample dilution, FSA 1:26
2. **Digestion preparation:** total and soluble samples, calibration standards, digestion standards, digestive reagent
3. **Digestion:** 1.5 hours at 200°C then 3.5 hours at 380°C
4. **Dilutions:** digested samples and standards diluted to 100 mL
5. **Ammonia Analysis:** dialysis unit for detection of ammonia in digested and FSA samples

During the first step, preserved samples were diluted with deionized water. Following dilution, 1.0 mL of each sample was added to a semi-macro TKN digestion vial with a total capacity of approximately 80 mL. A set of TKN calibration standards was prepared at 0, 125, 250, 500, and 1000 mg NH_4-N/L. In addition, glutamic acid standards were prepared at 125 and 500 mg NH_4-N/L, based on the theoretical ammonia composition after digestion. These standards were used to ensure that sample digestion was complete. Glutamic acid standards at 250 and 375 mg NH_4-N/L were also used in earlier digestions and analyses to increase the number of digestion standards and confidence in full digestion. Following preparation, 1.0 mL of each standard was added to a semi-macro TKN digestion vial. After sample and standard addition, 3.0 mL of the digestive reagent was added to each of the semi-macro TKN digestion vials. A recipe for this reagent is provided along with the overall procedure in Appendix C.

Once the reagent was added, two glass boiling beads were added to each vial, and the vials were placed in a block heater for digestion. The digestion took place for 1.5 hours at 200°C and then for 3.5 hours at 380°C. Following digestion, the digested samples and standards were diluted with deionized water to 100 mL by rinsing each digestion vial into a graduated cylinder three times. Because the original sample and standard volume added to the vials was 1.0 mL, this constitutes a 1:100 dilution. A Brann and Luebbe AA3 ammonia analysis system was used to determine the ammonia content in the digested samples and standards as well as the FSA samples. System calibration standards were required at 0.5, 1.0, 5.0, 10.0, and 30.0 mg NH_4-N/L. Analytical cups for each digested standard were prepared in at least duplicate, with triplicate and quadruplicate analysis in earlier analyses to ensure good performance. Each sample was analyzed in duplicate. The digested standards were used to

construct a calibration curve for digested samples, while the digested glutamic acid standards provided a correction factor for digestion completion. FSA samples were compared to the system calibration standards to obtain FSA concentrations. FSA samples were not digested, so comparison to non-digested system calibration standards prevented any digestion biases from being applied to the FSA sample measurements. Refer to the standard methods for water and wastewater analysis, 4500-NorgC Semi-Micro Kjeldahl Method and 4500-NH_3G Automated Phenate Method, as published by the American Public Health Association - American Water Works Association - Water Environment Foundation.

2.4.4. Anolyte pH

The wastewater pH was measured throughout most of the second experiment. The measurement was made using a standard pH probe and meter on the soluble wastewater anolyte samples before preservation. As mentioned earlier, preservation of the soluble sample required the addition of sulphuric acid, so pH measurements were taken prior to this step.

2.4.5. Ferricyanide

The catholyte ferricyanide concentration was the primary variable for the cathode side of MFC#2. The procedure for its determination is given below:

1. **Serial dilution:** duplicate samples diluted to 1:100
2. **Optical Density (OD) measurements:** $\lambda = 420$ nm, sample absorbance values recorded

A calibration curve of ferricyanide concentration versus optical density at a wavelength of 420 nm was established in advance of both experiments and used thereafter. The calibration curve was valid for concentrations up to 0.05 M, which was the feed concentration for both experiments. Following serial dilution of the samples, OD measurements were taken at a wavelength of 420 nm using a spectrophotometer (Spectronic Genesys 2). Sample OD values were compared to the calibration curve to obtain ferricyanide concentrations. The feed system for the fresh ferricyanide catholyte solution allowed a relatively constant ferricyanide concentration to be maintained throughout system operation.

A simple molar balance yields the amount of ferricyanide reduced to ferrocyanide at the cathode. Equation 2.5 shows this balance. The moles of ferricyanide reduced to ferrocyanide

was equal to the moles of electrons gained from the cathode. This was related to the moles of oxygen that are theoretically required to liberate these electrons through oxidation. The equivalent mass of oxygen was equal to the COD mass. This value was compared to the COD_{Elec} found for MFC#2 through coulombic analysis.

$$Ferri_{Reacted} = Ferri_{In} - Ferri_{Out} \tag{2.5}$$

where,
$Ferri_{Reacted}$ = moles of ferricyanide reacted during MFC operation (moles)
$Ferri_{In}$ = moles of ferricyanide added to MFC#2 during operation, includes start up (moles)
$Ferri_{Out}$ = moles of ferricyanide removed from MFC#2 during operation, includes shut down (moles)

2.4.6. Dissolved Oxygen

Dissolved oxygen (DO) data were used as indicators of electron acceptor concentrations in the cathode of MFC#1. It was not possible to calculate the total amount of oxygen that reacted at the cathode of MFC#1 for comparison to the COD_{Elec} found for MFC#1. However, it was important to ensure that the DO concentration in the phosphate-buffered saline catholyte of MFC#1 remained relatively constant. Low DO concentrations would theoretically hinder electricity production, influencing the anodic side of the MFC and limiting MFC performance on the cathode side. It was desired that the catholyte concentration in both MFCs remain relatively constant to minimize any cathodic limitations impacting the system performance.

2.4.7. Head Space Gas

The head space gas theoretically contains nitrogen, originating from any air that may have entered the system, along with carbon dioxide and methane from system operation. Analysis of the head space gas samples was accomplished using gas chromatography. The head space gas volume (V_{Total}) was approximated from system design dimensions and known anolyte volumes to be 10 mL. The steps required for analysis are outlined as follows:

1. **Gas chromatography system setup:** power up and carrier gas, Peak software

2. **Triplicate air sample injection:** prime system with air, 2 minute runtime each
3. **Head space gas sample injection:** samples injected, 2 minute runtime each
4. **Gas composition:** calculated against known system calibration curve
5. **Gas volumes:** head space gas volume estimated, with composition gives individual gas quantities

The gas chromatography (GC) system consisted of the GC unit (SRI 310C Gas Chromatograph, silica gel carrier medium), helium carrier gas cylinder and lines, a thermoconductivity detector and a lab computer with PeakSimple 3.29 software for data collection. A calibration curve was established using gas standards before experimentation. Methane was the component of interest since nitrogen was inert in the system and carbon dioxide has a zero COD equivalence. Head space gas samples were taken with every sample/feed cycle, resulting in gas samples every 48∓3 hours. Head space gas samples were only 2 mL in size, while the head space was approximated as 10 mL, leaving 8 mL of head space gas and probable methane to confound later measurements. However, the sample/feed procedure for the wastewater anolyte was assumed to effectively 'reset' the head space gas composition and eliminate methane presence. Thus, the amount of methane calculated for each sample was assumed to be independent of previous methane calculations. Since the gas composition of each sample provided the volumetric fraction of each component including methane (X_{CH4}), the methane volume in each sample(V_{CH4}) was easily calculated from Equation 2.6:

$$V_{CH4} = X_{CH4} \times V_{Total} \tag{2.6}$$

A cumulative methane volume was calculated from the sum of each head space gas sample result and converted to a molar equivalent using Equation 2.7, derived from the ideal gas law. The mass of oxygen required to fully oxidize this amount of methane provides the theoretical COD equivalent (COD_{Gas}) for use in the COD balance in Equation 2.4.

$$N_{CH4} = \frac{(P_{sys} \times V_{CH4})}{(R \times T_{sys})} \tag{2.7}$$

where,
N_{CH4} = number of moles of methane produced

P_{sys} = system operative pressure: 1 atm (abs)
V_{CH4} = volume of methane produced in litres
R = gas constant: 0.08206 L*atm/mol*K
T_{sys} = system operative temperature: 310.15 K

The presence of oxygen in the head space gas was assumed to be negligible, considering the anaerobic conditions maintained in the anodic chamber. However, during GC analysis, any trace amounts of oxygen would be measured as part of the total nitrogen component of the head space gas. The GC analytical method is unable to distinguish between these two gases.

2.5. Results and Discussion

Following the analysis of the data, several significant conclusions were drawn from the results. A few of these results are presented and discussed below, in the same order as in the previous section. Since the primary focus of this chapter is to introduce and describe the MFC experiments, a more thorough examination of the results is presented in Chapter 4.0.

2.5.1. Electrical Parameters

A brief summary of the electrical parameter results from the second experiment are given in Table 2.4 for MFC#1 and Table 2.5 for MFC#2. The controlled voltage was maintained at 0.3V throughout most of the experiment, though it was dropped to 0.25V following sample/feed procedures during the first few months of operation. This was due to a reversal of current flow direction immediately following the sample/feed procedure. After approximately 2 hours of operation at 0.25V, the controlled voltage was set back to 0.3V.

Results are presented in approximately 15 day intervals to highlight the changes during the acclimation period and the carbon dosing period. The acclimation period was defined as the operational time before the carbon source pulse tests (CSPTs) and lasted from December 5th, 2006 to February 20th, 2007. The carbon dosing period encompasses the CSPTs from February 20th, 2007 to April 23rd, 2007. There was also a post-experimental monitoring period from April 23rd, 2007 to June 5th, 2007, which completed the 182 day duration of the second experiment. On April 19th, 2007 the anolyte in both MFCs was manually stirred for a period of 5 minutes prior to the sample/feed procedure. Current and power production

Table 2.4.: *Electrical Parameter Results for MFC#1*

Date	Current and Current Density			Power and Power Density			Total Coulombs produced	
	(mA)	(mA/m^2)		(mW)	(mW/m^2)		(C)	
Densities calculated with		EESA	EMSA		EESA	EMSA		
Acclimation Period								
December 21st, 2006	0.0244	0.87	34.9	0.0086	0.30	12.3	85.726	
January 5th, 2007	0.0172	0.61	24.6	0.0052	0.18	7.43	188.456	
January 20th, 2007	0.0340	1.21	48.6	0.0102	0.36	14.6	280.197	
February 5th, 2007	0.0386	1.37	55.1	0.0116	0.41	16.6	379.802	
February 20th, 2007	0.0235	0.83	33.6	0.0071	0.25	10.1	420.637	
CS Dosing Period								
March 5th, 2007	0.0593	2.10	84.7	0.0178	0.63	25.4	520.243	Post Sodium Acetate
March 20th, 2007	0.0456	1.62	65.1	0.0137	0.49	19.6	617.674	Post Glucose
April 5th, 2007	0.0654	2.32	93.4	0.0196	0.70	28.0	760.586	Post Glycerol
April 19th, 2007	0.2296	8.14	328	0.0690	2.45	98.6	965.529	Post BSA
May 5th, 2007	0.2550	9.04	364	0.0765	2.71	109	x	Anolyte mixed Apr 19th
May 20th, 2007	0.1700	6.03	243	0.0510	1.81	72.9	x	
June 5th, 2007	0.0350	1.24	50.0	0.0105	0.37	15.0	x	

levels were observed to rise and remain high for over 2 weeks.

With a constant voltage, current and power were proportional to each other, so the trends shown in Table 2.4 and Table 2.5 for these two parameters followed a similar pattern. There were several interesting trends to note:

MFC#1

- current/power was relatively stable throughout the acclimation period
- addition of sodium acetate significantly increased current/power production from sludge

Table 2.5.: *Electrical Parameter Results for MFC#2*

Date	Current and Current Density			Power and Power Density			Total Coulombs produced	
	(mA)	(mA/m^2)		(mW)	(mW/m^2)		(C)	
Densities calculated with		EESA	EMSA		EESA	EMSA		
Acclimation Period								
December 21st, 2006	0.2796	9.91	399	0.0980	3.48	140	501.662	
January 5th, 2007	0.2659	9.43	380	0.0799	2.83	114	900.679	
January 20th, 2007	0.2706	9.60	387	0.0815	2.89	116	1240.002	
February 5th, 2007	0.2439	8.65	348	0.0734	2.60	105	1623.378	
February 20th, 2007	0.3186	11.3	455	0.0958	3.40	137	2015.667	
CS Dosing Period								
March 5th, 2007	0.2788	9.89	398	0.0839	2.98	120	2389.976	Post Sodium Acetate
March 20th, 2007	0.3087	11.0	441	0.0929	3.29	133	2776.565	Post Glucose
April 5th, 2007	0.3251	11.5	464	0.0977	3.46	140	3219.783	Post Glycerol
April 19th, 2007	0.2999	10.6	428	0.0902	3.20	129	3639.926	Post BSA
May 5th, 2007	0.3900	13.8	557	0.1170	4.15	167	x	Anolyte mixed Apr 19th
May 20th, 2007	0.3400	12.1	486	0.1020	3.62	146	x	
June 5th, 2007	0.2900	10.3	414	0.0870	3.09	124	x	

- addition of glucose and glycerol maintained this increased current/power production from sludge
- addition of bovine serum albumin drastically increased current/power production from sludge
- following CSPTs, the system returned to previous current/power production levels
- current/power densities calculated with the EMSA approached literature values derived from electrode surface areas, on the order of 150 mW/m^2 (Oh & Logan, 2006)
- current/power densities calculated with the EESA were significantly less than the same

literature values, on the order of 150 mW/m^2 (Oh & Logan, 2006)

MFC#2

- current/power was relatively stable throughout the acclimation period
- current/power was relatively stable throughout the carbon dosing period
- following CSPTs, the system returned to previous current/power production levels
- current/power densities calculated with the EMSA were on the same order as literature values derived from electrode surface areas, on the order of 150 mW/m^2 (Oh & Logan, 2006)
- current/power densities calculated with the EESA were significantly less than the same literature values, on the order of 150 mW/m^2 (Oh & Logan, 2006)

The power densities calculated from the EESA and the EMSA represent the theoretical minimum and maximum power densities for each MFC. It is reasonable to conclude that the actual effective surface area is bounded by the EESA and EMSA. If the actual effective surface area was close to the EESA, power densities were very low during system operation, while the opposite is true if the EMSA is closer to the actual effective surface area. It is recommended that future MFC designs incorporate a larger proton exchange membrane and equivalent, evenly-spaced, single electrodes.

The addition of the carbon sources increased current and power levels slightly, but only for short periods. This was due to their relatively low COD equivalence and the unsustained addition of the carbon sources. Spot sample values for the current, no matter how well placed, are a poor indicator of overall performance. MFC#1 operated at a much lower current than MFC#2 due to the differing catholytes. Therefore, the long term effects of the carbon source pulse tests were more easily identified by looking at the coloumb production averaged over time. Table 2.6 presents the average coulomb production for each time period in Tables 2.4 and 2.5.

From Table 2.6, the MFCs show similar electrical behaviour with respect to each carbon source pulse test.

Table 2.6.: *Daily Coulomb Production for MFCs*

Start-End Dates	MFC#1 (Q/day)	MFC#2 (Q/day)	
December 5–21, 2006	5.20	30.41	
December 21, 2006–January 5, 2007	6.90	26.79	
January 5–20, 2007	6.12	22.62	
January 20–February 5, 2007	6.23	23.96	
February 5–20, 2007	2.73	26.18	
February 20–March 5, 2007	7.66	28.80	Sodium Acetate dosing
March 5–20, 2007	6.51	25.83	Glucose dosing
March 20–April 5, 2007	8.95	27.77	Glycerol dosing
April 5–19, 2007	14.58	29.88	BSA dosing

- sodium acetate increased daily coulomb production by approximately 15% over acclimation period levels for both MFCs
- glucose decreased daily coulomb production to acclimation period levels for both MFCs
- glycerol increased daily coulomb production by approximately 30% and 10% over acclimation period levels for MFC#1 and MFC#2, respectively
- bovine serum albumin increased daily coulomb production by approximately 180% amd 20% over acclimation period levels for MFC#1 and MFC#2, respectively

Organics in the wastewater anolyte were oxidized by micro-organisms in the wastewater anolyte. This biocatalytic reaction occurred either at the anode surface or within the bulk anolyte solution. Because the anode side of the MFC was under anaerobic conditions, the liberated electrons could either:

- travel through the anode to the cathode to reduce the associated electron acceptor if the reaction took place at the anode surface, or
- chemically reduce carbon in solution, resulting in the production of methane if the reaction took place in the bulk anolyte solution

When the reaction takes place at the anode and electrons travel through the circuit, coulomb production occurs. When the reaction takes place in the bulk anolyte resulting in methane production, coulomb production does not occur. Therefore, a decrease in coulomb production likely favours methanogenesis in the bulk solution over reaction at the anode and coulomb production. At a microbial level, if glucose resulted in a competitive growth advantage for methanogens, electron-producing micro-organisms may have been at a relative disadvantage, resulting in a lower coulomb output. It is interesting that this phenomenon was noted in both MFCs. Also of interest, was the return to pre-CSPT current/power production levels during the post-experimental monitoring period. However, this may have been due to a 'washout' effect from the sample/feed procedure.

2.5.2. Chemical Oxygen Demand (COD)

The COD results from the second experiment are given in Table 2.7. The COD totals are given as sums over the course of the acclimation and carbon dosing periods. Some approximated results from the post-experimental monitoring period are presented in Table 2.8. The analytical error ranges are provided for the COD balance variables in both tables, based on a 95% confidence interval and triplicate analysis.

Table 2.7.: *Cumulative Chemical Oxygen Demand Results without Post-Experimental Period Extrapolations*

COD Variable	MFC#1 (mg)	MFC#2 (mg)
COD_{Feed}	19120∓2500	19120∓2500
COD_{CSP}	92.9∓4.6	92.9∓4.6
COD_{Smpl}	5070∓1810	5470∓1930
COD_{Elec}	88.4∓3.0	318.6∓59.7
COD_{Gas}	141.7∓278.3	175.2∓148.3
COD_{Acc} (calculated from Equation 2.4)	13914.8∓4594.7	13255.3∓4642.6

As can be seen in Table 2.7, the system mass transfer terms, $COD_{Feed,Smpl,Acc}$, constitute a majority of the overall balance. The COD_{CSP} associated with the carbon source pulse tests, was very small in comparison, as was the COD_{Elec} associated with electricity production and the COD_{Gas} associated with methane production. During system design, it was under-

stood that the sub-optimal geometry would lead to lower current/power production than previously published values (Oh & Logan, 2006), but the impact on the overall COD mass balance was not fully investigated. The balance on both MFCs indicated a very large COD accumulation term. The COD accumulation terms were 73% and 69% of the total sludge feed for MFC#1 and MFC#2, respectively.

During the post-experimental period, sampling and feeding continued, as did electricity and methane production. Based on the acclimation and carbon dosing periods, approximate values for the COD balance terms were extrapolated for the post-experimental period. Analysis of feed and effluent samples was discontinued during this period and a representative sample for the accumulation term was not taken immediately following the carbon dosing period. A representative sample would have required the scraping of the anode surface, which was avoided to preserve any biofilm activity during the post-experimental period. The COD results with the extrapolated values included can be seen in Table 2.8.

Table 2.8.: *Cumulative Chemical Oxygen Demand Results with Post-Experimental Period Extrapolations*

COD Variable	MFC#1 (mg)	MFC#2 (mg)
COD_{Feed}	24800∓3240	24800∓3240
COD_{CSP}	92.9∓4.6	92.9∓4.6
COD_{Smpl}	6690∓2390	7200∓2550
$COD_{Elec,Gas}$	307∓375	658∓277.4
COD_{Acc} (calculated from Equation 2.4)	17900∓6010	17040∓6070

Because the post-experimental period results were extrapolated from the previous operational results, the same general trends can be seen. Following the system shut down, samples to determine the COD accumulation were taken from both MFCs. The MFCs were opened up and the accumulated wastewater sludge on the lid, anodes, and within the anodic chamber were vigorously stirred into the anolyte. These sample volumes were 100 mL, constituting 20% of the entire anolyte for each MFC to minimize the possibility of unrepresentative samples. The measured accumulation was found to be 6244.0 mg and 6135.7 mg for MFC#1 and MFC#2, respectively.

From the results of the accumulation term analysis, a discrepancy of 11660 mg and 10900 mg was seen for MFC#1 and MFC#2, respectively. This constitutes approximately 47% of the total feed to MFC#1 and 44% of the total feed to MFC#2. Although it was likely that the measured accumulation samples would provide low estimates of the COD accumulation, it was not expected that the discrepancy would be of such a large magnitude. There are several possible causes for this:

1. head space gas leakage leading to the loss of methane from the system and unmeasured COD_{Gas}
2. oxygen presence in the anodic chamber providing a chemical short circuit of the MFC and unmeasured COD loss through oxidation
3. liquid phase anolyte leakage to MFC surroundings, leading to the loss of wastewater anolyte and the associated COD
4. other sources of error in addition to the calculated analytical error, such as operator and measurement error

Head space gas leakage was considered unlikely during MFC design and early operation. The Tedlar bags attached to the head space volume consistently showed little to no swelling and negligible amounts of methane when gas was present. However, if the discrepancy in the COD accumulation was due to methane leakage, it would only require a rate of approximately 25 mL/day or 1 mL/hr of methane production from each MFC. Carbon dioxide would not account for any of the COD balance discrepancy, but may have been produced beyond the measured amounts. This would increase the leakage rate of any gas from the system, but only by an equivalent or lesser rate. Therefore, the total leakage rate may have approached 50 mL/day, with methane, carbon dioxide and trace amounts of nitrogen leaving the system. Since these volumetric production rates are very small, a slight leak in the Tedlar bag system could account for the discrepancy. In addition, carbon dioxide and methane production in the head space during MFC operation would cause a slight positive pressure, forcing the gas into the Tedlar bag.

Oxygen presence in the anodic chamber was considered a minimal and unavoidable side effect of the sample/feed procedure. It was unlikely that oxygen was able to enter the anode side

during the feeding procedure in particular. However, if the Tedlar bags were leaking, oxygen could be introduced during sampling. If 100 mL of air was able to enter the anodic chamber during sampling, it would be quickly forced out during the feeding procedure. Any residual air would be a source of oxygen. If it is assumed that approximately 2 mL of oxygen, 20% of the 10 mL head space volume, was present in the anode chamber after the sample/feed procedure, this only represented about 2.5 mg of the undetected COD oxidation. If this leakage occured throughout the entire second experiment, this would only represent 228.8 mg of undetected COD oxidation and would not adequately explain the discrepancy in the measured COD accumulation. It was also unlikely that oxygen was able to leak into the anodic chamber on a continuous basis, considering the gas production and slight positive pressure in the head space.

Liquid phase anolyte leakage would provide a direct loss of COD from the anode chamber. However, this type of leak would be very noticeable and was not observed at any point during experimentation. Although additional sources of error beyond the analytical error from the 95% confidence level provided in Tables 2.7 and 2.8 is possible, it is unlikely to explain the full magnitude of the discrepancy in the COD accumulation measurement. Error associated with sample preparation would affect both MFC samples and the feed that was analyzed. It is possible that any under- or over-estimates would occur in both terms, and this could at least partially negate the effects on the COD accumulation term.

2.5.3. Total Kjeldahl Nitrogen (TKN) and Free and Saline Ammonia (FSA)

The TKN results from the second experiment are presented in Figure 2.4 for the feed, Figure 2.5 for MFC#1 and Figure 2.6 for MFC#2. Error bars are also included on the figures and are indicative of the analytical error calculated from duplicate samples at a 95% confidence level.

In Figure 2.4, the feed TKN between December 5th, 2006 and January 23rd, 2007 was interpolated based on the surrounding values. Unfortunately, direct analysis was not carried out due to TKN digestion equipment constraints. The error bars associated with these interpolated values essentially paints a black box with a width of the associated time period and a height equal to the difference between surrounding values. Subsequent TKN measurements throughout the experiment suggest that this was a reasonable range for estimated TKN

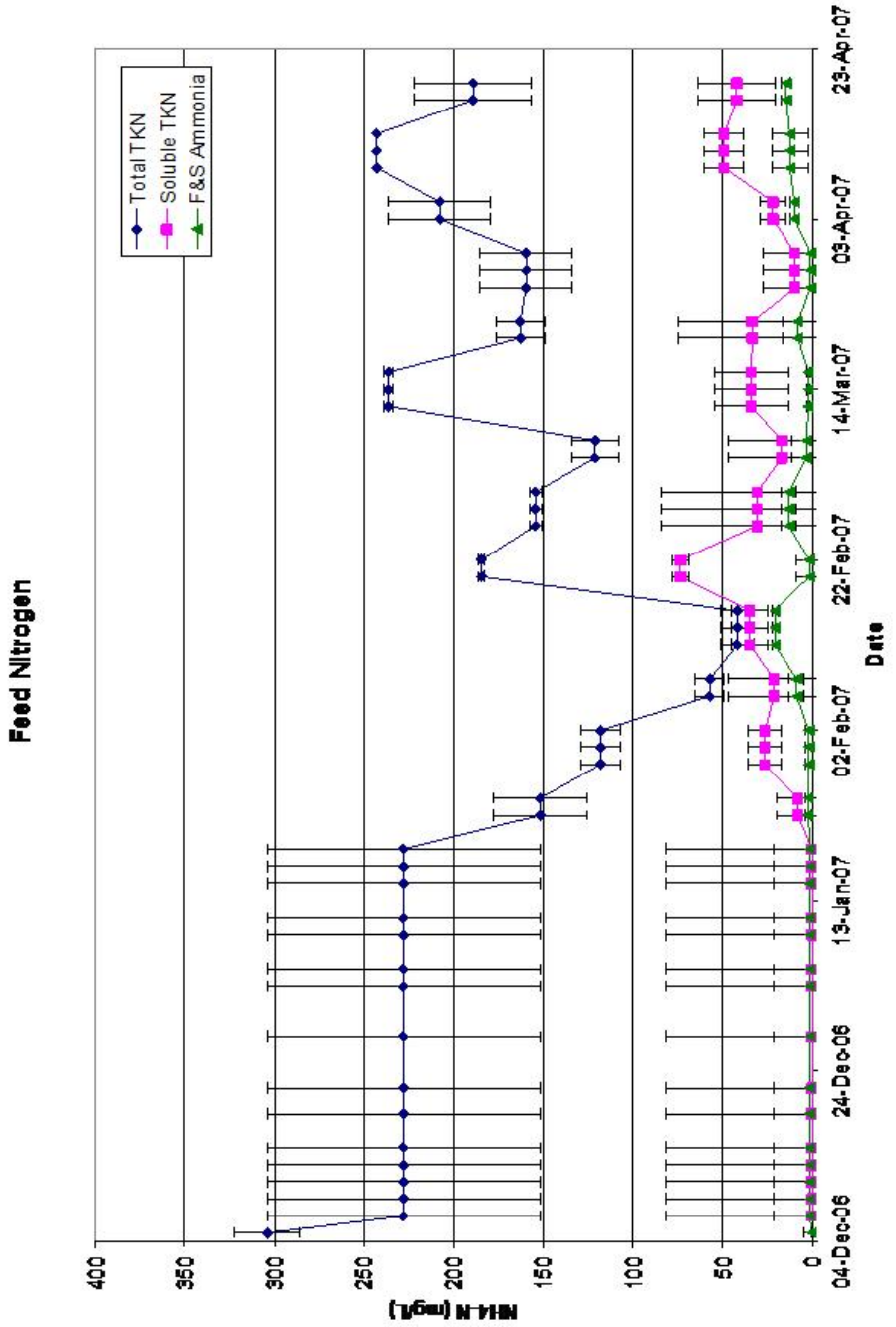

Figure 2.4.: *Feed TKN (Total and Soluble) and FSA*

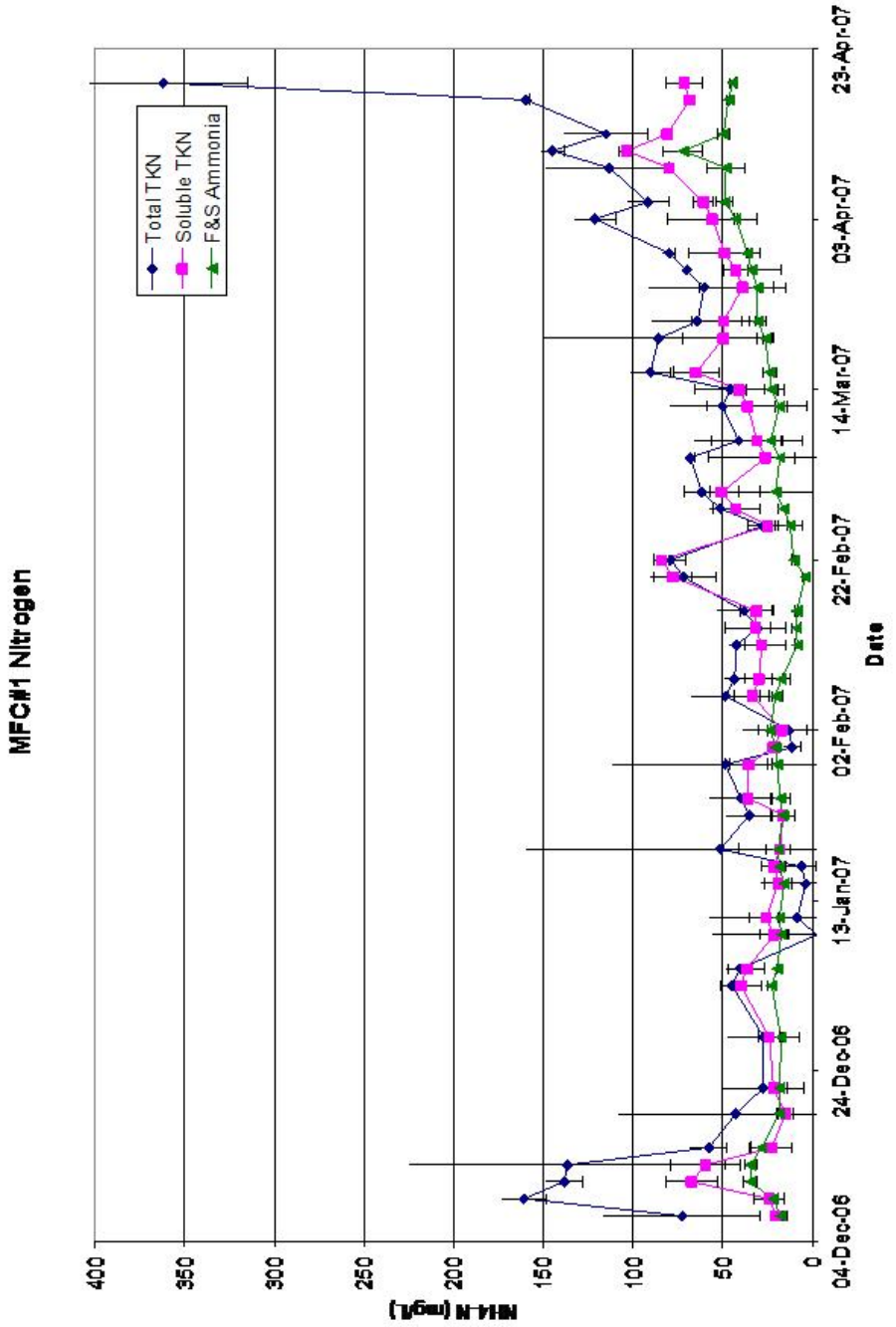

Figure 2.5.: *MFC#1 TKN (Total and Soluble) and FSA*

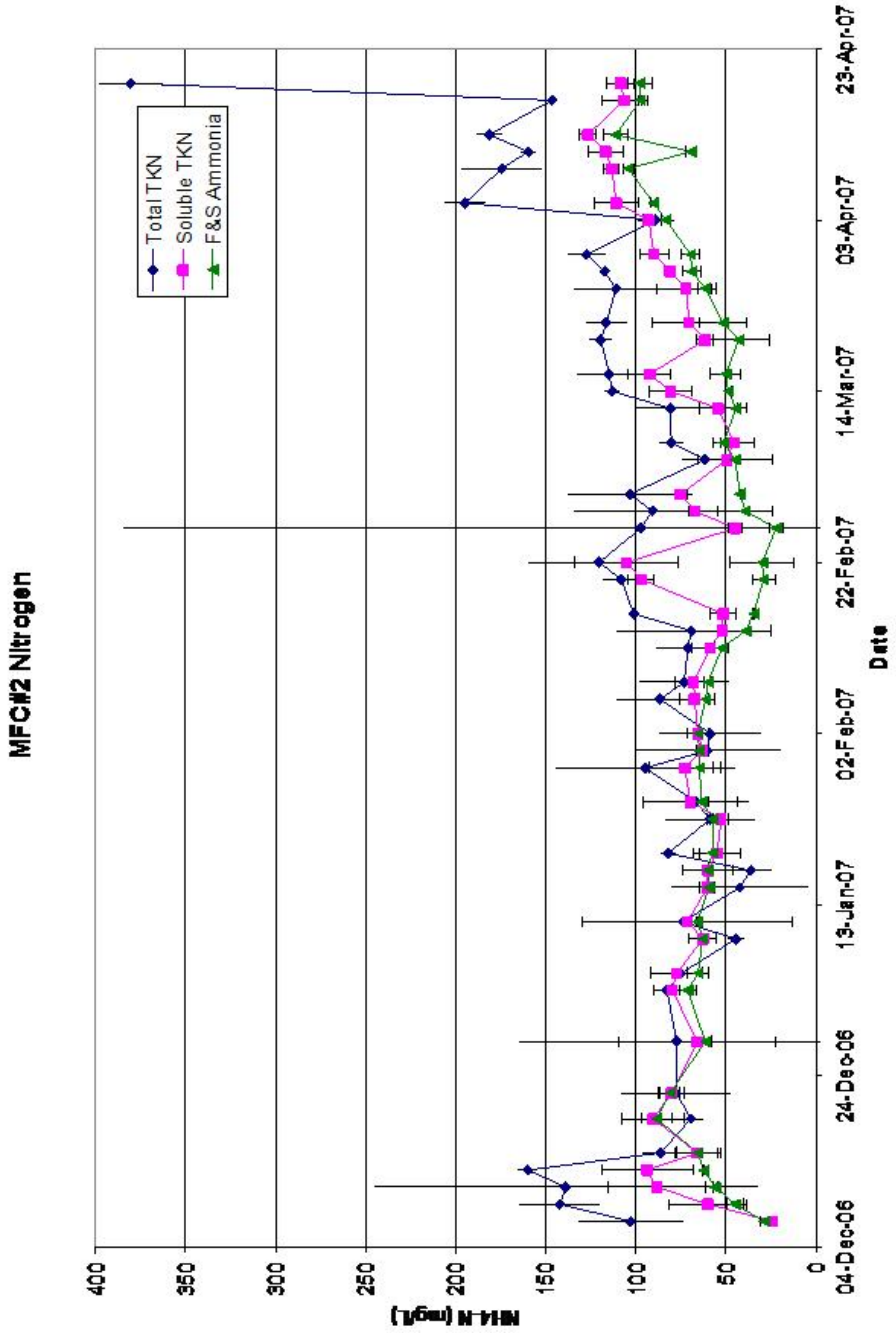

Figure 2.6.: *MFC#2 TKN (Total and Soluble) and FSA*

values. There are two decisive conclusions noted from the feed TKN results:

- other than early-mid February, total TKN had significantly larger concentrations than the associated soluble TKN and FSA concentrations
- FSA concentrations represent most of the soluble TKN concentrations

These results indicate that a significant portion of the waste activated sludge feed contained insoluble nitrogen components. In addition, most of the soluble nitrogen exists as ammonia rather than alternative soluble nitrogen species.

The TKN in MFC#1 samples (Figure 2.5), indicated generally lower TKN values leaving the MFC than those entering, suggesting a nitrogen accumulation in addition to the COD accumulation observed earlier. However, soluble TKN and FSA were comparable to the waste activated sludge feed values, indicating that any nitrogen accumulation was likely prevalent in the insoluble particulate matter. The TKN in MFC#2 samples, Figure 2.6, followed a similar trends to those seen in MFC#1. Also, as part of the biodegradation process of particulate matter, total TKN was expected to be broken down into soluble TKN and FSA, which would increase the percentage of the total TKN that exists as soluble TKN.

The final TKN sample taken from both MFCs on April 19th, 2007 was obtained after manually mixing the wastewater anolyte of each MFC for five minutes. Particulate accumulation in corners and other hydraulically dead areas were stirred into the wastewater anolyte for the purpose of gaining a more representative sample. It should be noted that any particulate matter accumulated on the lid and electrodes was not included in the mixing and final sample points. It is interesting to note that the final TKN samples indicated a significantly higher total TKN, while the soluble TKN and FSA did not show significantly higher amounts. This provides further support that nitrogen accumulation in the MFCs was mainly attributable to insoluble, particulate forms.

The TKN values for both MFCs between April 8th, 2007 and April 18th, 2007 are also of particular interest. The final CSPT of BSA took place during this time period, and BSA is a source of soluble nitrogen. It was difficult to determine the exact response for both MFCs considering the continued sample/feed procedure. However, it appeared that the addition of BSA resulted in higher TKN values for each MFC. This increase appeared in total and

soluble TKN as well as FSA. The increase was slight and it was difficult to conclude that this was due to BSA with any statistical significance.

2.5.4. Anolyte pH

The pH of the wastewater anolyte and feed waste activated sludge was measured for the last 38 days of the acclimation period and throughout the carbon dosing period. The results are presented in Figure 2.7.

Most pH measurements indicated that the wastewater anolyte in each MFC remained close to neutrality. The feed pH was consistently slightly basic, maintaining values below a pH of 8.2. During biodegradation of the organic matter in the wastewater anolyte, protons were liberated in addition to the electrons for electricity production. These protons theoretically migrated through the proton exchange membrane to the catholyte to maintain electro-neutrality in the system. However, any accumulation of protons in the wastewater anolyte during operation would result in lower pH values for the wastewater anolyte. Although unlikely, small amounts of proton accumulation could be a result of mass transfer limitation through the proton exchange membrane due to biofouling or particulate accumulation on the membrane surface.

MFC#1 consistently showed lower pH values than MFC#2. Another explanation for pH changes is the production of volatile fatty acids (VFAs). VFAs are a product of fermentation of the organics; a process that was likely partially active in the anaerobic anode chamber with few oxidizing agents present. The presence of VFAs would lower the pH. The higher current in MFC#2 allowed for more oxidation of the anolyte and less accumulation of any VFAs, resulting in a higher pH than MFC#1 throughout the experiment. In addition, the pH values observed during system operation were close enough to a neutral pH that biological activity would not be adversely affected.

2.5.5. Ferricyanide

The ferricyanide concentration in the catholyte of MFC#2 was measured throughout the acclimation and carbon dosing periods of the second experiment. Ferricyanide effluent concentrations ranged from 0.34 M to 0.46 M throughout the experiment. The measured feed and effluent concentrations were used to determine the total amount of ferric iron reduced

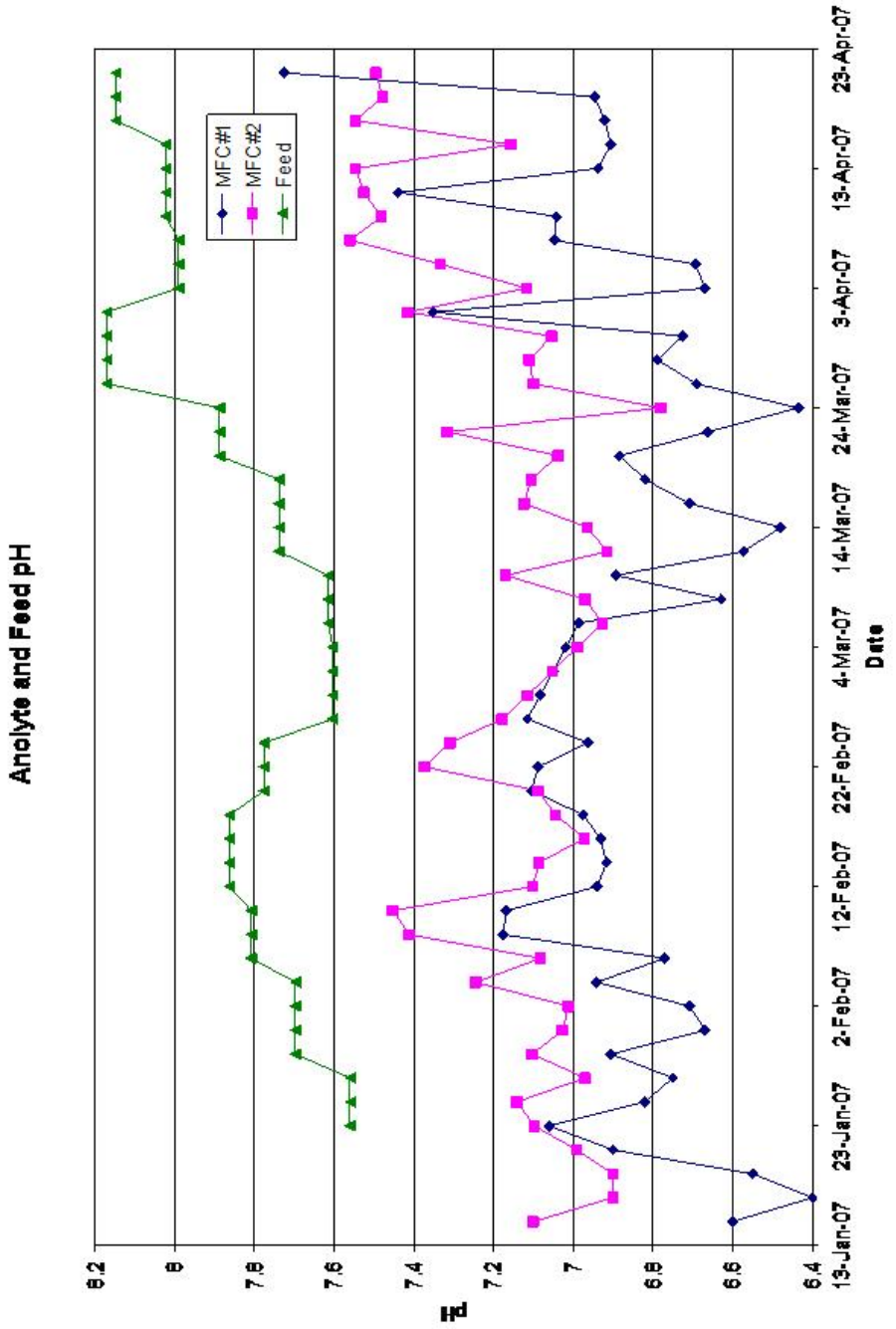

Figure 2.7.: *Anolyte and Feed pH*

to ferrous iron. This value was converted to a COD mass equivalent for comparison to the COD_{Elec} obtained for MFC#2. The value was calculated as 266.4∓911.2 mg with a 95% confidence level. The median value was in good agreement to the value obtained for MFC#2 (Table 2.7) on the basis of the measured current, but the 95% confidence range was significantly greater due to the ferricyanide analysis technique. It was expected that the value calculated from the ferricyanide results may be lower due to the effects of protons and any oxygen content in the ferricyanide catholyte providing an alternate final electron acceptor.

2.5.6. Dissolved Oxygen

The DO of the phosphate buffered catholyte for MFC#1 was measured for the last 40 days of the acclimation period and throughout the carbon dosing period. The results are presented in Figure 2.8.

The DO measurements taken during the first few weeks of the carbon dosing period were not considered reliable, since a recalibration of the DO meter was required. From Figure 2.8, it can be seen that the DO ranged from approximately 45%−85% saturation, or 3−6 mg/L during the acclimation period, while the DO ranged from 35%−75% saturation, or 2−5 mg/L during the carbon dosing period. This coincides with the higher current production observed in MFC#1 during the carbon dosing period. With higher current production, more oxygen would be consumed from solution as electron acceptors. Due to the range and relatively unstable DO measurements, it was difficult to identify a direct relationship outside of this expected theoretical relationship. Also, the wide range of oxygen concentration in MFC#1 introduces an uncertainty in the cathodic effects on coulomb production for MFC#1. A higher oxygen concentration was desired throughout the second experiment to eliminate cathodic influences on MFC#1 performance, but unfortunately, the system was unable to maintain reliable, high oxygen levels.

2.5.7. Head Space Gas

The main result from the head space gas analysis was the COD_{Gas} term, which is reported in Table 2.7 with the COD results. This result was based on an approximated head space volume of 10 mL. Over the course of the second experiment, the volumes of methane produced in order to equal the COD_{Gas} values in Table 2.7 were 56.3∓110.7 mL for MFC#1 and 69.7∓59.0 mL for MFC#2, with a 95% confidence level. These production rates were very

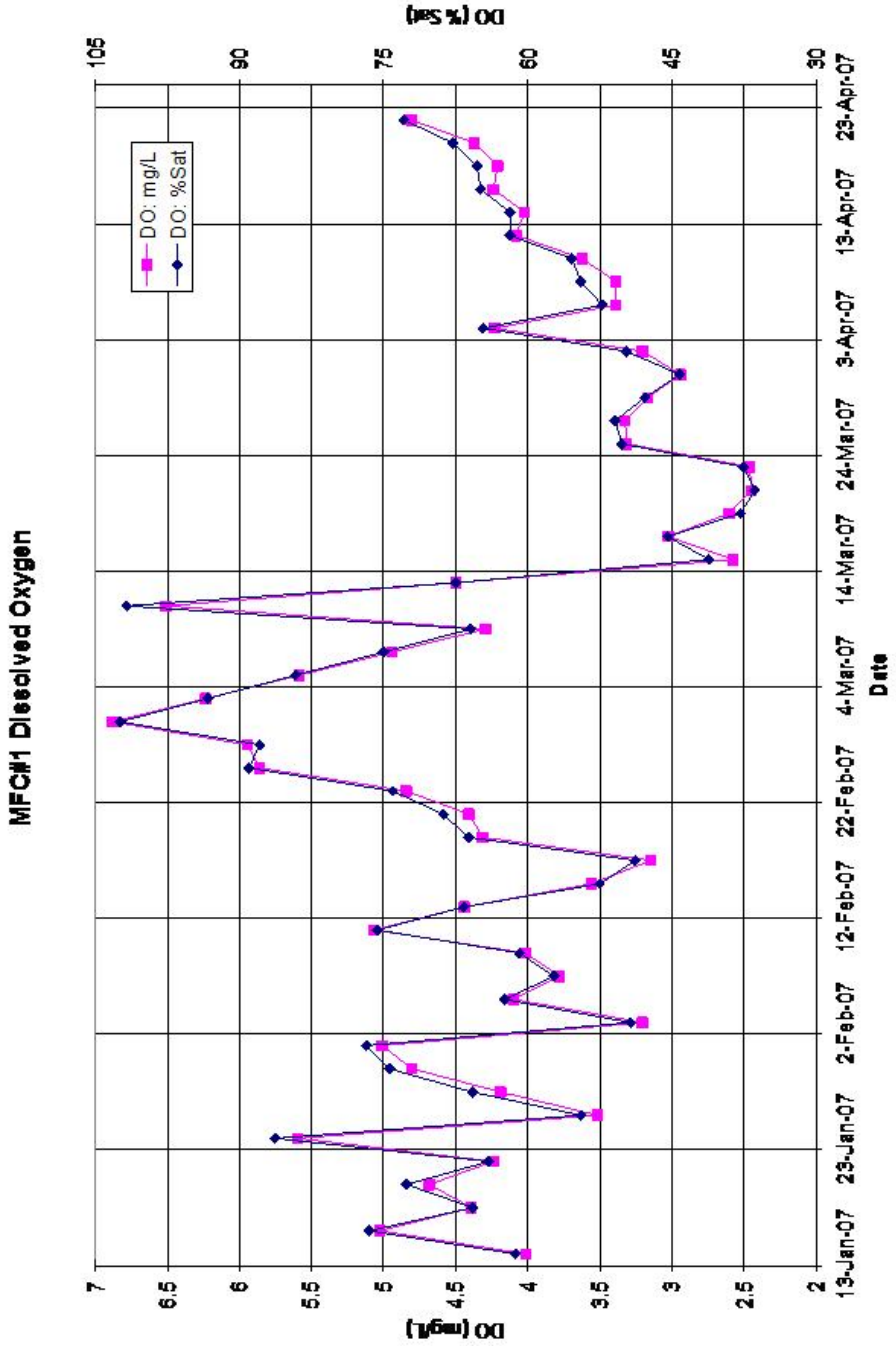

Figure 2.8.: *Dissolved Oxygen Content of MFC#1 Catholyte*

small, and it was assumed that volumetric methane production was very close to negligible. However, as discussed with the COD results, methane production of only 25 mL/day could account for the discrepancy observed between the measured and calculated COD_{Acc} values. If the Tedlar bags were leaking, it is possible that this methane production took place and went unmeasured.

2.6. Conclusions

Two MFCs were operated in parallel successfully for a period of 182 days, or approximately 6 months. The system was operated at a controlled voltage of 0.3V and under a fed-batch sample/feed protocol. Several system variables were measured throughout the experiment: cell voltage, individual MFC current, waste activated sludge feed and wastewater anolyte variables (COD, TKN, FSA, and pH), ferricyanide concentration in MFC#2 catholyte, DO in MFC#1 catholyte, and the head space gas composition. The calculation of current and power densities was performed using two effective surface areas, EESA based on the entire cathode surface area and EMSA based on the Nafion® proton exchange membrane surface area. Power densities of up to 167 mW/m^2 were observed from MFC#2 using the EMSA, while the same power production resulted in a power density of 4.15 mW/m^2 using the EESA. These areas represent upper and lower bounds on the effective surface area. The power density calculated with the EMSA was comparable to reported literature values in similar systems operated with a glucose feed.

A COD balance was calculated for each MFC, which resulted in a COD accumulation term. Measurement of the final accumulation term resulted in an accumulation discrepancy of 11660.8 mg and 10901.1 mg for MFC#1 and MFC#2, respectively. This is in excess of 40% of the overall COD feed to each MFC. It was suggested that the most likely cause for the COD discrepancy was greater methane production than that which was measured. TKN measurements further suggested that particulate matter was accumulating within the system. It was also noted that the addition of BSA appeared to increase the TKN leaving each MFC, as was suspected based on the BSA nitrogen content. The feed and anolyte pH remained relatively close to neutrality, reducing the possibility of pH effects on biological activity in the anode chamber. The change in ferricyanide concentration was consistent with that expected from the measured current in MFC#2. DO measurements generally showed oxygen concentration in the catholyte of MFC#1 to range between 30% and 80% of

saturation. Lower oxygen concentrations were observed during higher current production. Finally, the head space gas analysis indicated the presence of nitrogen, carbon dioxide, and methane, but the overall production of these gases was found to be very low, unless gas phase leakage was prevalent. Methane production represents the suspected discrepancy in the COD balances for each MFC.

References

References marked with an asterisk indicate studies included in the meta-analysis.

Aelterman, P., Rabaey, K., Clauwaert, P., & Verstraete, W. (2006). Microbial fuel cells for wastewater treatment. *Water Science & Technology*, *54*(8), 9-15.

*Bell, S., Foster, G., Fuller, M. W., Hughes, D., Le Brocq, K.-M. F., Leslie, E., et al. (1986). Spectrophotometric measurement of rates of hexacyanoferrate reactions. *International Journal of Chemical Kinetics*, *18*, 651-653.

Bond, D. R., & Lovley, D. R. (2003). Electricity production by *Geobacter sulfurreducens* attached to electrodes. *Applied and Environmental Microbiology*, *69*, 1548-1555.

Cheng, S., Liu, H., & Logan, B. E. (2006a). Increased performance of single-chamber microbial fuel cells using an improved cathode structure. *Electrochemistry Communications*, *8*, 489-494.

Cheng, S., Liu, H., & Logan, B. E. (2006b). Power densities using different cathode catalysts (pt and cotmpp) and polymer binders (nafion and ptfe) in single chamber microbial fuel cells. *Environmental Science and Technology*, *40*(1), 364-369.

*Collins, C. H., Lyne, P. M., & Grange, J. M. (Eds.). (1991). *Microbiological methods* (6th ed.). Butterworth-Heinemann.

*Engenhorst, T. (2006). *Design and characterization of a microbial fuel cell for simultaneous sewage treatment and electricity generation.* (research project at University of Waterloo, submitted as partial fulfilment of the requirements for the degree of Diplom Ing. in Biochemical Engineering)

Gil, G. C., Chang, I. S., Kim, B. H., Kim, M., Jang, J. K., Park, H. S., et al. (2003). Operational parameters affecting the performance of a mediator-less microbial fuel cell. *Biosensors and Bioelectronics*, *18*, 327-334.

*Haselrieder, W. (2005). *Utilization/design of sludge microbial fuel cells for sewage treatment and simultaneous electricity generation.* (research project at University of Waterloo, submitted as partial fulfilment of the requirements for the degree of Diplom Ing. in Biochemical Engineering)

He, Z., Minteer, S. D., & Angenent, L. T. (2005). Electricity generation from artificial wastewater using an upflow microbial fuel cell. *Environmental Science and Technology*, *39*, 5262-5267.

Kim, N., Choi, Y., Jung, S., & Kim, S. (2000). Effect of initial carbon sources on the

performance of microbial fuel cells containing *Proteus vularis*. *Biotechnology and Bioengineering*, *70*(1), 109-114.

Liu, H., & Logan, B. E. (2004). Electricity generation using an air-cathode single chamber microbial fuel cell in the presence and absence of a proton exchange membrane. *Environmental Science & Technology*, *38*(14), 4040-4046.

*Logan, B. E., Hamelers, B., Rozendal, R., Schröder, U., Keller, J., Freguia, S., et al. (2006). Microbial fuel cells: Methodology and technology. *Environmental Science and Technology*, *40*(17), 5181-5192.

Min, B., Kim, J. R., Oh, S. E., Regan, J. M., & Logan, B. E. (2005). Electricity generation from swine wastewater using microbial fuel cells. *Water Research*, *39*, 4961-4968.

Moon, H., Chang, I. S., & Kim, B. H. (2006). Continuous electricity production from artificial wastewater using a mediator-less microbial fuel cell. *Bioresource Technology*, *97*, 621-627.

Oh, S.-E., & Logan, B. E. (2006). Proton exchange membrane and electrode surface areas as factors that affect power generation in microbial fuel cells. *Applied Microbiology and Biotechnology*, *70*(2), 162-169.

Park, D. H., & Zeikus, J. G. (2002). Impact of electrode composition on electricity generation in a single-compartment fuel cell using *Shewanella putrefaciens*. *Applied Microbiology and Biotechnology*, *59*, 58-61.

Ringeisen, B. R., Ray, R., & Little, B. (2007). A miniature microbial fuel cell operating with an aerobic anode chamber. *Journal of Power Sources*, *165*, 591-597.

You, S. J., Zhao, Q. L., Jiang, J. Q., & Zhang, J. N. (2006). Treatment of domestic wastewater with simultaneous electricity generation in microbial fuel cell under continuous operation. *Chemical and Biochemical Engineering Q.*, *20*(4), 407-412.

3. Microbial Community Analysis in MFCs using BIOLOG® ECOplates

Abstract

Microbial fuel cells (MFCs) utilize bacteria to biodegrade organics such as those in wastewaters, and liberate electrons for electricity production. The microorganisms represent a critical component in these complex systems. A better understanding of the microbial community and the impacts of various disturbances is crucial to the future design of commercial level MFC systems. This study used BIOLOG® ECOplates to obtain ecological data on the microbial communities in two separate MFCs. A Taylor power law transform and a natural logarithm transform were applied to the resulting datasets to compare the impact of these transforms on dataset normality, homoscedasticity and the number of linear correlations between variables to these dataset qualities before transformation. While the Taylor power law transform was found to optimize homoscedasticity, the natural logarithm transform was identified as the best choice when evaluating all the dataset parameters. Principal component analysis (PCA) was used to determine the community level physiological profiling (CLPP) of the microbial communities present at different times or under different conditions in the two MFCs. The largest differences were found to exist between microbial communities developed during different experiments and those developed over the course of a four week experiment. The microbial communities in the wastewater anolyte and on the anode surface were not found to differ significantly. Likewise, microbial communities in two separate waste activated sludge samples were found to be similar. The functional diversity of the microbial communities in the MFCs was also evaluated throughout the experiment and was found to decrease over a 28 day period of operation. Further analysis of longer acclimation period impacts and the effects of dosing various carbon sources are discussed in Chapter 4.

Keywords: BIOLOG® ECOplates, Functional Diversity, Microbial Ecology, Microbial Fuel Cell, Principal Component Analysis

3.1. Introduction

As with most biological systems, it is desirable to identify the microorganisms present in the anodic chambers of microbial fuel cells (MFCs). Unfortunately, identification of each type of microorganism present would be both resource intensive and time consuming. As an alternative, community level physiological profiling (CLPP) through the use of BIOLOG® ECOplates allows the characterization of the microbial community as a whole. If the characteristics of the community rather than the individual microorganisms is of greater interest and potential application in future research, then the use of ECOplates for CLPP provides a relatively quick and simple way to obtain this information. Ecological stability and community response to disturbances are of particular interest in both natural and engineered environments such as the anodic chambers of MFCs, as these may be indications of overall system performance or potential failure.

ECOplates were introduced to address systems where the community level profile is of greater interest than that of individual microorganisms. The ECOplates provide a large ecological dataset based on the microbial metabolism of a mixed culture. The dataset represents a series of responses based on the growth of microbe populations on 31 carbon sources contained in the ECOplate wells. The 31 carbon sources are the variables contained in the ECOplate dataset. These variables can be interdependent because some of the carbon sources in the ECOplate are similar or are metabolized in a similar manner. This interdependency makes the dataset analysis particularly difficult. One solution to this analytical predicament is the use of multivariate data analysis techniques.

When using multivariate analysis techniques, there are two constraints to which the dataset should adhere. These constraints are homoscedasticity, which is a measure of the equivalence of variance of each variable, and a normal distribution of the data. Of particular interest to this study is principal component analysis (PCA). PCA linearly combines the variables in the dataset into principal components, preserving the maximum amount of the original dataset variance for each variable through an eigenanalysis. The first two principal components contain the greatest percentage of the original dataset variance and are used in the principal component analysis. Two more dataset constraints arise with the use of PCA. It is necessary to ensure that the variables within the dataset are linearly correlated, since PCA is based on linear combinations. In addition, the number of objects should be

greater than the number of variables in the dataset. An object is represented by one value for each of the variables. In this study, each ECOplate contained triplicate results for each carbon source. Therefore, each ECOplate provided 3 objects in the associated dataset. Data collection limitations often make it difficult to ensure that the number of objects is greater than the number of variables. However, the results from the PCA will not be significantly affected if they are drawn from the first two principal components (Legendre & Legendre, 1998). The analysis employed in this study utilized only the first two principal components, so this particular constraint on PCA was ignored.

The BIOLOG® ECOplate is used for microbial community analysis and CLPP from the environment. It consists of 96 wells, containing 31 different carbon sources and a blank, all in triplicate. A tetrazolium violet dye is present in each well as a redox indicator, which changes colour in response to carbon utilization. Hence, optical density (OD) measurements are carried out on the ECOplate to identify growth on a substrate. Earlier BIOLOG® microplates contained 96 different carbon sources in the wells, lacking the single plate replicate system added to the ECOplates. BIOLOG® plates and ECOplates in conjunction with PCA have been used in several recent microbial ecology studies (Garland & Mills, 1991; Garland, 1996; Franklin, Garland, Bolster, & Mills, 2001; Garland, Mills, & Young, 2001; Grove, Kautola, Javadpour, Moo-Young, & Anderson, 2004; Weber, 2006). ECOplates and PCA were used by Grove *et al*, (2004) to profile laboratory biofilters and Weber *et al*, (2006) to profile laboratory wetland mesocosms.

Weber *et al*, (2006) transformed the data before PCA was applied to an ecological dataset obtained from BIOLOG® ECOplates. The PCA constraints of dataset homoscedasticity and normality as well as linearly correlated variables were calculated and compared for transformed and and untransformed datasets. Only the first two principal components were used, so the constraint of the number of objects being greater than the number of variables was also ignored in this study.

In this chapter, the use of BIOLOG® ECOplates and PCA for the analysis of MFC microbial ecology datasets is presented. An approach similar to Weber *et al*, (2006) was used before PCA was performed. The homoscedasticity, normality, and number of linear correlations between variables were compared for transformed and untransformed data in order to

evaluate the effectiveness of the data transforms. The data are drawn from 16 ECOplates that were obtained across two separate experiments. An anaerobic sampling procedure for the wastewater anolyte was developed to ensure that the wastewater anolyte remained under anaerobic conditions before and during data collection. The ECOplates for the second experiment were prepared at intervals that permitted evaluation of the MFC microbial ecology before and after selected carbon sources were added to the system. Bulk wastewater anolyte samples and samples scraped from the anode surface were compared, and a comparison of MFC innoculant samples from the beginning of each experiment is also presented. In addition, the ECOplate variables, represented by the 31 carbon sources in the ECOplate wells, were classified based on their associated organic chemistry. PCA results are presented for transformed ECOplate datasets containing all variables as well as variable subsets, which represent the specific carbon source subset classifications. Chapter 4 details the microbial ecology and operational performance of the two MFCs used throughout the second study in this research.

3.2. Materials and Experimental Methods

The materials and experimental methods are divided into five sections. The MFC system is presented first followed by the BIOLOG® ECOplates, ECOplate experimental design, carbon source pulse tests (CSPTs), and finally, the anaerobic procedure. The anaerobic sampling procedure is presented in detail in Appendix B. The ECOplate and data analysis procedures are presented in Section 3.3.

3.2.1. Microbial Fuel Cell (MFC) System

The MFC system design and operation are essential to the overall experimental design, anaerobic sampling procedure, and associated ecological data. Chapter 2 presents a detailed account of the system design and operation.

3.2.2. BIOLOG® ECOplates

BIOLOG® ECOplates (BIOLOG Inc., Hayward CA., USA) were used to obtain ecological data for the community level physiological profiling (CLPP) of anolyte samples drawn from the two MFCs. The ECOplates consist of 96 wells containing 31 carbon sources and a blank in triplicate. Each of the wells was inoculated with 100μL of diluted and homogenized

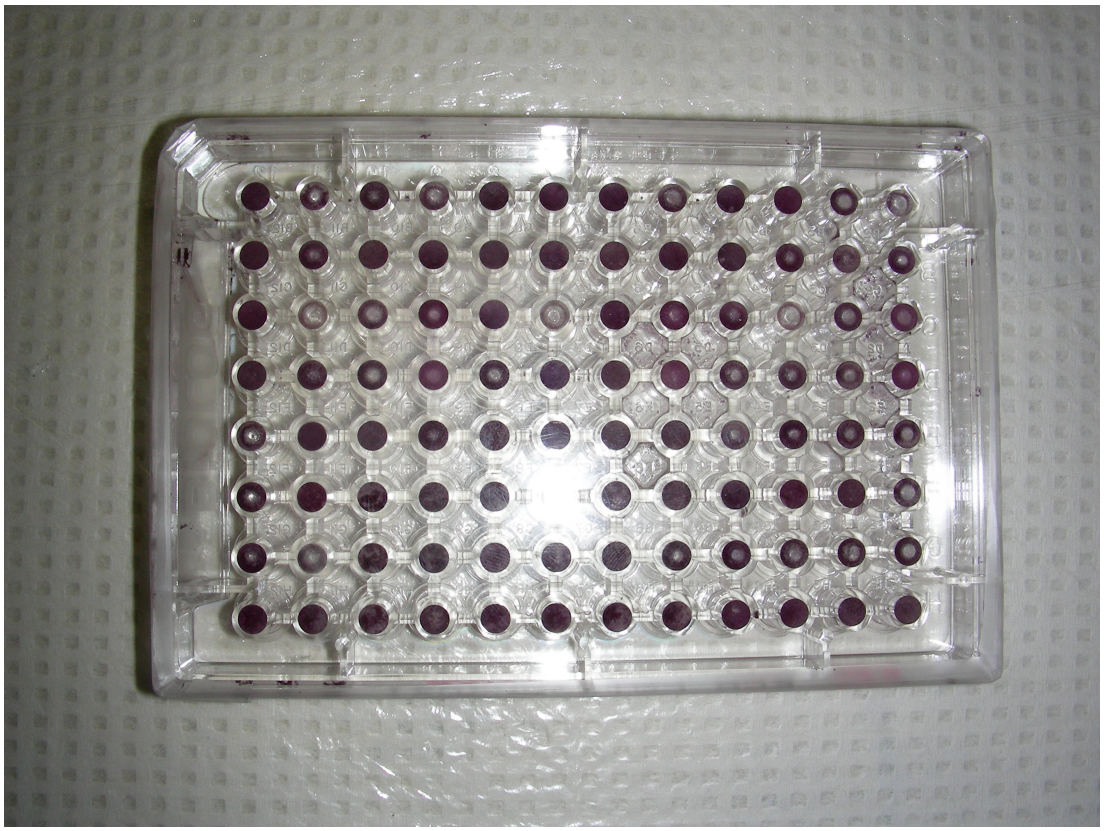

Figure 3.1.: *BIOLOG® ECOplate 42 hours post inoculation*

anolyte. Optical density (OD) or absorbance readings at 590nm were taken every hour for 42 hours with a microplate reader (Molecular Devices, VERSAmax tunable microplate reader). The data were recorded using a lab computer and the SOFTmax PRO 3.1.1 software. The anaerobic anolyte sampling technique is outlined at the end of this section while the ECOplate analysis during anaerobic incubation is described in Section 3.3.1. Figure 3.1 shows a BIOLOG® ECOplate after 42 hours of OD measurements. Figure 3.2 is a carbon source legend for the BIOLOG® ECOplates (BIOLOG, 2007).

The carbon sources in Figure 3.2 were labeled as c0 through c31 for ease of reference and subsequent carbon source classification. From Figure 3.2, carbon source A1, which represents the blank well, was designated as c0 and labeling continued from left to right. Only the first 4 columns were labeled, since the last 8 columns in the ECOplate were replicates for the carbon sources in the first 4 columns and would have the same associated label. For example,

A1 Water	A2 β-Methyl-D-Glucoside	A3 D-Galactonic Acid γ-Lactone	A4 L-Arginine	A1 Water	A2 β-Methyl-D-Glucoside	A3 D-Galactonic Acid γ-Lactone	A4 L-Arginine	A1 Water	A2 β-Methyl-D-Glucoside	A3 D-Galactonic Acid γ-Lactone	A4 L-Arginine
B1 Pyruvic Acid Methyl Ester	B2 D-Xylose	B3 D-Galacturonic Acid	B4 L-Asparagine	B1 Pyruvic Acid Methyl Ester	B2 D-Xylose	B3 D-Galacturonic Acid	B4 L-Asparagine	B1 Pyruvic Acid Methyl Ester	B2 D-Xylose	B3 D-Galacturonic Acid	B4 L-Asparagine
C1 Tween 40	C2 i-Erythritol	C3 2-Hydroxy Benzoic Acid	C4 L-Phenylalanine	C1 Tween 40	C2 i-Erythritol	C3 2-Hydroxy Benzoic Acid	C4 L-Phenylalanine	C1 Tween 40	C2 i-Erythritol	C3 2-Hydroxy Benzoic Acid	C4 L-Phenylalanine
D1 Tween 80	D2 D-Mannitol	D3 4-Hydroxy Benzoic Acid	D4 L-Serine	D1 Tween 80	D2 D-Mannitol	D3 4-Hydroxy Benzoic Acid	D4 L-Serine	D1 Tween 80	D2 D-Mannitol	D3 4-Hydroxy Benzoic Acid	D4 L-Serine
E1 α-Cyclodextrin	E2 N-Acetyl-D-Glucosamine	E3 γ-Hydroxybutyric Acid	E4 L-Threonine	E1 α-Cyclodextrin	E2 N-Acetyl-D-Glucosamine	E3 γ-Hydroxybutyric Acid	E4 L-Threonine	E1 α-Cyclodextrin	E2 N-Acetyl-D-Glucosamine	E3 γ-Hydroxybutyric Acid	E4 L-Threonine
F1 Glycogen	F2 D-Glucosaminic Acid	F3 Itaconic Acid	F4 Glycyl-L-Glutamic Acid	F1 Glycogen	F2 D-Glucosaminic Acid	F3 Itaconic Acid	F4 Glycyl-L-Glutamic Acid	F1 Glycogen	F2 D-Glucosaminic Acid	F3 Itaconic Acid	F4 Glycyl-L-Glutamic Acid
G1 D-Cellobiose	G2 Glucose-1-Phosphate	G3 α-Ketobutyric Acid	G4 Phenylethyl-amine	G1 D-Cellobiose	G2 Glucose-1-Phosphate	G3 α-Ketobutyric Acid	G4 Phenylethyl-amine	G1 D-Cellobiose	G2 Glucose-1-Phosphate	G3 α-Ketobutyric Acid	G4 Phenylethyl-amine
H1 α-D-Lactose	H2 D,L-α-Glycerol Phosphate	H3 D-Malic Acid	H4 Putrescine	H1 α-D-Lactose	H2 D,L-α-Glycerol Phosphate	H3 D-Malic Acid	H4 Putrescine	H1 α-D-Lactose	H2 D,L-α-Glycerol Phosphate	H3 D-Malic Acid	H4 Putrescine

Figure 3.2.: *Carbon Source Legend for the BIOLOG® ECOplate*

itaconic acid, shown as F3 in Figure 3.2, was labeled as c22. A classification system was developed to create carbon source variable subsets for further PCA (Zak, Willig, Moorhead, & Wildman, 1994). The carbon sources were divided into 4 subgroups based on their general organic chemistry. The subsets are presented in Table 3.1 below:

Table 3.1.: *BIOLOG® ECOplate Carbon Source Subset Classifications*

Classification	Carbon Sources
Carbohydrates	c1,c5,c9,c13,c17,c24,c28
Carboxylic Acids	c2,c4,c6,c10,c14,c18,c21,c22,c26,c30
Polymers & Miscellaneous	c8,c12,c16,c20,c25,c29
Amines & Amino Acids	c3,c7,c11,c15,c19,c23,c27,c31

3.2.3. ECOplate Experimental Design

A total of 16 ECOplates were prepared over the duration of two experiments with the MFCs. During the first experiment, ECOplates were only prepared from MFC#2, which operated with a ferricyanide catholyte. The purpose of conducting the ECOplate testing in the first experiment was to evaluate the difference between bulk anolyte samples and anode scraping samples. During the second experiment, ECOplates were prepared from both of the MFCs.

The purpose of the ECOplate testing in the second experiment was to evaluate the changes in microbial ecology over time during system acclimation and after the carbon source pulse tests (CSPTs). Table 3.2 outlines the ECOplate sampling timeline and experimental design significance. Table 3.3 presents the ECOplate case organization for PCA.

Table 3.2.: *ECOplate Preparation Timeline*

ECOplate #	Date Prepared	Design Significance
Experiment#1		
1	October 17, 2006	1st Experiment Initial Feed
2	October 30, 2006	Centrepoint Bulk Solution
3	November 1, 2006	Centrepoint Anode Scraping
4	November 11, 2006	Endpoint Bulk Solution
5	November 13, 2006	Endpoint Anode Scraping
Experiment#2		
6	December 5, 2006	2nd Experiment Initial Feed
7	February 15, 2007	MFC#1 Steady State Operation
8	February 20, 2007	MFC#2 Steady State Operation
9	March 5, 2007	MFC#1 Post Sodium Acetate Dosing
10	March 7, 2007	MFC#2 Post Sodium Acetate Dosing
11	March 19, 2007	MFC#1 Post Glucose Dosing
12	March 21, 2007	MFC#2 Post Glucose Dosing
13	April 2, 2007	MFC#1 Post Glycerol Dosing
14	April 4, 2007	MFC#2 Post Glycerol Dosing
15	April 16, 2007	MFC#1 Post Bovine Serum Albumin Dosing
16	April 18, 2007	MFC#2 Post Bovine Serum Albumin Dosing

Table 3.3.: *ECOplate Case Organization for PCA*

Case #	ECOplates Used	Comparison Significance
1.0	All	Entire ECOplate Set Comparison
2.0	2,3,4,5	Bulk Solution vs. Anode Scraping Samples
3.0	1,4	Inoculant vs Endpoint (Experiment #1)
4.0	1,6	Inoculants Comparison
5.0	6,7,8	Inoculant vs Steady States (Experiment #2)
6.0	7,8,9,10	Pre and Post Sodium Acetate Comparison (both MFCs)
7.0	9,10,11,12	Pre and Post Glucose Comparison (both MFCs)
8.0	11,12,13,14	Pre and Post Glycerol Comparison (both MFCs)
9.0	13,14,15,16	Pre and Post BSA* Comparison (both MFCs)

*Bovine Serum Albumin

A total of 4 sub-cases were developed for each of the cases in Table 3.3 based on the variable subsets presented in Table 3.1. All first sub-cases were based on the carbohydrate variable subset and were designated as Case #x.1. Similarly for the other three variable subsets,

sub-cases #x.2, #x.3 and #x.4 were designated for carboxylic acids, polymers/miscellaneous and amines/amino acids, respectively.

3.2.4. Carbon Source Pulse Tests (CSPTs)

The CSPTs involved the injection of a known chemical oxygen demand (COD) equivalence of a simple carbon source. The CSPTs took place after the MFCs had reached operational steady state with respect to current production. There were a total of 4 substances included in the CSPTs. Table 3.4 outlines these substances, in addition to the COD equivalent mass of each substance added, and their solution preparation.

Table 3.4.: *Carbon Source Pulse Test Substances*

Substance	COD Mass per Pulse (mg)	Solution Preparation
Sodium Acetate	50 (1 pulse) 2.857 (3 pulses)	2.44137 g per 100 mL DI 1 mL above solution to 16.5 mL DI
Glucose	2.857 (4 pulses)	0.08928 g per 100 mL DI
Glycerol	2.857 (4 pulses)	0.07831 g (0.0621 mL) per 100 mL DI
Bovine Serum Albumin (BSA)	2.857 (4 pulses)	0.06806 g per 100 mL DI

The choice of substances used in the CSPTs was based on several factors. Simple substances were desired to minimize the microbial response time required before utilization could occur. Considering the anaerobic environment that was maintained in the anode chambers of each MFC, the substances were chosen based on their categorization in anaerobic digestion processes. Acetate as sodium acetate represented a low molecular weight volatile fatty acid, which is a typical intermediate in anaerobic digestion processes. Acetate is also utilized by some methanogens to produce methane and carbon dioxide. Glucose represented a simple sugar or carbohydrate, while glycerol represented a lipid and bovine serum albumin (BSA) represented a protein. In an anaerobic environment, each of these three carbon sources would be biodegraded to simpler substances including organic acids, alcohols, ketones, carbon dioxide and hydrogen. While all three are similarly utilized by bacteria, they each represent a particular classification of substrate: carbohydrate, lipid and protein.

The steps involved in the CSPTs are listed below:

1. prepare each carbon source solution beforehand

2. withdraw 3 mL from the prepared solutions with syringe
3. inject carbon source solution into anode chamber via multi-functional, 1/2 inch NPT port in MFC lid, plug with rubber cap during MFC operation and throughout CSPT

The act of injecting the carbon source solution was called a 'pulse'. Each carbon source was pulsed four times. The pulses were spaced between sample/feed procedures, taking place every 48 ∓ 3 hours. Once the fourth pulse was completed, the MFCs continued to operate for $2-4$ days before samples were taken for the ECOplate analyses. An ECOplate was prepared for each MFC, before and after the set of 4 pulses was completed for each carbon source.

The first CSPT of sodium acetate had a COD equivalency of 50 mg COD. This value was chosen based on the soluble COD levels observed in the feed waste activated sludge. However, following this first pulse of sodium acetate, a period of higher current production was observed for both MFCs. The higher current levels were observed for almost 4 days. Subsequent CSPTs were performed with a COD equivalency of approximately 2.857 mg COD to avoid confounding electrical results from the CSPTs with regular sampling and feeding performed every 48 ∓ 3 hours. These levels of COD addition were less than 2% of the feed waste activated sludge COD addition levels. When considering the impact of the CSPTs on the CLPP and the microbial ecology as a whole, the very low COD dosage levels suggest responses were more likely due to microbial activity shifts rather than a shift in the microbial population.

3.2.5. Anaerobic Sampling

As part of the experimental design, anaerobic conditions were maintained for the anolyte during sampling, ECOplate inoculation and analysis. If strict anaerobes comprised a significant portion of the viable and active biological community, oxygen exposure would be toxic and would have significant effects on the microbial community. The steps to the anaerobic sampling procedure are outlined below:

1. gather equipment, ECOplate and MFC and place in the glove bag
2. establish anaerobic environment in the glove bag using nitrogen gas
3. collect an anolyte sample, dilute with buffer solution (4 parts buffer solution to 1 part anolyte sample) and manually homogenize with a Potter Elvehejm Homogenizer

4. measure the OD_{590} of the homogenized solution, repeat the previous step if the OD value is greater than 0.35 (dilution level may vary)

5. once homogenized solution has OD reading of 0.25−0.35 at a wavelength of 590nm, plate out the resulting solution on the ECOplate

6. seal the ECOplate by placing the ECOplate lid on the ECOplate and taping the edge

7. open the glove bag to atmosphere and immediately transfer the sealed ECOplate to the microplate reader for analysis

3.3. Analysis

The description of the analytical procedures is divided into six sub-sections. The first section outlines the optical density (OD) measurement procedure, which is presented in greater detail in Appendix C. Once ECOplate data were collected, the time point determination was carried out, followed by the data transformations. These transformations were evaluated against each other and the set of untransformed data based upon the statistical constraints placed on PCA: normality, homoscedasticity and linear correlation of variables. The natural logarithm transform was found to be optimal, and PCA was performed on these transformed datasets to produce ordinate plots for the determination of CLPP. From Table 3.3, only cases 1.0 to 4.0 with the associated sub-cases are presented and discussed in Section 3.4. Finally, ECOplate data were used in a series of ecological tests to determine the functional diversity of the microbial community in the samples. The results of these analyses for ECOplates 1 through 5 are presented and discussed in Section 3.4

3.3.1. Kinetic Optical Density (OD) Measurements

Once the ECOplate was prepared anaerobically, the OD analysis was carried out. During ECOplate analysis, the ECOplate remained sealed with optical density (OD) readings taken through the microplate lid. A VERSAmax tunable microplate reader was used to take OD readings at 590nm every hour for 42 hours. The ECOplate was incubated at 37°C during OD measurements. The SOFTmax PRO 3.1.1 software allowed for automation of these readings and recording of the ECOplate OD measurements for each timepoint into a text file. The maintenance of an anaerobic environment and continued incubation during analysis was a

novel application of the BIOLOG® ECOplates.

The overall dataset consisted of 43 readings for each of 16 ECOplates, each with 96 OD readings for the ECOplate wells. This resulted in over 66000 data points. The first step in data treatment was time point determination. The choice of a single time point for ECOplate analysis and latter comparisons reduced the dataset by a factor of 43.

3.3.2. Time Point Determination

It was recommended by Garland (1996) that a single time point be used for well comparisons between microplates (Weber, 2006). Also, the use of a single, but optimal, time point reduces the analytical workload by a factor equal to the number of time points measured while preserving a maximum amount of the variance in the dataset. The determination of the time point required preliminary numerical analysis. The standard deviation values of the 96 well OD readings at each time point for each ECOplate were calculated. The number of well OD readings greater than 2 was also calculated at each time point for each ECOplate. These values were used to determine which time point or range of time points for each ECOplate met the following criteria:

1. maximization of the variance between the 96 well OD readings measured at a time point
2. minimization of the number of well OD readings greater than 2

The maximum OD reading of 2 represents the upper boundary of absorbance values that maintain a linear correlation with carbon source utilization in the ECOplate wells. Using these criteria, a range of optimal time points were identified for each ECOplate. An overall optimal time point of 23 hours was chosen as the comparison point used in this study.

3.3.3. Data Transforms

Following the time point determination, data pretreatment was performed. The data in each ECOplate was normalized by the average well colour development (AWCD) of the respective plate (Weber, 2006; Garland, 1996). Each OD measurement was also adjusted by the blank OD measurement, which represented a zero value on the OD measurement scale. Equation 3.1 illustrates this data pretreatment.

$$\overline{A_k} = \frac{A_k - A_0}{\sum_{i=1}^{31}(A_i - A_0)} \tag{3.1}$$

Where,
$\overline{A_k}$: pretreated OD reading of well 'k'
A_k: OD reading of well 'k'
A_0: corresponding OD reading of the blank well on the ECOplate containing well 'k'
A_i: corresponding OD readings of the wells for each of the 31 carbon sources on the ECOplate containing well 'k'

This data pretreatment helps to eliminate any biases of the original data due to well inoculation variability, allowing later PCA to be based on carbon source utilization differences. Another pretreatment step recommended by Garland (1996) follows data normalization. All pretreated OD values that were below zero were set to zero. Any well with a negative OD value relative to the blank of zero was considered non-responsive, and equivalent to the blank. Negative OD readings can make PCA results difficult to interpret for the purpose of CLPP.

Similar to Weber *et al* (2006), following data pretreatment, the data was subjected to either no transformation, a Taylor power law transformation, and a natural logarithm transformation. These two transformations chosen by Weber *et al* (Weber2006) are common in the analysis of ecological data and were considered equally valid for the MFC ecological data. The Taylor power law transformation is used to increase the homoscedasticity and the normality of a dataset (Legendre & Legendre, 1998). Equation 3.2 presents the fundamental assumption of the Taylor power law transformation. By taking the logarithm of each term in Equation 3.2, Equation 3.3 was derived. A plot of the logarithm of carbon source variances versus the logarithm of carbon source means allows for the determination of the Taylor transform slope, 'b'. The determination of the Taylor transform slope was the required element for the application of the Taylor power law transformation. Equations 3.4 and 3.5 represent the transforms applied to the pretreated data subject to a single constraint on the value Taylor transform slope.

$$S^2 \;=\; a\,\overline{y}^{b} \tag{3.2}$$

Where,
S^2: variance of a sample variable/carbon source
$\overline{y}$: mean of a sample variable/carbon source
a: sampling factor
b: Taylor transform slope
Note: Each variance and mean value was obtained from data for a single carbon source across the ECOplates applicable to the case being analyzed

$$log(S^2) \;=\; log(a) \;+\; b \cdot log(\overline{y}) \tag{3.3}$$

$$\overline{A_k}' \;=\; \overline{A_k}^{(1\,-\,b/2)} \qquad\qquad where\ b \;\neq 2 \tag{3.4}$$

Where,
$\overline{A_k}'$: transformed and pretreated OD reading of well 'k'

$$\overline{A_k}' \;=\; ln(\overline{A_k}) \qquad\qquad where\ b \;=\; 2 \tag{3.5}$$

The natural logarithm transform is often used to normalize skewed datasets (Legendre & Legendre, 1998). Equation 3.6 represents the natural logarithm transform used in this study.

$$\overline{A_k}' \;=\; ln(\overline{A_k} \;+\; 1) \tag{3.6}$$

3.3.4. Statistical Constraint Diagnostics

The Taylor power law and natural logarithm transformed datasets were evaluated against each other and the non-transformed dataset. The datasets for each case defined in Table 3.3 were each evaluated to ensure that the use of PCA was applicable to the datasets of each

case. As discussed earlier, PCA is subject to several statistical constraints. The transformed and pre-treated datasets were evaluated based on diagnostics of these statistical constraints. The statistical constraints are:

1. homogeneity of variance or homoscedasticity
2. normality of data
3. linear correlations between variables/carbon sources

Although it is difficult to evaluate homogeneity of variance, the ratio of the highest variance to lowest variance was chosen for this study (Weber, 2006). Equation 3.7 illustrates the variance ratio as it was determined for each dataset. The ratio was calculated by dividing the greatest variance found for a carbon source in a dataset by the least variance found for a carbon source in the same dataset.

$$VarianceRatio = \frac{Var_{high}}{Var_{low}} \tag{3.7}$$

Where,
Variance Ratio = ratio of greatest variable variance to least variable variance within a dataset
Var_{high} = the greatest variance in a dataset, associated with one variable
Var_{low} = the least variance in a dataset, associated with one variable

The variance ratio approaches the desired value of one for complete variance homogeniety, but increases as the difference between the variances increases. However, there is a weakness in this evaluation when there is a consistent response in one variable, since the variance is zero. The resulting variance ratio is always infinity regardless of how close to zero the greatest variance value is. In addition, variables with no response are not included in the PCA. To address this, the definition of the least variance was adapted to:

Var_{low} = the least **non-zero**, variance in a dataset, associated with one variable

While this may appear to be an erroneous method to increase homoscedasticity, it should be recognized that the variable or carbon source with zero variance in the dataset was not included in subsequent PCA. In fact, a non-zero variance is required of every variable in PCA

in order to complete the eigenanalysis and define the principal components. Therefore, the removal of zero variances from datasets before homoscedasticity evaluation had no impact on the applicability of PCA to these datasets.

The normality of the pretreated and transformed datasets in this study were evaluated using a series of statistical tests. The kurtosis of the datasets characterizes the peakedness or flatness of the distribution relative to a normal distribution. A positive kurtosis indicates more peakedness while a negative value relates to a flatter distribution. The skewness of the datasets characterizes the asymmetry of the distributions around their means. A positive skewness indicates an asymmetric tail in the distribution, extending toward positive values. A negative skewness indicates the same asymmetry in the distribution, but toward negative values. Kurtosis and skewness were calculated using predefined equations in Microsoft Excel.

The standard error for the kurtosis and skewness was needed to complete the diagnostics. Equations 3.8 and 3.9 represent the standard error for kurtosis and skewness, respectively.

$$SE_{kurtosis} = \sqrt{\frac{24}{n}} \tag{3.8}$$

Where,
$SE_{kurtosis}$ = the standard error of the kurtosis
n = the number data points within a dataset or data subset

$$SE_{skewness} = \sqrt{\frac{6}{n}} \tag{3.9}$$

Where,
$SE_{skewness}$ = the standard error of the skewness

Statistical methods for the diagnostic tests require a z-value to determine normality at a 95% confidence level. Z-values for the kurtosis and skewness of the datasets were calculated from Equations 3.10 and 3.11.

$$z_{kurtosis} = \frac{kurtosis}{SE_{kurtosis}} \tag{3.10}$$

Where,
$z_{kurtosis}$ = the z-value of the kurtosis
kurtosis = the kurtosis of the dataset

$$z_{skewness} = \frac{skewness}{SE_{skewness}} \tag{3.11}$$

Where,
$z_{skewness}$ = the z-value of the skewness
skewness = the skewness of the dataset

The data was considered normally distributed if the absolute values of the $z_{kurtosis}$ and $z_{skewness}$ were less than 1.96 for a 95% confidence level. Optimally conditioned datasets would contain most of the z-values close to or equal to zero.

Two methods were used to determine the normality of the datasets, following the procedure of Weber *et al*, (2006). In the first method, the averages of the absolute values for the kurtosis and skewness of each of the 31 variables or carbon sources were used to determine a $z_{kurtosis}$ and $z_{skewness}$. In the second method, the kurtosis and skewness values for all of the 31 variables or carbon sources were used to calculate a $z_{kurtosis}$ and $z_{skewness}$ for each of the 31 variables. All of these z-values were evaluated at the 95% confidence level and the number of signifcantly normal z-values for each full dataset were compared.

Finally, the correlation between variables was evaluated for linearity using a correlation matrix for the 31 variables or carbon sources. If the absolute value of the correlation coefficient was greater than the Pearson's critical r-value, the two variables were considered linearly correlated with a 95% confidence level. Pearson's critical r-values were chosen based on the number of observations or objects that constitute the dataset. The total number of linearly correlated variables was calculated, and this value was used as a comparitive basis between the pretreated and transformed data, where more linearly correlated variables was favoured.

3.3.5. Principal Component Analysis (PCA)

PCA is a multivariate analysis technique based on the eigenanalysis of an R-mode, variance-covariance matrix. PCA is used with datasets in higher dimensional spaces by ordinating objects from the dataset on a 2-dimensional plane, while preserving the maximum amount of variance contained in the dataset. This leads to the determination of any shifts or differences between samples or objects based on the number of variables (Legendre & Legendre, 1998) Within this study, the carbon sources were the variables, constituting a 31 dimensional space. The objects for PCA were the ECOplate well replicate sets. Therefore, each ECOplate consisted of three objects, since there were triplicate sets of carbon source on each ECOplate. The result of performing PCA is the ordination of the dataset objects on a 2-dimensional space for visual analysis. The first two principal components, or eigenvectors, were used throughout the PCA of the datasets in this study. As mentioned earlier, this minimizes the impact of having fewer objects than variables, which was true for most of the analyzed cases. Typically, 40% to 80% of the original dataset variance are contained within the first two principal component axes. Based on these properties and the recommendations of Garland (1996), PCA was used to analyze the ECOplate datasets from this study.

3.3.6. Functional Diversity

The data from the BIOLOG® ECOplates were also subjected to another analysis to evaluate the functional diversity of the samples, as suggested by Zak *et al* (1994). Weber *et al* (2006) carried out a similar analysis using ECOplates as compared to the BIOLOG®gram negative and gram positive microplates used by Zak *et al* (1994). Zak *et al* (1994) also defined functional diversity as the "numbers, types, activities, and rates at which a suite of substrates are utilized by the bacterial community". The ECOplate preparation timeline presented earlier in Table 3.2 provided the samples for the functional diversity analysis. Each ECOplate was evaluated for the functional diversity indices: substrate diversity, substrate richness and substrate evenness.

The term 'substrate diversity' was used because the ECOplate data represented substrate utilization patterns rather than microbial colony direct counts from inoculated nutrient agar plates. Substrate diversity (H) was calculated from Equation 3.12, as derived by Weber *et al* (Weber2006):

$$H = -\sum p_i \cdot ln(p_i) \tag{3.12}$$

Where,
p_i = ratio of the pretreated OD reading of a particular substrate to the sum of the pretreated OD readings of all substrates

The substrate richness (S) equals the number of different substrates utilized by the microbial community within the sample. As there are a maximum of 31 carbon source substrates in the ECOplates, the substrate richness values for this study were integers bounded by 0 and 31. A substrate was considered utilized if the pretreated optical density value was greater than 0.25. The substrate evenness is defined as the equitability of activities across all utilized substrates. Substrate evenness (E) is calculated from Equation 3.13, as derived by Weber *et al* (2006):

$$E = H/log(S) \tag{3.13}$$

The inherent triplicates in the pretreated ECOplate data was analyzed using the above equations, and an average substrate diversity, evenness and richness was calculated for each ECOplate. The substrate diversity, richness and evenness was normalized to the first ECOplate of each experiment to allow for normalized comparison. Therefore, ECOplates 1 through 5 were normalized to ECOplate 1, while ECOplates 6 through 16 were normalized to ECOplate 6.

3.4. Results and Discussion

The presentation and discussion of results is separated into three sub-sections. The pretreated and transformed datasets are compared and evaluated using the statistical constraint diagnostics outlined in Section 3.3.4. The natural logarithm transformed dataset was found to be optimal. PCA was performed on this dataset using the cases outlined in Table 3.3 and the sub-cases discussed in Section 3.2.3. Finally, the functional diversity was evaluated for each ECOplate.

3.4.1. Data Transformations and Statistical Diagnostics

Tables 3.5 through 3.13 present the statistical constraint diagnostic results for each of the 9 cases outlined in Table 3.3. Each case compares the pretreated (no transform) dataset, the Taylor power law transformed dataset and the natural logarithm transformed dataset. The diagnostics were performed on the full datasets, inclusive of all carbon source variables. No statistical diagnostics were performed on the data subsets used in the sub-cases. It was important to perform these diagnostics on the datasets in each case to ensure that PCA was applicable to each case being analyzed. The optimal 'average z-value of the kurtosis and skewness' value is 0, while the optimal '# of significant kurtosis and skewness z-values' value is 31. This would represent an ideal normal distribution. The optimal '# of linear correlations' value is 465, while the optimal 'variance ratio' is 1. This variance ratio would result in an ideal homoscedasticity, where each variable had an equal variance and equal impact on the PCA.

Table 3.5.: *Case 1 Statistical Constraint Diagnostics Results*

Diagnostic Test	Pretreated (No Transform)	Taylor Power Transform	Ln Transform
Average Kurtosis z-value	2.98	3.41	1.85
# of Significant Kurtosis Values	14	16	21
Average Skewness z-value	3.04	-2.65	1.29
# of Significant Skewness Values	14	6	11
# of Linear Correlations	239	262	249
Variance Ratio	1063	14.9	58.5

All of the ECOplates were used when evaluating the statistical diagnostics presented in Table 3.5 for Case 1.0 The z-value for both the kurtosis and skewness of the pretreated data was greater than 1.96, meaning that the dataset could not be considered normally distributed. The Taylor power transform did not improve normality, while the natural logarithm transform did. However, the natural logarithm transform resulted in a decrease in the '# of significant skewness values' as compared to the pretreated dataset. The linear correlation between variables was best for the natural logarithm transform, while the Taylor power transform was best for the variance ratio. The results for the two transforms were

comparable with respect to the '# of linear correlations' and the 'variance ratio'. Considering all of the diagnostic tests, the natural logarithm transform was found to be optimal because of the significant increase in dataset normality.

Table 3.6.: *Case 2 Statistical Constraint Diagnostics Results*

Diagnostic Test	Pretreated (No Transform)	Taylor Power Transform	Ln Transform
Average Kurtosis z-value	1.26	0.91	0.53
# of Significant Kurtosis Values	21	25	28
Average Skewness z-value	1.61	-1.29	0.97
# of Significant Skewness Values	17	22	23
# of Linear Correlations	93	130	119
Variance Ratio	1237	34.9	90.4

ECOplates 2 through 5 were used when evaluating the statistical diagnostics presented in Table 3.6 for Case 2.0. The z-value for both the kurtosis and skewness of all three datasets was less than 1.96, meaning that all three datasets could be considered normally distributed. The # of significant kurtosis and skewness values supported these findings. The natural logarithm transform increased normality with respect to all four diagnostic tests. The linear correlation between variables and variance ratio were best for the Taylor power transform, but the results for the two transforms were comparable with respect to these diagnostics. Once again, considering all of the diagnostic tests, the natural logarithm transform was found to be optimal.

ECOplates 1 and 4 were used when evaluating the statistical diagnostics presented in Table 3.7 for Case 3.0. The z-value for both the kurtosis and skewness of all three datasets was less than 1.96, meaning that all three datasets could be considered normally distributed. The # of significant kurtosis and skewness z-values supported these findings. The natural logarithm transform increased normality with respect to the # of significant z-value diagnostic tests. The linear correlation between variables and variance ratio were also best for the natural logarithm transform. Again, considering all of the diagnostic tests, the natural logarithm transform was found to be optimal.

Table 3.7.: *Case 3 Statistical Constraint Diagnostics Results*

Diagnostic Test	Pretreated (No Transform)	Taylor Power Transform	Ln Transform
Average Kurtosis z-value	-0.15	-0.24	-0.43
# of Significant Kurtosis Values	26	29	30
Average Skewness z-value	0.75	-0.37	0.45
# of Significant Skewness Values	27	29	30
# of Linear Correlations	224	233	241
Variance Ratio	1788	63.3	60.1

Table 3.8.: *Case 4 Statistical Constraint Diagnostics Results*

Diagnostic Test	Pretreated (No Transform)	Taylor Power Transform	Ln Transform
Average Kurtosis z-value	0.24	0.19	0.15
# of Significant Kurtosis Values	27	28	28
Average Skewness z-value	0.58	0.38	0.35
# of Significant Skewness Values	28	28	28
# of Linear Correlations	143	110	138
Variance Ratio	28.7	20.6	25.5

ECOplates 1 and 6 were used when evaluating the statistical diagnostics presented in Table 3.8 for Case 4.0. The z-value for both the kurtosis and skewness of all three datasets was less than 1.96, meaning that all three datasets could be considered normally distributed. The # of significant kurtosis and skewness z-values supported these findings. All three datasets were essentially equal with respect to normality. The linear correlation between variables and variance ratio were close for all three datasets as well, though the linear correlations between variables was noticeably lower for the Taylor power transform dataset. Considering the close nature of the diagnostic results for all three datasets, it was difficult to choose an optimal dataset for the PCA. The natural logarithm transform was chosen for consistency with previous cases.

Table 3.9.: *Case 5 Statistical Constraint Diagnostics Results*

Diagnostic Test	Pretreated (No Transform)	Taylor Power Transform	Ln Transform
Average Kurtosis z-value	0.01	-0.05	-0.08
# of Significant Kurtosis Values	28	28	29
Average Skewness z-value	0.52	0.39	0.25
# of Significant Skewness Values	29	30	30
# of Linear Correlations	119	115	123
Variance Ratio	18.3	14.2	26.2

ECOplates 6 through 8 were used when evaluating the statistical diagnostics presented in Table 3.9 for Case 5.0. The z-value for both the kurtosis and skewness of all three datasets was less than 1.96, meaning that all three datasets could be considered normally distributed. The # of significant kurtosis and skewness z-values supported these findings. All three datasets were essentially equal with respect to normality. The linear correlation between variables and variance ratio were close for all three datasets as well. Considering the close nature of the diagnostic results for all three datasets, it was difficult to choose an optimal dataset for the PCA. The natural logarithm transform was chosen for consistency with previous cases and the optimal 'average skewness z-value' and '# of linear correlations'.

ECOplates 7 through 10 were used when evaluating the statistical diagnostics presented in Table 3.10 for Case 6.0. The z-value for both the kurtosis and skewness of all three datasets

Table 3.10.: *Case 6 Statistical Constraint Diagnostics Results*

Diagnostic Test	Pretreated (No Transform)	Taylor Power Transform	Ln Transform
Average Kurtosis z-value	<0.01	-0.03	-0.03
# of Significant Kurtosis Values	30	30	30
Average Skewness z-value	0.52	0.18	0.22
# of Significant Skewness Values	29	30	30
# of Linear Correlations	166	169	169
Variance Ratio	147155	2815	57598

was very close to the optimal value of 0, meaning that all three datasets were normally distributed. The # of significant kurtosis and skewness z-values supported these findings. All three datasets were essentially equal with respect to normality. The linear correlation between variables was close for all three datasets as well. As a result of a very low variance for one variable, the variance ratio was very high for the pretreated dataset. Both transforms improved the homoscedasticity, but the Taylor power transform reduced it by the greatest factor. Considering the close nature of the diagnostic results for all three datasets, it was difficult to choose an optimal dataset for the PCA. The Taylor power transform was optimal, but the natural logarithm transform was chosen for consistency with previous cases. The performance of the two transforms was so close that choosing either transform for PCA was considered appropriate.

Table 3.11.: *Case 7 Statistical Constraint Diagnostics Results*

Diagnostic Test	Pretreated (No Transform)	Taylor Power Transform	Ln Transform
Average Kurtosis z-value	0.29	0.28	0.34
# of Significant Kurtosis Values	30	27	29
Average Skewness z-value	0.48	-0.07	0.14
# of Significant Skewness Values	27	27	28
# of Linear Correlations	175	169	169
Variance Ratio	147964	1024	46950

ECOplates 9 through 12 were used when evaluating the statistical diagnostics presented in Table 3.11 for Case 7.0. The z-value for both the kurtosis and skewness of all three datasets was less than 1.96, meaning that all three datasets could be considered normally distributed. The # of significant kurtosis and skewness z-values supported these findings. All three datasets were essentially equal with respect to normality. The linear correlation between variables was close for all three datasets as well. As a result of a very low variance for one variable, the variance ratio was very high for the pretreated dataset. Both transforms improved the homoscedasticity, but the Taylor power transform reduced it by the greatest factor. Considering the close nature of the diagnostic results for all three datasets, it was difficult to choose an optimal dataset for the PCA. The Taylor power transform was optimal, but the natural logarithm transform was chosen for consistency with previous cases. The performance of the two transforms was so close that choosing either transform for PCA was considered appropriate.

Table 3.12.: *Case 8 Statistical Constraint Diagnostics Results*

Diagnostic Test	Pretreated (No Transform)	Taylor Power Transform	Ln Transform
Average Kurtosis z-value	0.67	0.27	0.69
# of Significant Kurtosis Values	27	29	27
Average Skewness z-value	0.81	-0.05	0.40
# of Significant Skewness Values	26	27	26
# of Linear Correlations	91	82	95
Variance Ratio	428	30.5	84.8

ECOplates 11 through 14 were used when evaluating the statistical diagnostics presented in Table 3.12 for Case 8.0. The z-value for both the kurtosis and skewness of all three datasets was less than 1.96, meaning that all three datasets could be considered normally distributed. The # of significant kurtosis and skewness z-values supported these findings. The Taylor power transform was optimal with respect to normality. The linear correlation between variables and variance ratio were close for all three datasets. Considering the close nature of the diagnostic results for all three datasets, it was difficult to choose an optimal dataset for the PCA. The Taylor power transform was optimal, but the natural logarithm transform was chosen for consistency with previous cases. The performance of the two transforms was

so close that choosing either transform for PCA was considered appropriate.

Table 3.13.: *Case 9 Statistical Constraint Diagnostics Results*

Diagnostic Test	Pretreated (No Transform)	Taylor Power Transform	Ln Transform
Average Kurtosis z-value	0.94	0.82	0.89
# of Significant Kurtosis Values	27	26	27
Average Skewness z-value	0.99	0.11	0.51
# of Significant Skewness Values	22	26	24
# of Linear Correlations	94	90	88
Variance Ratio	125931	172	21648

ECOplates 13 through 16 were used when evaluating the statistical diagnostics presented in Table 3.13 for Case 9.0. The z-value for both the kurtosis and skewness of all three datasets was less than 1.96, meaning that all three datasets could be considered normally distributed. The # of significant kurtosis and skewness z-values supported these findings. The Taylor power transform was optimal with respect to normality. The linear correlation between variables was close for all three datasets. As a result of a very low variance for one variable, the variance ratio was very high for the pretreated dataset. Both transforms improved the homoscedasticity, but the Taylor power transform reduced it by the greatest factor. Considering the close nature of the diagnostic results for all three datasets, it was difficult to choose an optimal dataset for the PCA. The Taylor power transform was optimal, but the natural logarithm transform was chosen for consistency with previous cases. The performance of the two transforms was so close that choosing either transform for PCA was considered appropriate.

From the statistical diagnostics performed on all 9 cases, the natural logarithm transform was found to be best for the first 3 cases. Statistical diagnostic performance was very nearly equivalent for both transforms with respect to the last 6 cases. The natural logarithm transformed datasets were chosen for PCA for several reasons:

1. The natural logarithm transform was optimal for Case 1.0, using all the ECOplate data

2. When the Taylor power transform was optimal, the natural logarithm transform performed almost as well

3. The natural logarithm transform was chosen for all cases for consistency in comparison between cases

4. Previous studies (Weber, 2006) found natural logarithm transformed datasets optimal for PCA ordination

When pretreated datasets were distributed non-normally, both transforms were found to improve the normality, though the natural logarithm transform resulted in the greatest degree of normality. For most cases, linear correlations between variables was maintained or increased when either transform was applied to the pretreated dataset. Both transforms were found to increase homoscedasticity, though the Taylor power transform resulted in the greatest increase. When approaching PCA as an analytical technique for BIOLOG® ECOplate data, it is recommended that these two transforms be applied to increase dataset normality, homoscedasticity, and linear correlations between variables. Additional transforms should also be tested for their effects. The choice of which transform should be based on the results of the statistical diagnostics discussed above.

3.4.2. Principal Component Analysis (PCA)

Principal component analysis (PCA) ordination has several key features to understand before evaluation. The first principal component calculated from PCA contains the largest amount of the preserved dataset variance and represents the x-axis in PCA ordination. The second principal component calculated from PCA contains the second largest amount of the preserved dataset variance and represents the y-axis in PCA ordination. Therefore, the total preserved dataset variance is equal to the amount preserved by the first two principal components. Each point on the PCA ordination represents an object, which was an ECOplate replicate for this study. When objects are aggregated together, there is little difference with respect to either principal component. In this study, aggregated objects had very similar results for most or all of the carbon sources in the ECOplate wells. When objects are horizontally separated, they vary with respect to the first principal component, which carries more of the dataset variance than the second principal component. Therefore, objects separated vertically, or with respect to the second principal component, show less carbon source utilization differences than objects separated horizontally. Objects in this

study were labeled with the ECOplate number and either an 'A', 'B' or 'C' to denote the replicates on each ECOplate.

Figures 3.3 through 3.6 present the PCA results for the natural logarithm transformed datasets for the first 4 cases outlined in Table 3.3. The last 5 cases are presented in Chapter 4. Each figure presents the original case, designated as Case x.0, and the 4 sub-cases, designated as Cases x.1 to x.4, based on the carbon source subsets. Case x.1 represents the carbohydrate subset, Case x.2 the carboxylic acid, Case x.3 the polymer and miscellaneous and Case x.4 represents the amine and amino acid subset. No PCA was performed on the pretreated (no transform) and Taylor power law transformed datasets. The principal component analysis was performed using Statistica 7.1, and all PCA figures were originally generated by Statistica 7.1.

Figure 3.3 shows the results of the PCA performed on all ECOplates. The purpose of this case and set of sub-cases was to compare all of the ECOplates prepared during this study to determine if any single or group of ECOplates appeared distinct from the rest. With such a large amount of data in one analysis, no particular hypothesis was proposed. The primary observation was the segregation of the samples between experiments #1 and #2. ECOplates 2 through 5 were distinctly separate from the remaining ECOplates. In addition, ECOplates 2 through 5 were illustrated, in Case 1.0 (a), as distinct groups with respect to each other. These ECOplates were compared in Case 2, so this distinct grouping in Case 1.0 received further attention in the discussion of Case 2. The segregation of the experiments was prevalent in all Case 1 results, though the grouping for ECOplates 2 through 5 were not as defined for the sub-cases. The starting waste activated sludge samples were represented by ECOplates 1 and 6 for experiment #1 and #2, respectively. It is interesting to note that both of these ECOplates were grouped with ECOplates 7 though 16, which represented samples from experiment #2. Some of the replicates from ECOplate 1 showed divergence from this aggregation in Case 1.3 (d) and 1.4 (e). Most of the divergence was with respect to the second principal component, which represented approximately 15% of the dataset variance for each of these sub-cases. ECOplates 1 and 6 are compared in Case 4, so this behaviour receives further attention in the discussion of Case 4. The results of Case 1 suggest that the development of the microbial community in the MFCs was unique to the experiment being run and the variables and conditions that differed between experiments.

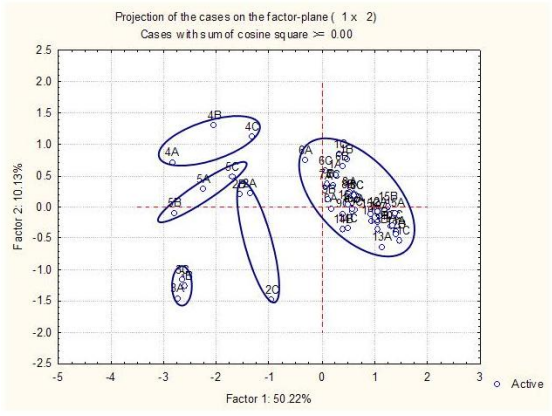

(a)

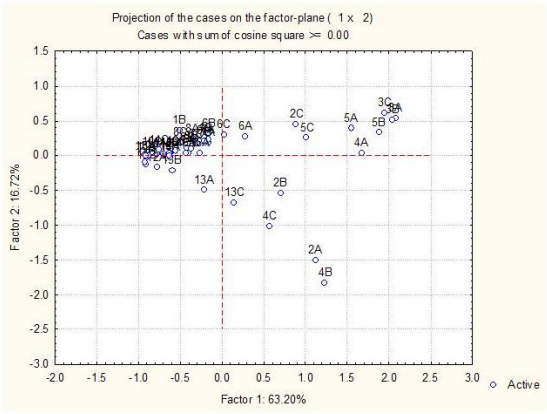

(b)

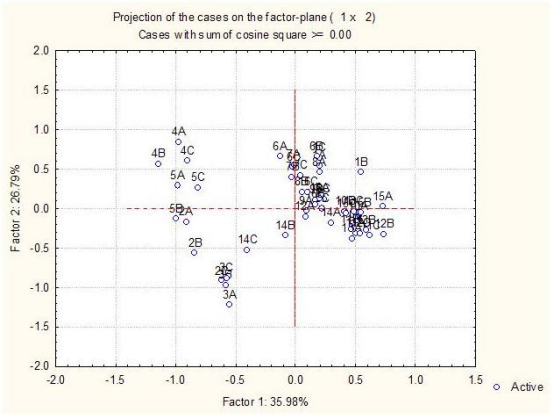

(c)

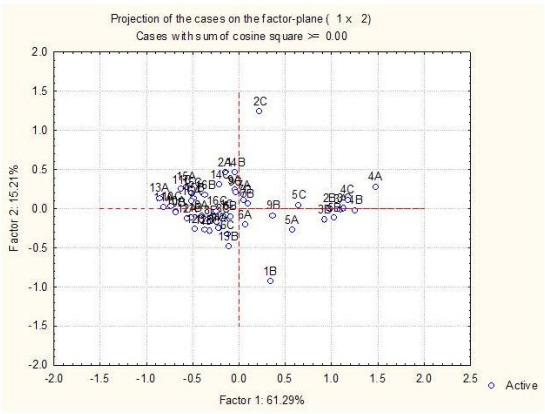

(d)

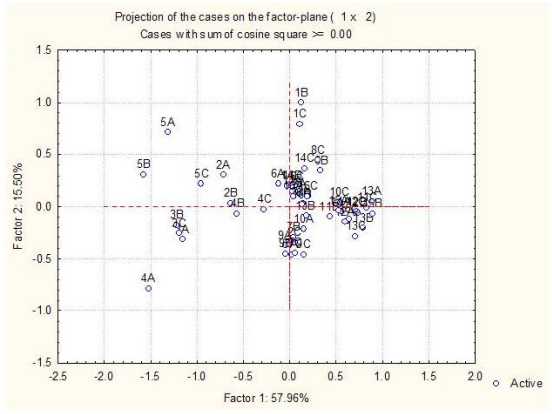

(e)

(a) = Case 1.0 - All ECOplate substrates
(b) = Case 1.1 - Carbohydrate substrates only
(c) = Case 1.2 - Carboxylic Acid substrates only
(d) = Case 1.3 - Polymer and Miscellaneous substrates only
(e) = Case 1.4 - Amine and Amino Acid substrates only

Figure 3.3.: *PCA Ordinations for Cases 1.0 through 1.4 - All ECOplates - Both Experiments*

Figure 3.4 shows the results of the PCA performed on ECOplates 2 through 5. ECOplates 2 and 4 were taken from the bulk anolyte at the middle and end of experiment #1, respectively. ECOplates 3 and 5 were prepared from biofilm scrapings from the side of the nearest anode to the proton exchange membrane at the middle and end of experiment #1, respectively. The purpose of this case and set of sub-cases was to compare the samples taken from the bulk anolyte and those removed from the anode as scrapings. It was hypothesized that they would not differ significantly throughout operation. From Case 2.0 (a), it was difficult to conclude that ECOplates 2, 4 and 5 were significantly different. However, replicates for the bulk anolyte samples, ECOplates 2 and 4, were not well aggregated. The variance between these replicates may have disguised a more pronounced difference between ECOplates 2, 4 and 5. The anode scrapings samples, ECOplates 3 and 5, did not appear to demonstrate the same replicate variance. In addition, ECOplate 3, which represented an anode scraping in the middle of the first experiment, was found to be significantly different from the other ECOplates for the parent case, Case 2.0. Though it was difficult to conclude that the bulk anolyte samples were significantly different from later anode scrapings, it appeared that earlier samples were significantly different. From Case 1.0, presented in Figure 3.3, each of the ECOplates in Case 2 were distinctly grouped. Interestingly, Case 1.0 provided the best illustration that ECOplates 2 and 3 were distinct in the first principal component, while ECOplates 4 and 5 were distinct in the second principal component. This supported the Case 2 results that later ECOplates showed less differentiation between anolyte samples and anode scraping samples than earlier ECOplates did.

There were several interesting results from the analysis of Cases 2.1 (b) to 2.4 (e). The carbohydrates (Case 2.1 - b) and carboxylic acids (Case 2.2 - c) behaved similarly to the full carbon source variable set (Case 2.0). The replicates for ECOplate 3 showed a much higher variance in the second principal component for the carboxylic acids, indicating a higher degree of variability with respect to this component. However, the second principal component represented only 19.5% of the dataset variance, so the replicate differentiation in ECOplate 3 carboxylic acid use would be subtle. The results for ECOplate 2 were highly variable with respect to the first principal component for the parent case and all sub-cases. This was attributed to ECOplate inoculation variance. ECOplate 2 represented a bulk anolyte sample taken only 2 weeks after system start-up. It was expected that the microbial community, or

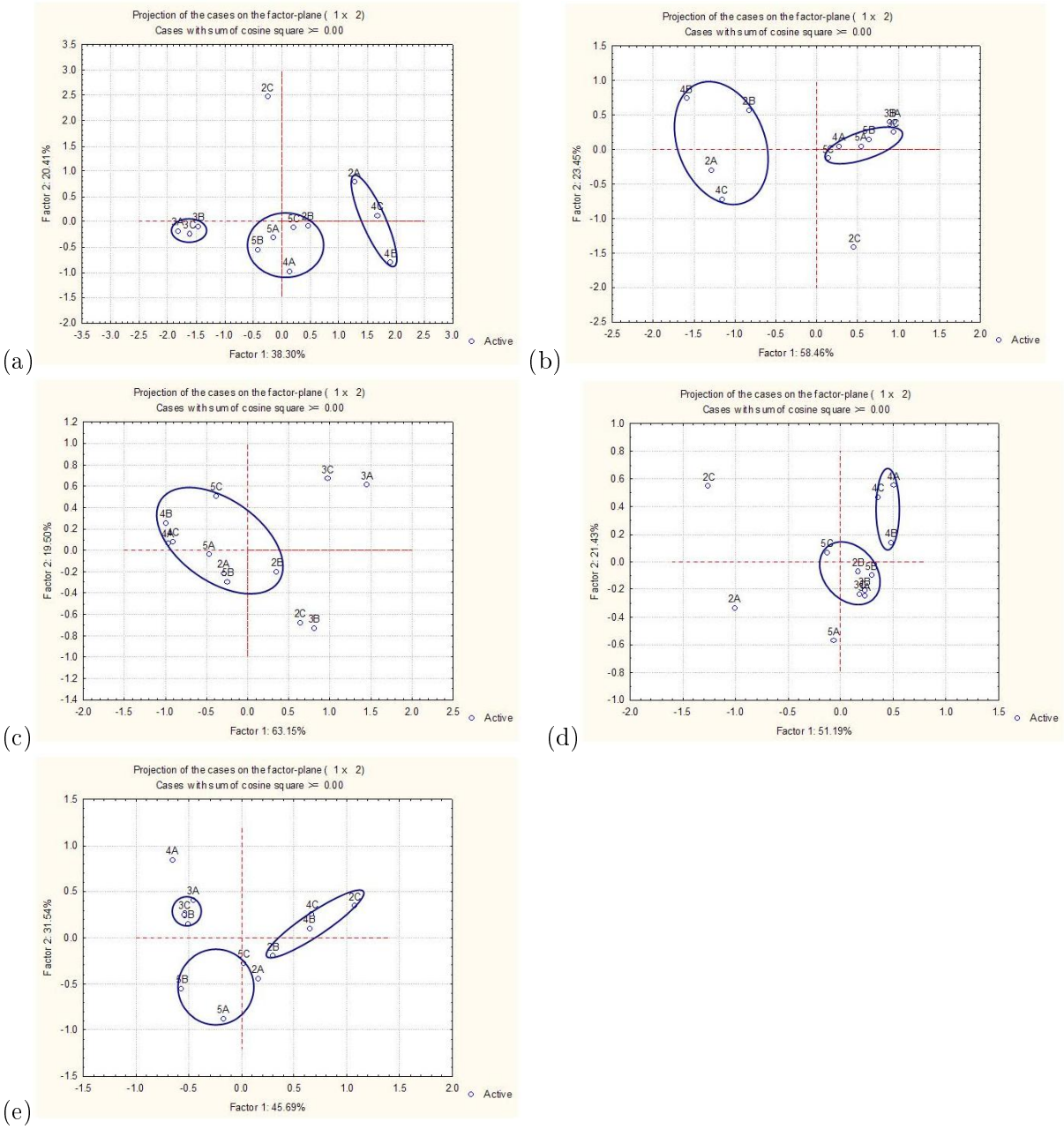

(a) = Case 2.0 - All ECOplate substrates
(b) = Case 2.1 - Carbohydrate substrates only
(c) = Case 2.2 - Carboxylic Acid substrates only
(d) = Case 2.3 - Polymer and Miscellaneous substrates only
(e) = Case 2.4 - Amine and Amino Acid substrates only

Figure 3.4.: *PCA Ordinations for Cases 2.0 through 2.4 - ECOplates 2 through 5 - Anolyte and Anode Scraping Comparison*

at least its activity, would still be diverse before system acclimation. The additional factor of small inoculation volumes added to each ECOplate well made it possible that each well of the ECOplate did not represent similar microbial components. The general consistency of ECOplate 3, prepared only 2 days later, suggests that this diversity was not present at the anodes. Similar observations were noted when comparing ECOplates 4 and 5 after approximately 1 month of system operation.

ECOplates 2 through 5 showed some differentiation, but it was difficult to conclude its significance. It was further concluded that the microbial community in the bulk anolyte and at the anode surface would converge as the system acclimated. This was based on the closer proximity of ECOplates 4 and 5 as compared to ECOplates 2 and 3 and was the driving reason behind allowing over 2 months for system acclimation in experiment #2.

Figure 3.5 shows the results of the PCA performed on ECOplates 1 and 4. ECOplate 1 represented the initial waste activated sludge for system start-up in experiment #1, while ECOplate 4 represented the bulk anolyte at the end of experiment #1. The purpose of this case and set of sub-cases was to compare the initial microbial community in the waste activated sludge to that in the anolyte following one month of operation. It was hypothesized that they would differ significantly. The results of Case 3 were consistent for the parent case and all sub-cases. ECOplates 1 and 4 showed very strong differentiation with respect to the first principal component. The first principal component represented 65% to 85% of the total variance; a representation level often not met by the first two principal components combined. Most of the variance between replicates was associated with the second principal component. These results indicate definitive microbial differences between MFC start-up and operational conditions after only 4 weeks.

Figure 3.6 shows the results of the PCA performed on ECOplates 1 and 6. ECOplates 1 and 6 represented the initial waste activated sludge for system start-up in experiments #1 and #2, respectively. The purpose of this case and set of sub-cases was to compare the initial microbial communities of the waste activated sludge used in experiment #1 with that of the waste activated sludge used in experiment #2. It was hypothesized that they would not differ significantly. The results of Case 4.0 supported this hypothesis, but some of the sub-cases indicated a certain amount of differentiation. Results from the carbohydrates

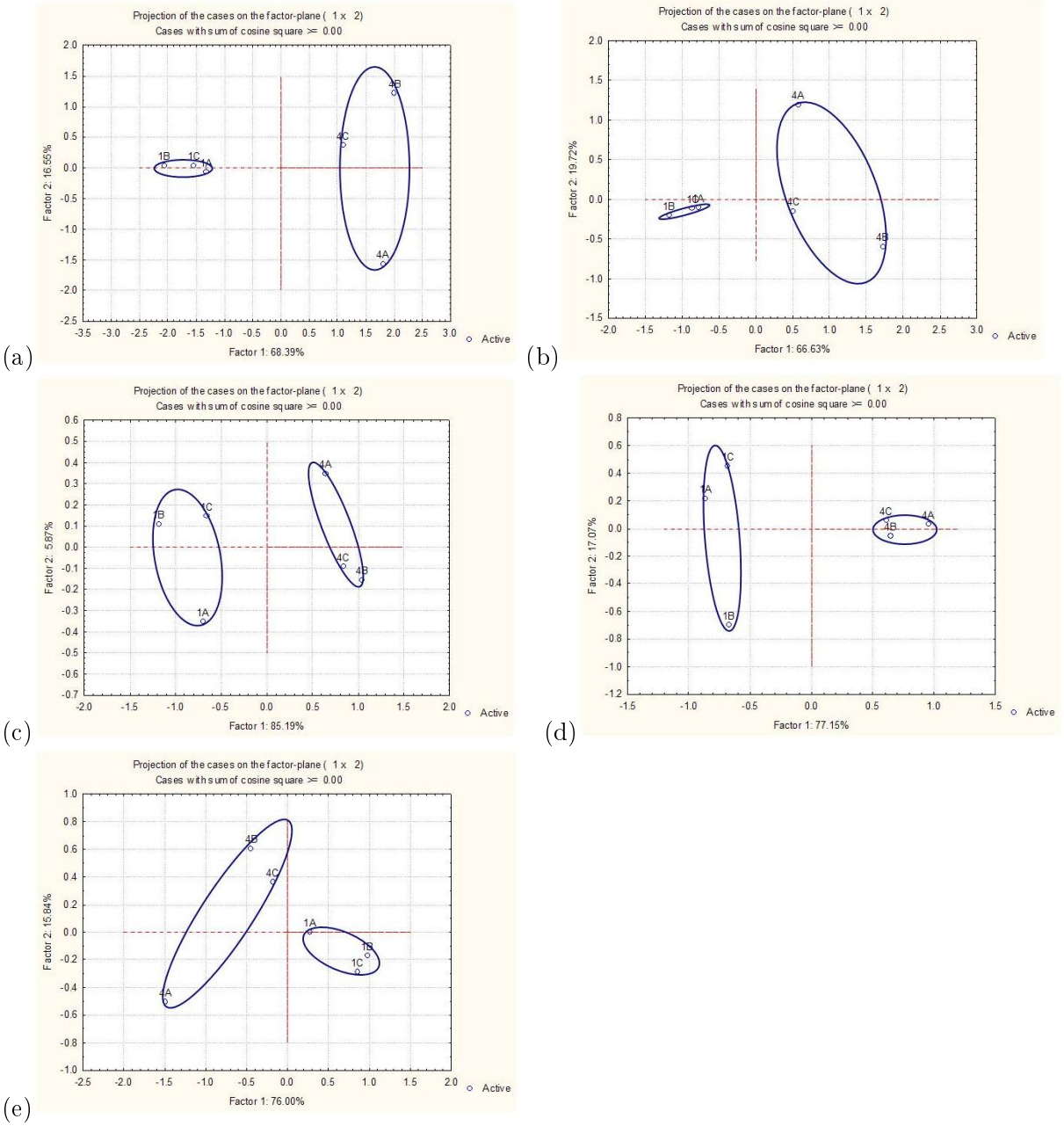

(a) = Case 3.0 - All ECOplate substrates
(b) = Case 3.1 - Carbohydrate substrates only
(c) = Case 3.2 - Carboxylic Acid substrates only
(d) = Case 3.3 - Polymer and Miscellaneous substrates only
(e) = Case 3.4 - Amine and Amino Acid substrates only

Figure 3.5.: *PCA Ordination for Cases 3.0 through 3.4 - ECOplates 1 and 4 - Exp#1 Acclimation Period*

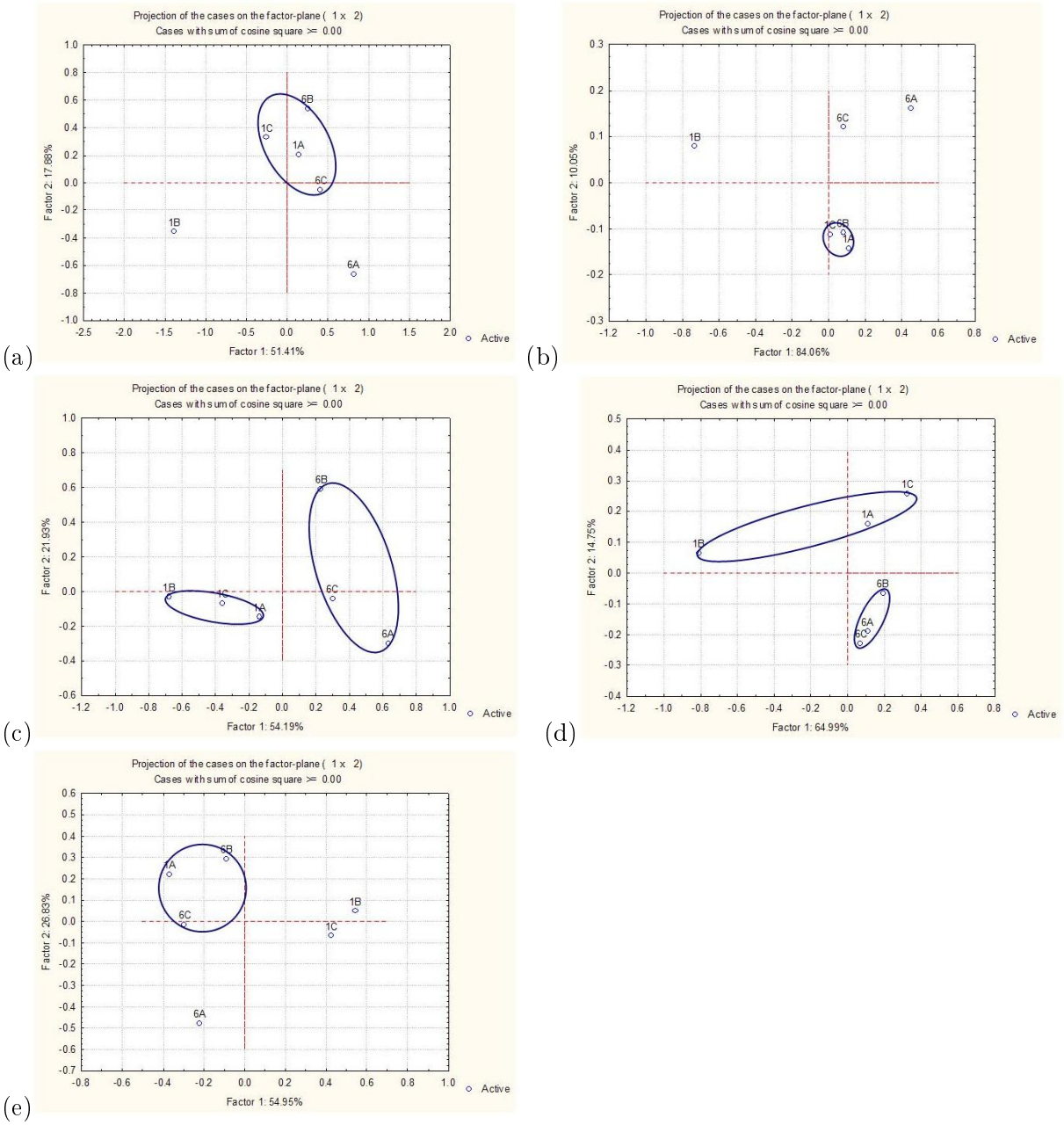

(a) = Case 4.0 - All ECOplate substrates
(b) = Case 4.1 - Carbohydrate substrates only
(c) = Case 4.2 - Carboxylic Acid substrates only
(d) = Case 4.3 - Polymer and Miscellaneous substrates only
(e) = Case 4.4 - Amine and Amino Acid substrates only

Figure 3.6.: *PCA Ordination for Cases 4.0 through 4.4 - ECOplates 1 and 6 - Waste Activated Sludge Innoculent Comparison*

(Case 4.1 - b) and amines and amino acids (Case 4.4 - e) were in agreement with the parent case. Results from the carboxylic acids (Case 4.2 - c) showed significant differentiation with respect to the first principal component, while results from the polymers and miscellaneous carbon sources (Case 4.3 - d) showed weaker differentiation through the second principal component. While the microbial communities of the two waste activated sludge samples did not differ with respect to general substrate use, the two samples appeared to differ significantly with respect to carboxylic acid utilization. The samples were taken from the Waterloo wastewater treatment plant approximately 7 weeks apart from each other. The differences in carboxylic acid utilization may have been due to a difference in volatile fatty acids (VFA) presence in earlier wastewater treatment processes.

Several conclusions were drawn from the PCA performed on the ECOplate data of the first 4 cases. From a PCA of all ECOplate data, the only noticeable difference was between the two experiments. ECOplates prepared from samples removed during experiment #1 were distinct from those prepared from samples removed during experiment #2. The waste activated sludge samples from the start-up of both experiments was grouped with the results of experiment #2.

From a PCA of ECOplates 2 through 5 data, it was concluded that the microbial communities in the bulk wastewater anolyte were different from those on the anode surface. However, these differences appeared to lessen with later samples, suggesting a convergence of microbial communities after sufficient MFC system acclimation.

From a PCA of ECOplates 1 and 4 data, it was concluded that the microbial communities in the initial waste activated sludge were significantly different than those in the wastewater anolyte after 4 weeks of operation. These distinctions were seen in all carbon source subset analyses as well.

From a PCA of ECOplates 1 and 6 data, it was concluded that the microbial communities in the initial waste activated sludge used in the two experiments were similar. The only point of differentiation appeared to be with carboxylic acid utilization, which may have been due to different conditions and VFAs present in earlier wastewater treatment processes at the Waterloo wastewater treatment plant.

3.4.3. Functional Diversity

Figure 3.7 presents the results of the functional diversity indices calculated from the pretreated ECOplate data from ECOplates 1 though 5, prepared during experiment #1. The functional diversity results for both MFCs in experiment #2 are presented in Chapter 4.

From Figure 3.7, the functional diversity was compared for samples taken from the anolyte versus those scraped from the anode surface. Both anolyte and anode scraping samples showed similar values for substrate diversity and substrate evenness at 75% to 90% of the initial waste activated sludge. The substrate richness differed significantly between the two types of samples. The anode scraping sample at 2 weeks after system start up showed only 60% of the substrate richness of the intial waste activated slugde, while the anode scraping sample at 4 weeks after system start up showed almost 100% of the substrate richness of the inital waste activated sludge. The substrate richness results from the wastewater anolyte samples showed a similar, but less drastic trend.

It was difficult to draw many conclusions from this single analysis. Anolyte and anode scraping samples had similar substrate diversity and substrate evenness, but substrate richness varied between the two types of samples. The substrate richness of the anolyte sample was greater than the anode scraping sample at 2 weeks, but the opposite was true after 4 weeks of operation. This indicated a much greater flux in substrate richness at the anode surface than in the anolyte. Acclimation period trends are discussed in Chapter 4.

3.5. Conclusions

BIOLOG® ECOplates were utilized during two experiments to perform community level physiological profiling (CLPP) of the microbial communities in microbial fuel cells (MFCs). A Taylor power law transform and a natural logarithm transform were applied to pretreated ECOplate data to ascertain the effects the transforms would have on dataset normality, homoscedasticity and linear correlation between variables. Principal component analysis (PCA) was applied to natural logarithm transformed datasets to visualize and interpret shifts in microbial community composition or activity for several cases. The functional diversity of the microbial communities was evaluated for each ECOplate to identify any shifts in substrate diversity, evenness and richness during experimentation.

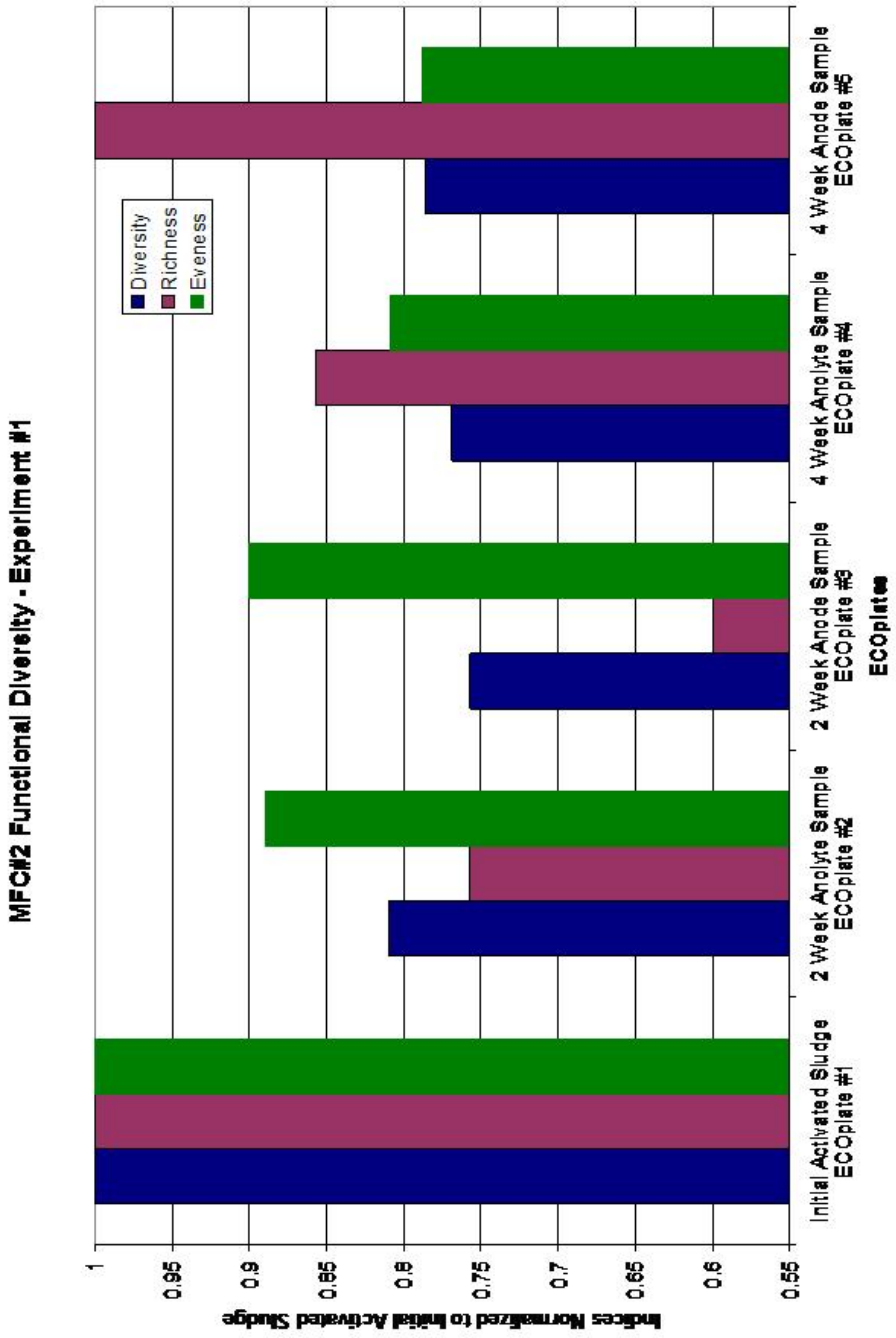

Figure 3.7.: *Functional Diversity Indices for Experiment #1*

The natural logarithm transformed datasets were found to be optimal with respect to dataset normality as compared to the Taylor power law transformed and pretreated datasets. The Taylor power law transform increased homoscedasticity by the greatest degree, while neither transform showed great improvement in the number of linear correlations between variables as compared to the pretreated datasets. The increase in homoscedasticity, preservation of linear correlations between variables and optimal dataset normality were the reasons behind the choice of the natural logarithm transformed datasets for subsequent PCA.

PCA of the first 4 cases yielded several interesting results. From the first case studied, the dominant trend was the segregation of the samples from the first experiment from those of the second experiment. In the second case, the differences between samples taken from the wastewater anolyte and those taken from the anode surface were compared. Though the samples showed some segregation, it was difficult to conclude that the behaviour was significantly different. In addition, comparison of samples taken later in the experimental period indicated convergence of behaviour of wastewater anolyte and anode surface samples with reference to samples taken earlier in the experimental period. In the third case, microbial communities in the initial waste activated sludge were compared to those in the wastewater anolyte after 4 weeks of MFC operation. The results were clearly segregated, identifying a shift in the microbial community level physiology and/or activity. From the fourth case studied, a comparison of two samples of initial waste activated sludge used in the two experiments resulted in only one discernible difference between the microbial communities. The utilization of carboxylic acids appeared to differ between the two waste activated sludge samples, suggesting a difference in initial composition or conditions, possibly related to VFAs in the initial sludge. The PCA of the last 5 cases is discussed in Chapter 4.

The functional diversity of the microbial communities of each ECOplate were calculated and compared to identify any further ecological trends. The indices used to evaluate the functional diversity were the substrate diversity, substrate evenness and substrate richness. All three indices were observed to decrease during the acclimation period of the MFC operation. Anolyte and anode scraping samples differed only in substrate richness, with the anode scraping samples showing much larger differences at the 2 and 4 week sample points than the anolyte samples.

References

References marked with an asterisk indicate studies included in the meta-analysis.

*Allen, M. J. (1972). *Methods in microbiology.* Academic Press, New York.

BIOLOG. (2007). *Biolog ecoplate.* `http://www.biolog.com/pdf/eco\_microplate\_sell\_sheet.pdf`. (accessed August 15, 2006)

*Forney, L. J., Liu, W.-T., Guckert, J. B., Kumagai, Y., Namkung, E., Nishihara, T., et al. (2001). Structure of microbial communities in activated sludge: Potential implications for assessing the biodegradability of chemicals. *Ecotoxicology and Environmental Safety*, *49*, 40-53.

*Fox, J. D., & Robyt, J. F. (1991). Miniaturization of 3 carbohydrate analyses using a microsample plate reader. *Analytical Biochemistry*, *195*, 93-96.

Franklin, R. B., Garland, J. L., Bolster, C. H., & Mills, A. L. (2001). Impact of dilution on microbial community structure and functional potential: comparison of numerical simulations and batch culture experiments. *Applied and Environmental Microbiology*, *67*(2), 702-712.

Garland, J. L. (1996). Analytical approaches to the characterization of samples of microbial communities using patterns of potential c source utilization. *Soil Biology & Biochemistry*, *28*(2), 213-221.

Garland, J. L., & Mills, A. L. (1991). Classification and characterization of heterotrophic microbial communities on the basis of patterns of community-level sole-carbon-source utilization. *Applied and Environmental Microbiology*, *57*(8), 2351-2359.

Garland, J. L., Mills, A. L., & Young, J. S. (2001). Relative effectiveness of kinetic analysis vs single point readings for classifying environmental samples based on community-level physiological profiles (clpp). *Soil Biology & Biochemistry*, *33*, 1059-1066.

Grove, J. A., Kautola, H., Javadpour, S., Moo-Young, M., & Anderson, W. A. (2004). Assessment of changes in the microorganism community in a biofilter. *Biochemical Engineering Journal*, *18*, 111-114.

Legendre, P., & Legendre, L. (1998). *Numerical ecology* (2nd ed.). Elsevier B.V. Amsterdam.

*Taylor, L. R. (1961). Aggregation, variance, and the mean. *Nature*, *189*, 732-735.

Weber, K. P. (2006). *Investigation of the mechanisms and fundamental variables affecting acid mine drainage treatment in wetland mesocosms.* Unpublished master's thesis, University of Waterloo, Ontario, Canada.

Zak, J. C., Willig, M. R., Moorhead, D. L., & Wildman, H. G. (1994). Functional diversity

of microbial communities: a quantitative approach. *Soil Biology & Biochemistry*, *26*, 1101-1108.

4. Impact of Carbon Source Dosing on MFCs Operating with Different Catholytes

Abstract

Microbial fuel cells (MFCs) utilize bacteria to biodegrade organics, such as those in wastewasters, and liberate electrons for electricity production.This study focused on the evaluation of several key features. The first MFC, MFC#1, was operated with a dissolved oxygen (DO) catholyte, while the second MFC, MFC#2, was operated with a ferricyanide catholyte. Both MFCs operated with a waste activated sludge anolyte. The operation was divided into two periods, an acclimation period and a carbon source dosing period. During the carbon source dosing period, the affects of several carbon sources were examined. These are referred to as the carbon source pulse tests (CSPTs). The substrates chosen for the CSPTs were sodium acetate, glucose, glycerol and bovine serum albumin (BSA). The two MFCs were compared throughout the operational periods with respect to current and power production, wastewater quality and microbial ecology. The microbial ecology was evaluated using ecological data obtained from BIOLOG® ECOplates and subsequent principal component analysis (PCA).

Electricity production was constant throughout operation, except during BSA dosing, where increases of 25% and 100% were seen for MFC#1 and MFC#2, respectively. Throughout operation, the chemical oxygen demand (COD) removal due to electricity production was less than 1% of the feed COD to each MFC. The majority of the feed COD was found to accumulate in each MFC, primarily as particulate matter, indicating that biodegradation rates of COD material or solubilization of particulate COD material was an operational bottleneck for both MFCs. Nitrogen results agreed with COD results, indicating an accumulation, primarily as particulate matter. Microbial community shifts were observed throughout operation. The COD equivalence of the CSPTs was minute in comparison to waste activated

sludge feed COD levels. As such, responses to CSPTs were attributed to shifts in the microbial community activity or primary metabolic activity rather than the microbial community composition. The microbial community activity of the MFCs tended to diverge during the acclimation period and following glycerol dosing, while convergence was observed following sodium acetate, glucose and BSA dosing. The impacts of BSA on electricity production translated into moderate shifts in the microbial community activity of MFC#1, but no shift was observed for MFC#2. Functional diversity was found to be nearly equal before and after the acclimation period. During the CSPTs, functional diversity decreased by 10% to 15% of the levels seen before the acclimation period, though increases to approximately 92% of the levels observed before the acclimation period were noted following BSA dosing.

Keywords: Carbon Source, Dissolved Oxygen, Ferricyanide, Functional Diversity, Microbial Ecology, Microbial Fuel Cell, Performance

4.1. Introduction

Sustainable electricity production and effective wastewater treatment are two major concerns leading into the twenty-first century. Natural sources of electricity generation, while sustainable, are not often possible in many regions of the world. Water usage is continually rising with global populations, making it increasingly necessary to find eco-friendly and effective wastewater treatment alternatives.

Microbial fuel cells (MFCs) are rapidly gaining popularity in both alternative energy production and wastewater treatment. While, typical wastewater treatment systems utilize biological treatment under aerobic conditions to degrade the organic components in the wastewater, MFCs utilize microorganisms to degrade organic components under anaerobic conditions. Through this process, electrons are liberated and provide the energy produced by the MFCs.

Early MFC studies used simple systems with single microorganisms and simple substrates (Kim, Choi, Jung, & Kim, 2000). Several microorganisms were found to behave ideally under anaerobic conditions, readily freeing electrons during biodegradation of the substrate, including some *Shewanella* and *Geobacter* species (Bond & Lovley, 2003; Ringeisen, Ray, & Little, 2007). The use of electron mediators was accepted in early research, but the concept of mediatorless MFCs became prominent only in the late 1990's and continues to be more widely researched over MFCs operated with mediators (Gil et al., 2003; Moon, Chang, & Kim, 2006). Over the past decade, many advances have been made with respect to system design and materials. Further studies have begun to focus on naturally diverse microbial systems and substrates, such as those provided in wastewater (Moon et al., 2006; Min, Kim, Oh, Regan, & Logan, 2005; He, Minteer, & Angenent, 2005; Aelterman, Rabaey, Clauwaert, & Verstraete, 2006; You, Zhao, Jiang, & Zhang, 2006). Further research is needed in many areas, including the use of multiple MFC reactor systems, the influence of various operational parameters, overall MFC performance and system responses to disturbance and upset.

In this chapter, the operation and microbial ecology of two MFCs were compared during an acclimation period and a subsequent carbon source dosing period. MFC#1 was operated with a dissolved oxygen catholyte, while MFC#2 was operated with a ferricyanide catholyte. The acclimation period was approximately 77 days in duration, lasting from system start-up

to the first carbon source pulse test (CSPT). The CSPTs involved the dosing of a known amount of a specific, soluble carbon source. Sodium acetate, glucose, glycerol, and bovine serum albumin (BSA) were chosen and dosed in that order. The carbon source dosing period was approximately 60 days in duration. Evaluation of MFC operation included monitoring of electricity production and anolyte quality as outlined in Chapter 2. The microbial ecology was evaluated using BIOLOG® ECOplates and principal component analysis (PCA) as outlined in Chapter 3.

4.2. Microbial Fuel Cell (MFC) System

4.2.1. System Design, Operation, Materials, and Experimental Methods

The MFC system design and materials were described in Chapter 2. The system was operated for a total of 182 days, consisting of the acclimation period (77 days), the carbon source dosing period (60 days) and a post-experimental monitoring period (45 days). Both MFCs were controlled at 0.3V while the current produced from each MFC was measured. The system was operated under a fed-batch mode with 100 mL of waste activated sludge fed every 48∓3 hours following the removal of a 100 mL sample of the wastewater anolyte. Sampling and feeding methodology are presented in detail in Appendix B.

The anolyte and the waste activated sludge feed were analyzed for chemical oxygen demand (COD), total Kjeldahl nitrogen (TKN) and pH. The dissolved oxygen and ferricyanide concentrations were measured in the catholytes of MFC#1 and MFC#2, respectively. The head space gas composition of each MFC was also analyzed for nitrogen, carbon dioxide and methane. The anolyte and waste activated sludge feed samples were fractionated via centrifugation and filtration, then preserved prior to digestion and analysis. During system operation, carbon source pulse tests (CSPTs) were performed by injecting a small, known amount of COD in the form of a known, soluble substrate. The MFC system operation and experimental methods are provided in detail in Chapter 2, while the CSPTs are described in Chapter 3. Analytical methods and reagent/solution chemistry are provided in detail in Appendix C.

Shifts in the microbial ecology of the wastewater anolyte in each MFC were identified through PCA of datasets obtained using BIOLOG® ECOplates. Wastewater anolyte sampling and

ECOplate preparation and analytical methods are presented in Appendices B and C. Dataset pretreatment, transformation and PCA methods are presented in Chapter 3.

As discussed in Chapter 2, evaluation of electrochemical performance, such as current and power production, are usually reported after normalization to the effective surface area of the transport media. The MFCs were identical with anodes having a surface area of 423 cm^3, cathodes having a surface area of 282 cm^3 and the proton exchange membranes having a surface area of 7 cm^3. The effective electrode surface area (EESA) was equal to the cathode surface area, while the effective membrane surface area (EMSA) was equal to the proton exchange membrane surface area. The EESA and EMSA were both used to report current and densities for this study. The surface area used to calculate the associated density is identified for each instance. From Chapter 2, the EESA and EMSA were assumed to bound the actual effective surface area, providing minimum and maximum densities for electrical variables, respectively.

4.2.2. MFC Differentiation

The differentiation between the two MFCs used in this study was made through the catholyte composition in each MFC. The first MFC, MFC#1, used a phosphate buffered, saline solution with a constant supply of air bubbled through it. The dissolved oxygen (DO) functioned as the electron acceptor at the cathode surface of MFC#1. MFC#2 used a phosphate buffered, ferricyanide solution. The ferricyanide served as the electron acceptor at the cathode surface of MFC#2. Catholyte composition is discussed further in the MFC system description in Chapter 2.

4.2.3. CSPTs and ECOplate Experimental Organization

Tables 4.1 and 4.2 were presented in Chapter 3 as Tables 3.3 and 3.4 and represent the experimental organization and case nomenclature used with the carbon source pulse tests (CSPTs) and BIOLOG® ECOplates during this study. They are presented here for ease of reference.

Table 4.1.: *ECOplate Case Organization for PCA*

Case #	ECOplates Used	Comparison Significance
1.0	All	Entire ECOplate Set Comparison
2.0	2,3,4,5	Bulk Solution vs. Anode Scraping Samples
3.0	1,4	Inoculant vs Endpoint (Experiment #1)
4.0	1,6	Inoculants Comparison
5.0	6,7,8	Inoculant vs Steady States (Experiment #2)
6.0	7,8,9,10	Pre and Post Sodium Acetate Comparison (both MFCs)
7.0	9,10,11,12	Pre and Post Glucose Comparison (both MFCs)
8.0	11,12,13,14	Pre and Post Glycerol Comparison (both MFCs)
9.0	13,14,15,16	Pre and Post BSA* Comparison (both MFCs)

*Bovine Serum Albumin

Table 4.2.: *Carbon Source Pulse Test Substances*

Substance	COD Mass per Pulse (mg)	Solution Preparation
Sodium Acetate	50 (1 pulse) 2.857 (3 pulses)	2.441g per 100 mL DI 1 mL above solution to 16.5 mL DI
Glucose	2.857 (4 pulses)	0.089g per 100 mL DI
Glycerol	2.857 (4 pulses)	0.078g (0.0621 mL) per 100 mL DI
Bovine Serum Albumin (BSA)	2.857 (4 pulses)	0.068g per 100 mL DI

4.3. System Acclimation Period Comparison

Results from the MFC acclimation period are divided into three sub-sections. The current and power production of each MFC is presented and discussed first, allowing for an operational comparison. Results of the analysis of the wastewater anolyte, catholyte and head space gas obtained from each MFC are compared next, with emphasis on a COD mass balance, ferricyanide concentration in the MFC#2 catholyte and methane presence in the head space gas. Finally, shifts in microbial community ecology and activity during the acclimation period are evaluated and discussed.

4.3.1. Current and Power Production

Table 4.3 presents current and power production results for MFC#1 and MFC#2 during the acclimation period. The average coulombs per day were calculated by dividing the sum of the coulombs produced during the acclimation period by the duration of the acclimation

period. The average power was calculated similarly, while the the maximum power was identified from the acclimation period data.

Table 4.3.: *Acclimation Period: Coulomb and Power Production*

Electrical Variable	MFC#1	MFC#2
Average Coulombs per day	5.49	26.34
Maximum Power (mW)	0.066	0.347
Average Power (mW)	0.020	0.093

For each MFC, the controlled voltage was 0.3V and the duration of the acclimation period was equal. Therefore, differences in coulomb production and power levels were solely due to differences in current. MFC#1 generated approximately 20% of the current and power that MFC#2 could achieve. The lower current levels observed for MFC#1 were a direct result of the electron accepetor used. Oxygen is relatively insoluble, with a solubility of less than 7 mg/L under the operational conditions of this study. This is equivalent to a maximum concentration of less than 0.22 mM. The measured DO concentration range in the MFC#1 catholyte during the acclimation period was 3.1-5.6 mg/L, which was equivalent to 0.10-0.18 mM. By contrast, ferricyanide concentrations in the MFC#2 catholyte were maintained at levels approaching 42 mM. In addition to a lower electron acceptor concentration, oxygen reduction kinetics are relatively slow as compared to that of ferricyanide. Therefore, the lower concentration and slower kinetics of oxygen limited the operation of MFC#1 during the acclimation period.

Using the average power calculated for each MFC and the EESA and EMSA, upper and lower estimates of the average power densities for each MFC were calculated. For MFC#1, the EESA resulted in a power density of 0.73 mW/m^2 while the EMSA resulted in a power density of 29.3 mW/m^2. For MFC#2, the EESA resulted in a power density of 3.29 mW/m^2 while the EMSA resulted in a power density of 132.5 mW/m^2. Power densities calculated with the EMSA were comparable to power densities reported in literature for similar systems run with glucose as a substrate (Oh & Logan, 2006). Current and power production is known to be limited when the surface area of the proton exchange membrane is less than that of the electrodes (Oh & Logan, 2006).

4.3.2. Wastewater Anolyte, Catholyte and Head Space Gas Analyses

Table 4.4 presents COD results during the acclimation period for the anolyte samples and head space gas. The analytical procedures and equations required for these calculations are presented in Chapter 2. The COD_{Feed} represents the COD mass equivalence of the waste activated sludge feed to the MFCs. The carbon source pulses, anolyte samples, electricity generation and methane production COD mass equivalences are represented by COD_{CSP}, COD_{Smpl}, COD_{Elec} and COD_{Gas}. From these terms and Equation 2.4, the mass of COD accumulated in each MFC, COD_{Acc}, was calculated. For MFC#2, the ferricyanide reduction was converted to a COD mass equivalence for comparison to the electricity generation results of MFC#2. A 95% confidence interval is also presented.

Table 4.4.: *Acclimation Period: Cumulative Chemical Oxygen Demand Results*

COD Variable	MFC#1 (mg)	MFC#2 (mg)
COD_{Feed}	11300∓1990	11300∓1990
COD_{CSP}	0∓0	0∓0
COD_{Smpl}	1976∓1193	2399∓1400
COD_{Elec}	35.0∓1.2	168.1∓31.5
COD_{Gas}	83.0∓115.0	86.0∓85.8
COD_{Acc} (calculated from Equation 2.4)	9210∓3300	8660∓3510
COD_{Ferri}		149.2∓303.7

Several points were evident from the data in Table 4.4:

- the COD withdrawn from both MFCs was approximately 20% of the COD fed to both MFCs
- the removal of COD due to electricity production was approximately 4 times higher in MFC#2
- the removal of COD in the MFCs was primarily due to the removal of the COD through sampling
- COD associated with methane production was comparable to the COD equivalence of electricity production

- both MFCs appeared to be accumulating a majority of the COD fed
- the change in the ferricyanide concentration in the catholyte was in agreement with that expected on the basis of current generation in MFC#2, though the 95% confidence interval was much greater

As was expected from the current and power production results, the COD removal due to electricity production in MFC#2 was greater than that in MFC#1. All other terms in the COD balance were similar for both MFCs. These results represent the accumulated totals from approximately 35 samples. The 95% confidence intervals associated with the results represents the accumulated error associated with the multiple sample analysis. Coulombic efficiencies were not calculated due to the large confidence intervals.

The pH of the feed and anolyte samples were also determined during the acclimation period. The pH of the feed ranged from 7.6 to 7.9, while the anolyte samples ranged from 6.4 to 7.2 and 6.9 to 7.5 for MFC#1 and MFC#2, respectively. Both MFCs showed lower pH values than the waste activated sludge feed. This was attributed to the accumulation of volatile fatty acids (VFAs) in the anolyte during any fermentation processes which were likely active during MFC operation. The lower pH values of the MFC#1 anolyte suggested a greater accumulation of VFAs as a result of more fermentation processes being active. With lower electricity production, active bacteria in MFC#1 were more likely involved in fermentation processes than bacteria in MFC#2.

Figure 4.1 presents the acclimation period nitrogen concentrations for the feed and both MFCs along with error bars that describe 95% confidence levels. The analytical procedures required to obtain these results are presented in Chapter 2.

There are a few key conclusions from Figure 4.1:

- feed waste activated sludge NH4-N content was present in the particulate matter for most of the acclimation period
- NH4-N content in MFC#1 samples was less than 50 mg/L throughout the acclimation period
- NH4-N content in MFC#2 samples was 50-100 mg/L throughout the acclimation period

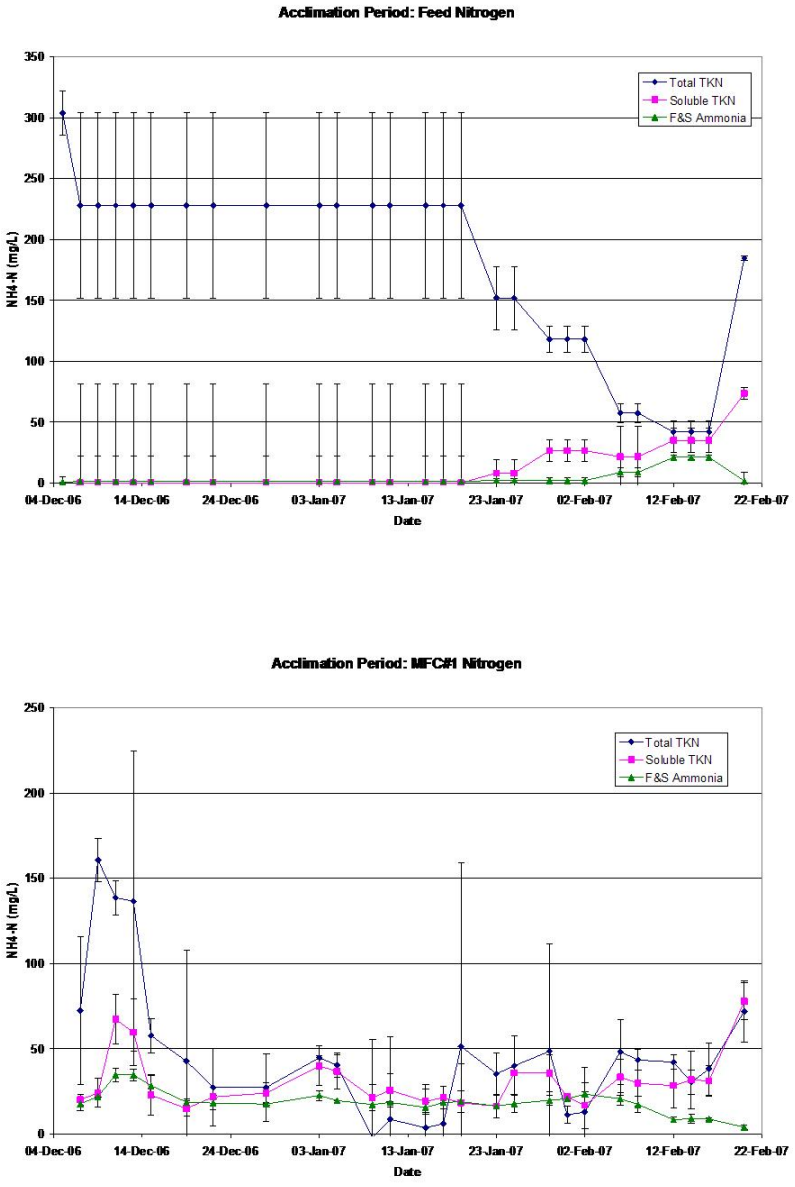

Figure 4.1.: *Nitrogen Content Results from the Acclimation Period*

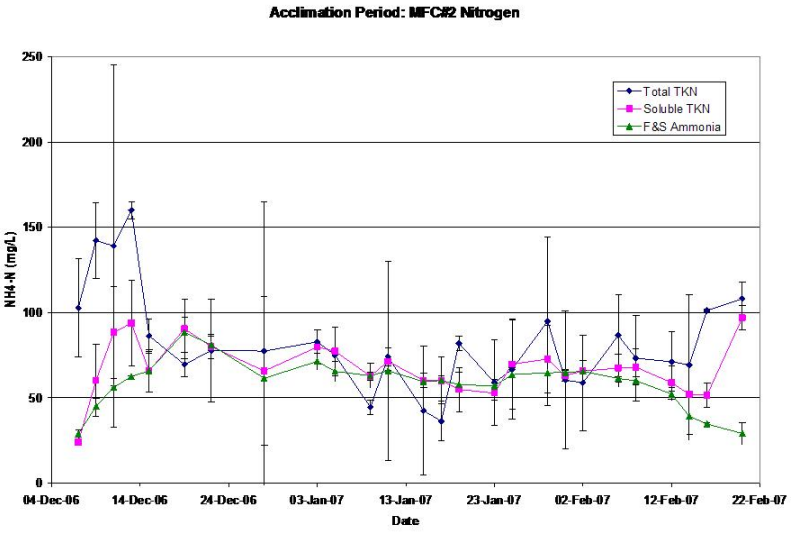

Figure 4.1.: *Cont'd*

- NH4-N content in both MFC anolyte samples was primarily composed of free and saline ammonia (FSA)

Both MFCs behaved similarly with respect to nitrogen analysis. While nitrogen species in the feed were primarily particulate in nature, the steady effluent of soluble, primarily FSA, nitrogen from both MFCs suggests that these particulate nitrogen species were solubilized and converted to ammonia. With feed nitrogen levels significantly greater than the samples, nitrogen accumulation in the MFCs was apparent.

4.3.3. Microbial Ecology

Following the treatment and transformation of the ecological data obtained from the BIOLOG® ECOplates, principal component analysis (PCA) was performed. Figure 4.2 shows the results of the PCA performed on ECOplates 6 through 8. ECOplate 6 represents the initial waste activated sludge at system start-up, while ECOplates 7 and 8 represent the bulk anolyte at the end of the acclimation period for MFC#1 and MFC#2, respectively. The first PCA ordination, Case 5.0, represents PCA performed on the dataset containing all the carbon source variables. The four following ordinations, Cases 5.1 to 5.4, represent

4. Impact of Carbon Source Dosing on MFCs Operating with Different Catholytes

PCA performed on datasets containing only subsets of the carbon source variables. These subsets represented carbohydrates (Case 5.1), carboxylic acids (Case 5.2), polymers and miscellaneous (Case 5.3) and amines and amino acids (Case 5.4). The analytical procedures and carbon source classifications are presented in Chapter 3. Evaluation of PCA ordinations is discussed in Chapter 3 as well.

The purpose of this case and set of sub-cases was to compare the initial microbial community in the waste activated sludge to that in the anolytes of both MFCs following an acclimation period of 77 days. It was hypothesized that the microbial communities of the MFCs would show significant differentiation from that of the initial waste activated sludge, identifying the existence of these shifts during MFC start up and acclimation. However no hypothesis was proposed as to how MFC#1 and MFC#2 may differ.

From Case 5.0 (a), the ECOplates showed strong differentiation from each other. In addition to being significantly different than the microbial community activity in the waste activated sludge, the microbial community activities in each MFC anolyte differed from each other. ECOplate 6 represented the same starting point for each MFC, with divergence to the states of ECOplate 7 and 8 after 77 days.

The sub-cases for the carbohydrates (Case 5.1 - b), polymers and miscellaneous (Case 5.3 - d) and amines and amino acids (Case 5.4 - e) showed similar results to the parent case. However, Case 5.2 (c), representing carboxylic acid utilization, showed no differentiation between the ECOplates. This was attributed to the continued anaerobic environmental state and the likely continued production of common volatile fatty acids (VFAs) through fermentation processes. Variance in the first principal component for ECOplate 6 replicates was apparent in the parent case and most sub-cases. By contrast, ECOplates 7 and 8 replicates showed little variation in the first principal component, indicating that the microbial community activity shift was toward a steadier state with more reproducible responses to carbon sources.

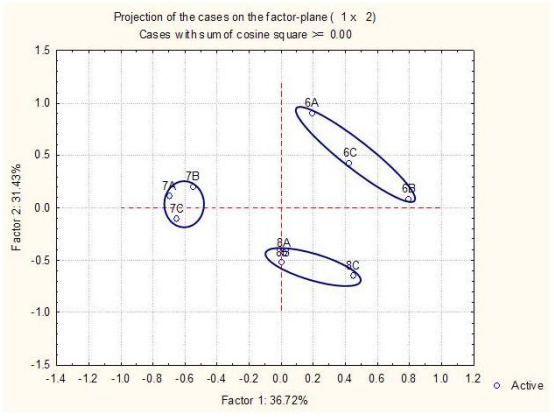

(a)

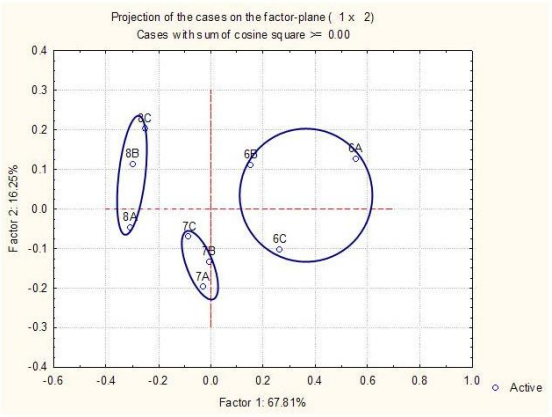

(b)

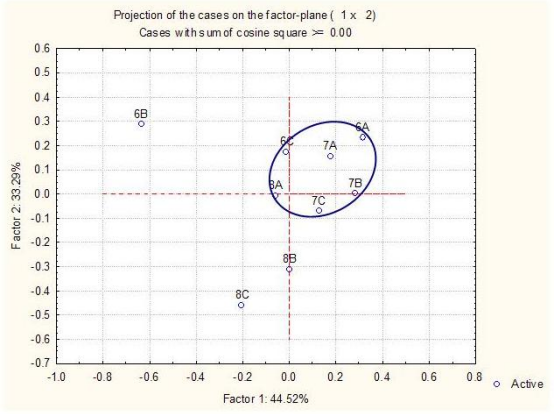

(c)

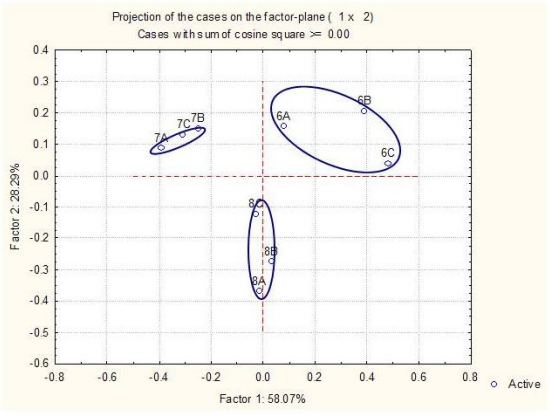

(d)

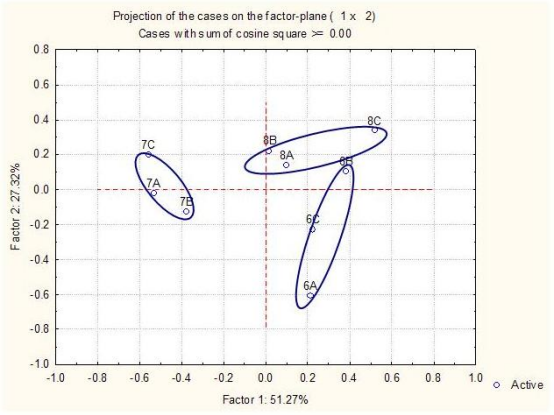

(e)

(a) = Case 5.0 - All ECOplate substrates
(b) = Case 5.1 - Carbohydrate substrates only
(c) = Case 5.2 - Carboxylic Acid substrates only
(d) = Case 5.3 - Polymer and Miscellaneous substrates only
(e) = Case 5.4 - Amine and Amino Acid substrates only

Figure 4.2.: *PCA Ordination for Cases 5.0 through 5.4 - ECOplates 6 through 8 - Acclimation Period*

4.4. Response to Sodium Acetate Dosing

4.4.1. Current and Power Production

Table 4.5 presents the current and power production results for MFC#1 and MFC#2 during sodium acetate dosing.

Table 4.5.: *Sodium Acetate Dosing: Coulomb and Power Production*

Electrical Variable	MFC#1	MFC#2
Coulombs per day	7.12	27.60
Maximum Power (mW)	0.050	0.162
Average Power (mW)	0.024	0.095

MFC#1 operated at approximately 25% to 30% of MFC#2 levels for all three electrical variables presented in Table 4.5. Similar to the performance comparison during the acclimation period, the lower current levels observed for MFC#1 were a direct result of the electron acceptor used. The measured DO concentration range in the MFC#1 catholyte during sodium acetate dosing was 4.3-6.9 mg/L, which was equivalent to 0.13-0.22 mM. Ferricyanide concentrations in the MFC#2 catholyte were maintained at levels approaching 40 mM. A lower electron acceptor concentration and slower electron acceptor kinetics limited MFC#1 operation during sodium acetate dosing.

Using the average power calculated for each MFC and the EESA and EMSA, upper and lower estimates of the average power densities for each MFC were calculated. For MFC#1, the EESA resulted in a power density of 0.87 mW/m^2 while the EMSA resulted in a power density of 34.9 mW/m^2. For MFC#2, the EESA resulted in a power density of 3.37 mW/m^2 while the EMSA resulted in a power density of 135.9 mW/m^2. With respect to current and power production, sodium acetate dosing appeared to increase the production only slightly when compared to results from the acclimation period. Maximum power values were actually found to be lower, while average power values were higher.

The current measurements carried out during this study were on the order of 0.01mA. This resulted in a system with strong sensitivity to variations in current. Current responses were immediately observed following sodium acetate dosing. These responses were particularly

profound in MFC#1, due to the lower operational current as compared to MFC#2. Figure 4.3 illustrates an increase in the MFC#1 current of 0.06mA over approximately 1.5 min and in response to sodium acetate dosing, which is indicated with the red line. Responses of this sensitivity raise the question as to the possibility of future application of MFC-like devices as sensors for readily biodegradable COD.

4.4.2. Wastewater Anolyte, Catholyte and Head Space Gas Analyses

Table 4.6 presents the COD results for the anolyte samples and head space gas during sodium acetate dosing. The analytical procedures and calculations are presented in Chapter 2.

Table 4.6.: *Sodium Acetate Dosing: Cumulative Chemical Oxygen Demand Results*

COD Variable	MFC#1 (mg)	MFC#2 (mg)
COD_{Feed}	2172∓244	2172∓244
COD_{CSP}	58.6∓2.9	58.6∓2.9
COD_{Smpl}	365∓195	660∓189
COD_{Elec}	10.6∓0.4	41.2∓7.7
COD_{Gas}	13.1∓44.2	17.6∓17.9
COD_{Acc} (calculated from Equation 2.4)	1841∓487	1512∓462
COD_{Ferri}		11.1∓280.7

The COD balance results during sodium acetate dosing were similar to those for the acclimation period. COD removal due to electricity production in MFC#2 was greater than that in MFC#1. In addition, the COD removal due to sampling of MFC#2 anolyte was noticeably larger than that of MFC#1. All other terms in the COD balance were similar for both MFCs. The ferricyanide catholyte results for MFC#2 were comparable to the electricity results. These results represent the accumulated totals from approximately 9 samples. The 95% confidence intervals associated with the results represents the accumulated error associated with the multiple sample analysis. Coulombic efficiencies were not calculated due to the large confidence intervals.

Figure 4.3.: *MFC#1 Current Response to Sodium Acetate Pulse*

The pH of the feed ranged from 7.6 to 7.8, while the anolyte samples ranged from 6.6 to 7.1 and 6.9 to 7.4 for MFC#1 and MFC#2, respectively. These results are nearly identical to those observed during the acclimation period. Lower observed pH values in the MFC anolytes as compared to the waste activated sludge feed were attributed to the accumulation of volatile fatty acids (VFAs) in the anolyte during fermentation processes.

Figure 4.4 presents the nitrogen content results for the feed and both MFCs during sodium acetate dosing. Error bars representing the 95% confidence level are indicated, and the CSPT dosage points are represented by red lines. The analytical procedures are presented in Chapter 2.

Similar points were drawn from Figure 4.4 as Figure 4.1:

- feed waste activated sludge nitrogen content was primarily found in the particulate matter
- NH4-N content in MFC#1 samples was 25-75 mg/L throughout sodium acetate dosing
- NH4-N content in MFC#2 samples was 75-100 mg/L throughout sodium acetate dosing
- NH4-N content in both MFC anolyte samples was primarily soluble, though not entirely composed of free and saline ammonia (FSA)

Both MFCs behaved similarly to each other with respect to nitrogen content results. The nitrogen content results during sodium acetate dosing were similar to those observed during the acclimation period. The total nitrogen levels in the waste activated sludge feed were approximately twice those observed in the anolyte samples, indicating further particulate nitrogen accumulation. The prevalence of FSA in the anolyte samples indicated that particulate nitrogen species were solubilized during MFC operation.

4.4.3. Microbial Ecology

Figure 4.5 shows the results of the principal component analysis (PCA) performed on ECOplates 7 through 10. ECOplates 7 and 9 represent the bulk anolyte samples from MFC#1, before and after sodium acetate dosing, respectively. ECOplates 8 and 10 represent the bulk anolyte samples from MFC#2, before and after sodium acetate dosing,

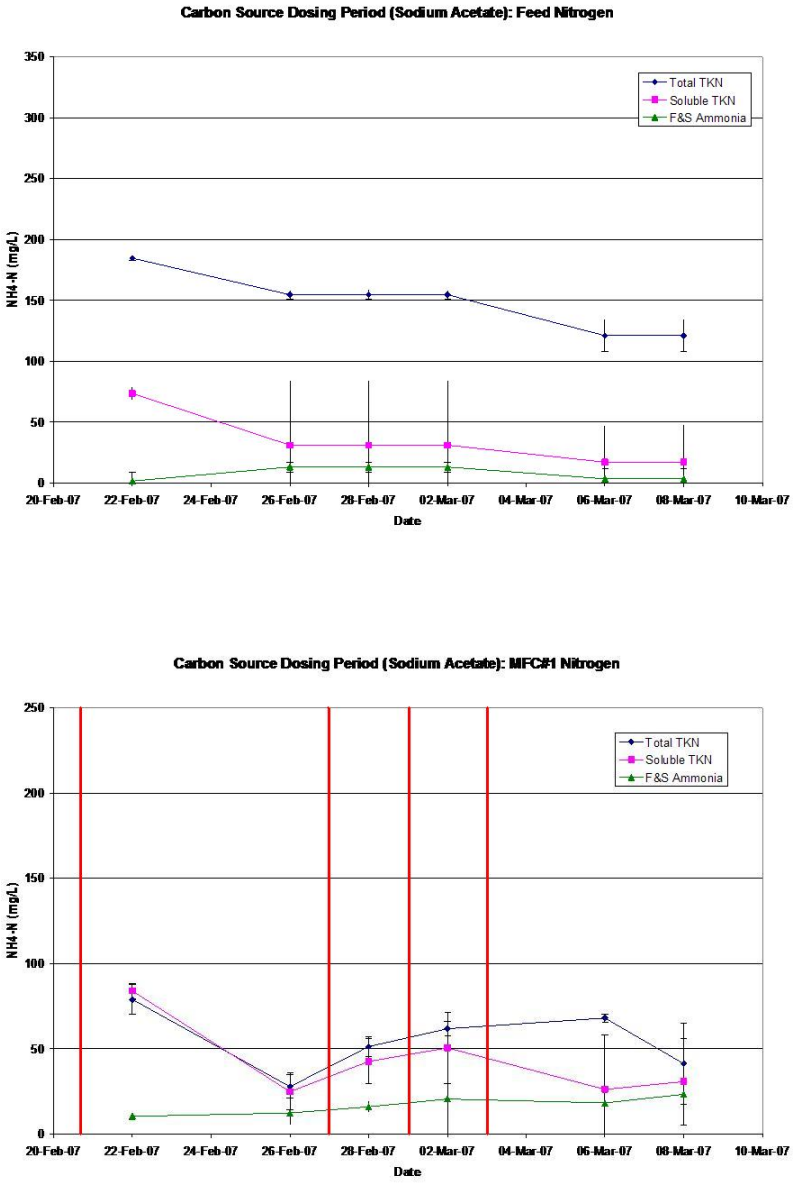

Figure 4.4.: *Nitrogen Content Results during Sodium Acetate Dosing*

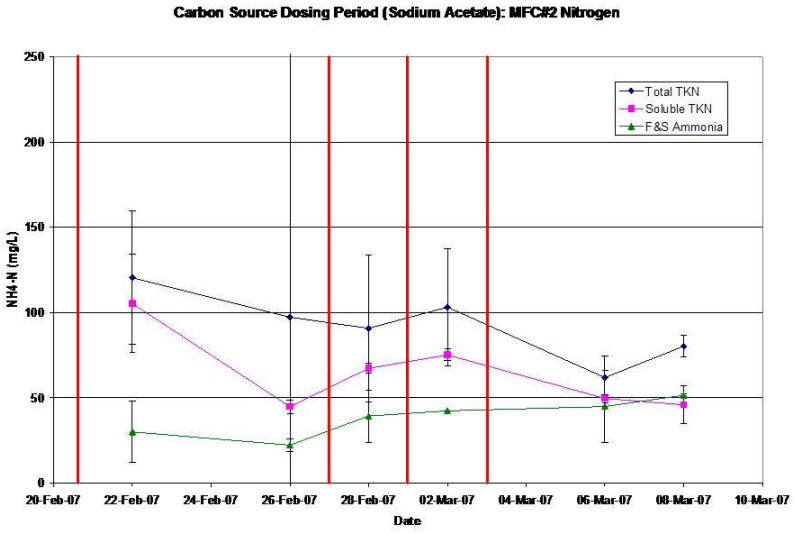

Figure 4.4.: *Cont'd*

respectively. The first PCA ordination, Case 6.0, represents PCA performed on the dataset containing all the carbon source variables. The four following ordinations, Cases 6.1 to 6.4, represent PCA performed on datasets containing only subsets of the carbon source variables. These subsets represented carbohydrates (Case 6.1), carboxylic acids (Case 6.2), polymers and miscellaneous (Case 6.3) and amines and amino acids (Case 6.4). The analytical procedures required to obtain these results and the carbon source classifications are presented in Chapter 3. Evaluation of PCA ordinations is discussed in Chapter 3 as well.

The purpose of this case and set of sub-cases was to compare the anolyte samples drawn from both MFCs, before and after sodium acetate dosing. It was hypothesized that the microbial communities of the MFCs would have converging shift responses, due to the common substrate dosing. Because sodium acetate was classified as a carboxylic acid, it was hypothesized that the primary microbial community activity shift would be due to carboxylic acid utilization.

From Case 6.0 (a), ECOplates 7 and 8 showed strong differentiation from each other. ECOplates 9 and 10 showed the same level of differentiation with respect to the first prin-

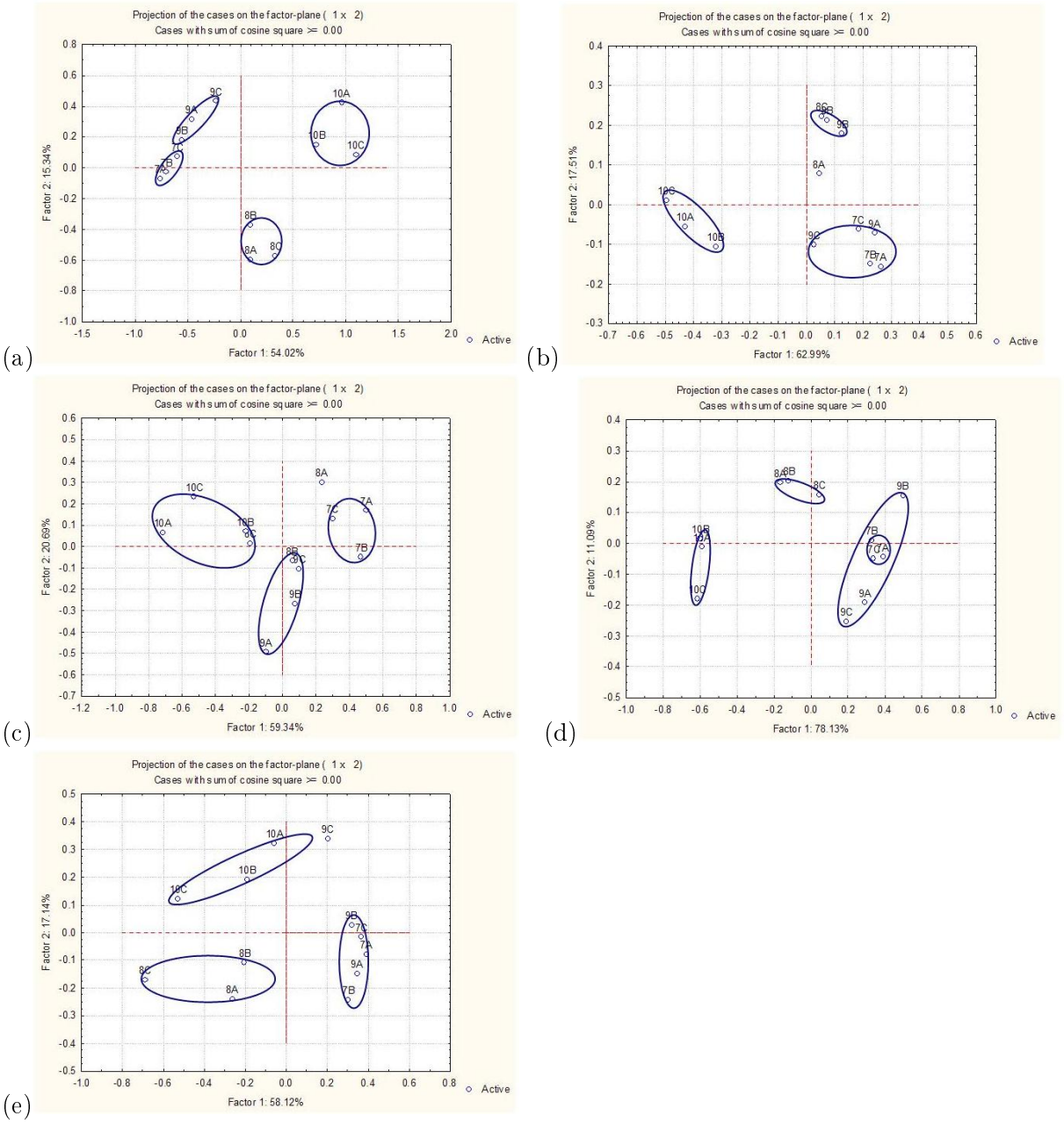

(a) = Case 6.0 - All ECOplate substrates
(b) = Case 6.1 - Carbohydrate substrates only
(c) = Case 6.2 - Carboxylic Acid substrates only
(d) = Case 6.3 - Polymer and Miscellaneous substrates only
(e) = Case 6.4 - Amine and Amino Acid substrates only

Figure 4.5.: *PCA Ordination for Cases 6.0 through 6.4 - ECOplates 7 through 10 - Sodium Acetate Dosing*

cipal component, having shifted from the positions of ECOplates 7 and 8 by the same magnitude. However, MFC#2 showed a greater shift with respect to the second principal component, which resulted in the same values as MFC#1. The sub-cases illustrate a divergence in behaviour between the two MFCs. MFC#1 was found to have little to no response in microbial community activity with respect to carbohydrate (Case 6.1), polymer and miscellaneous (Case 6.3) and amine and amino acid (Case 6.4) utilization. However, a shift in microbial community activity was observed for carboxylic acid utilization in MFC#1. ECOplate 9 appeared to be converging to a midpoint between ECOplates 8 and 10, suggesting a similar response to MFC#2, but a certain lag in that response. For MFC#2, definitive microbial community activity shifts were observed for all the sub-cases, though amine and amino acid utilization shifts were primarily in the second principal component. Table 4.6 indicates that the COD equivalency of all the sodium acetate added to each MFC was approximately 58.6 mg COD. During biodegradation of substrates, a portion of the energy is utilized for bacterial growth. A yield coefficient is used to identify the mass of bacterial growth due to a certain mass of substrate used. Yield coefficients under anaerobic conditions are typically 75% or less of those under aerobic conditions (Muller, Wentzel, & Ekama, 2004). Even if a yield coefficient of 1 is used, indicating that 1 mg of bacteria results from 1 mg of COD equivalence added, the sodium acetate dosing would have resulted in less than 60 mg of bacterial growth in each MFC. This indicated that shifts in carbon source utilization were more likely the result of a shift in microbial community activity rather than microbial community composition.

4.5. Response to Glucose Dosing

4.5.1. Current and Power Production

Table 4.7 presents the current and power production results for MFC#1 and MFC#2 during glucose dosing.

MFC#1 operated at approximately 28% to 32% of MFC#2 levels for all three electrical variables presented in Table 4.7. Similar to the performance comparison during sodium acetate dosing, the lower current levels observed for MFC#1 were a direct result of the electron acceptor used. The measured DO concentration range in the MFC#1 catholyte during glucose dosing was 2.5-4.5 mg/L, which was equivalent to 0.08-0.14 mM. Ferricyanide con-

Table 4.7.: *Glucose Dosing: Coulomb and Power Production*

Electrical Variable	MFC#1	MFC#2
Coulombs per day	7.66	27.47
Maximum Power (mW)	0.045	0.139
Average Power (mW)	0.027	0.096

centrations in the MFC#2 catholyte were maintained at levels approaching 39 mM. A lower electron acceptor concentration and slower electron acceptor kinetics limited MFC#1 operation during glucose dosing.

Using the average power calculated for each MFC and the EESA and EMSA, upper and lower estimates of the average power densities for each MFC were calculated. For MFC#1, the EESA resulted in a power density of 0.94 mW/m^2 while the EMSA resulted in a power density of 38.0 mW/m^2. For MFC#2, the EESA resulted in a power density of 3.39 mW/m^2 while the EMSA resulted in a power density of 136.6 mW/m^2. With respect to current and power production in MFC#1, glucose dosing appeared to increase the production only slightly when compared to results observed during sodium acetate dosing. MFC#2 results throughout dosing these two substrates were nearly identical, indicating glucose effects on current and power production in MFC#2 were negligible.

During glucose dosing, gradual responses in current were observed. These responses were more easily observable for MFC#1, due to the lower operational current as compared to MFC#2. Figure 4.6 illustrates an increase in the MFC#1 current of 0.015mA over approximately 40 min in response to glucose dosing, which is indicated with the red line. This was only 25% of the current increase response seen with sodium acetate dosing with a response time that was approximately 26 times longer.

4.5.2. Wastewater Anolyte, Catholyte and Head Space Gas Analyses

Table 4.8 presents the COD results for the anolyte samples and head space gas during glucose dosing. The analytical procedures and calculations required to obtain these values are presented in Chapter 2.

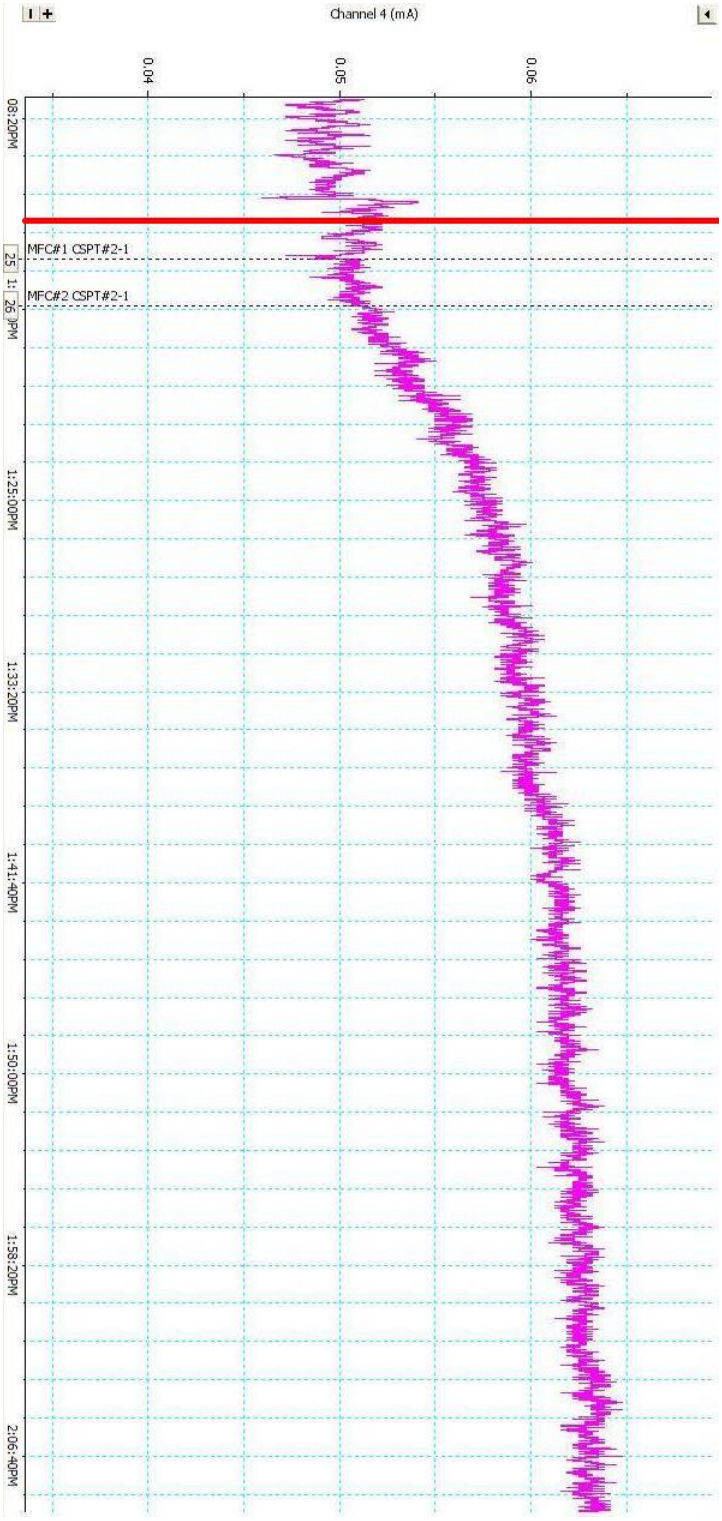

Figure 4.6.: *MFC#1 Current Response to Glucose Pulse*

Table 4.8.: *Glucose Dosing: Cumulative Chemical Oxygen Demand Results*

COD Variable	MFC#1 (mg)	MFC#2 (mg)
COD_{Feed}	1757∓119	1757∓119
COD_{CSP}	11.4∓0.6	11.4∓0.6
COD_{Smpl}	448∓126	500∓105
COD_{Elec}	8.9∓0.3	31.9∓6.0
COD_{Gas}	20.2∓49.2	28.8∓16.8
COD_{Acc} (calculated from Equation 2.4)	1291∓296	1209∓247
COD_{Ferri}		51.2∓50.2

The COD balance results during glucose dosing were similar to those during the sodium acetate dosing. COD removal due to electricity production in MFC#2 was greater than that in MFC#1, while all other terms in the COD balance were similar for both MFCs. The ferricyanide catholyte results for MFC#2 were comparable to the electricity results. These results represent the accumulated totals from approximately 7 samples. The 95% confidence intervals associated with the results represents the accumulated error associated with the multiple sample analysis. Coulombic efficiencies were not calculated due to the large confidence intervals.

The pH of the feed ranged from 7.7 to 7.9, while the anolyte samples ranged from 6.4 to 6.9 and 6.8 to 7.3 for MFC#1 and MFC#2, respectively. While the feed pH was higher during glucose dosing than during sodium acetate dosing, the anolytes showed lower pH values. The larger disparity between observed pH values in the MFC anolytes and the waste activated sludge feed were attributed to continued accumulation of volatile fatty acids (VFAs) in the anolyte during fermentation processes. Glucose is a precursor for VFA production during fermentation processes.

Figure 4.7 presents the nitrogen content results for the feed and both MFCs during glucose dosing. Error bars were added with a 95% confidence level, and the CSPT dosage points are represented by red lines.

Conclusions from Figure 4.7 were similar to those from Figure 4.4:

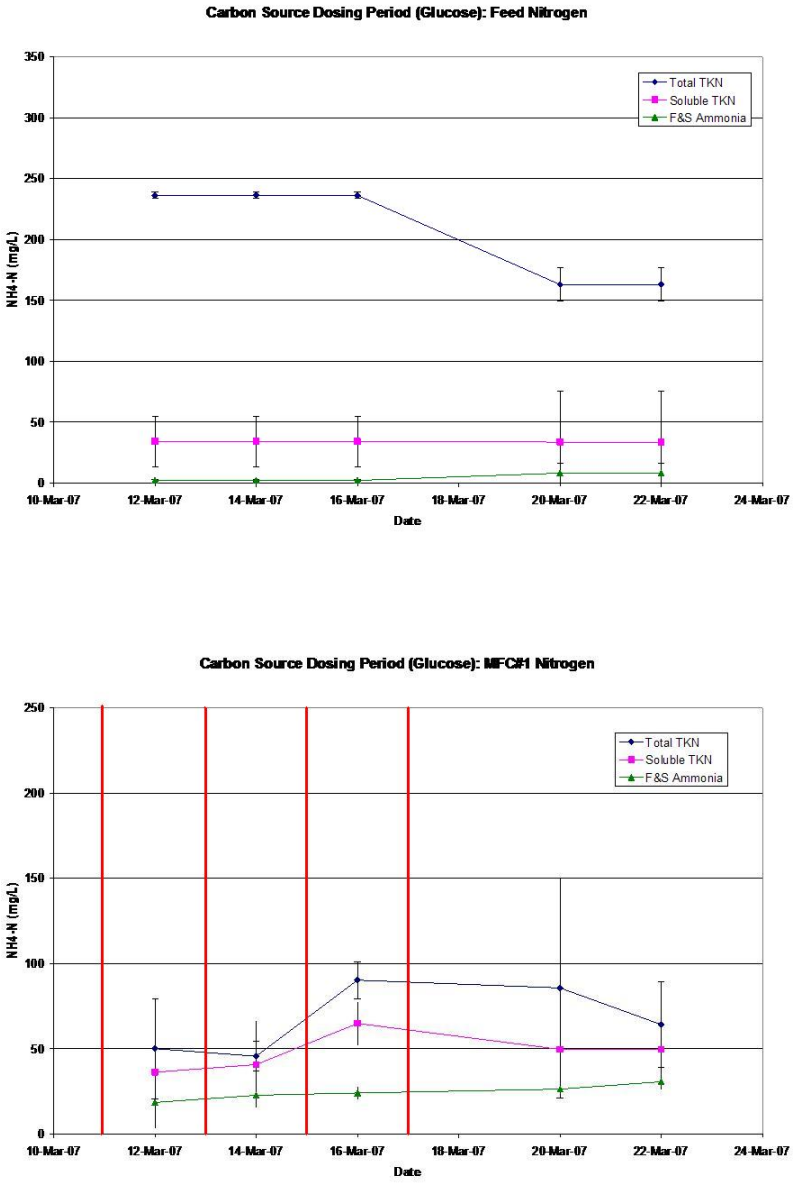

Figure 4.7.: *Nitrogen Content Results during Glucose Dosing*

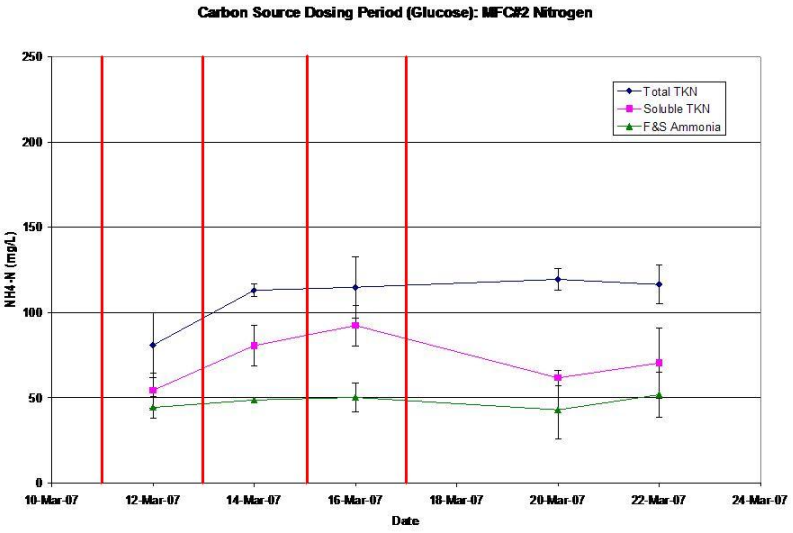

Figure 4.7.: *Cont'd*

- feed waste activated sludge nitrogen content was primarily found in the particulate matter
- NH4-N content in MFC#1 samples was 50-100 mg/L throughout glucose dosing
- NH4-N content in MFC#2 samples was 75-125 mg/L throughout glucose dosing
- NH4-N content in both MFC anolyte samples was primarily soluble, though not entirely composed of free and saline ammonia (FSA)

Both MFCs behaved similarly to each other with respect to nitrogen content results. The nitrogen content results during glucose dosing were similar to those observed during sodium acetate dosing. FSA presence in the anolytes was attributed to the solubilization of particulate nitrogen species.

4.5.3. Microbial Ecology

Figure 4.8 shows the results of the principal component analysis (PCA) performed on ECOplates 9 through 12. ECOplates 9 and 11 represent the bulk anolyte samples from MFC#1, before and after glucose dosing, respectively. ECOplates 10 and 12 represent the

bulk anolyte samples from MFC#2, before and after glucose dosing, respectively. The first PCA ordination, Case 7.0, represents PCA performed on the dataset containing all the carbon source variables. The four following ordinations, Cases 7.1 to 7.4, represent PCA performed on datasets containing only subsets of the carbon source variables. These subsets represented carbohydrates (Case 7.1), carboxylic acids (Case 7.2), polymers and miscellaneous (Case 7.3) and amines and amino acids (Case 7.4). The analytical procedures required to obtain these results and the carbon source classifications are presented in Chapter 3. Evaluation of PCA ordinations is discussed in Chapter 3 as well.

The purpose of this case and set of sub-cases was to compare the anolyte samples drawn from both MFCs, before and after glucose dosing. It was hypothesized that the microbial communities of the MFCs would have converging shift responses, due to the common substrate dosing. Because glucose is a carbohydrate, it was hypothesized that the primary microbial community activity shift would be due to carbohydrate utilization.

From Case 7.0 (a), ECOplates 10 and 11 showed an aggregation or grouping. This would suggest that MFC#1 had reached a similar state of carbon source utilization following glucose dosing as MFC#2 had before glucose dosing. ECOplates 10 and 12 showed differentiation with respect to the second principal component, resulting from a smaller portion of the dataset variance. ECOplate 9 was significantly segregated from the other ECOplates, indicating a difference in MFC#1 before and after glucose dosing. In essence, the glucose dosing appeared to have a converging effect on the microbial community activities of the two MFCs that originally diverged during acclimation and sodium acetate dosing. The carbohydrate sub-case (Case 7.1 - b) was almost identical to the parent case, indicating that carbohydrate utilization was the defining carbon source subset. The other sub-cases for carboxylic acid (Case 7.2 - c), polymer and miscellaneous (Case 7.3 - d) and amine and amino acid (Case 7.4 - e) utilization were similar to the parent case. MFC#1 showed a strong microbial community activity shift following glucose dosing, however, the main result was the convergence of the microbial community activities of the two MFCs. MFC#2 showed little change in microbial community activity following glucose dosing, with carboxylic acid utilization nearly identical. It was possible that the carbon source utilization shifts observed for the MFC#1 microbial community may have been part of a continued response to the sodium acetate dosing, rather than an independent response to glucose dosing. This was considered due to

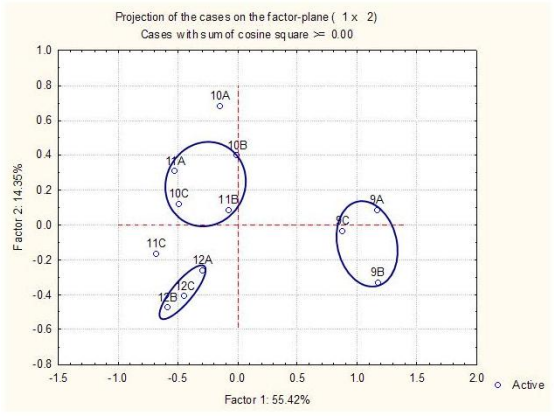

(a)

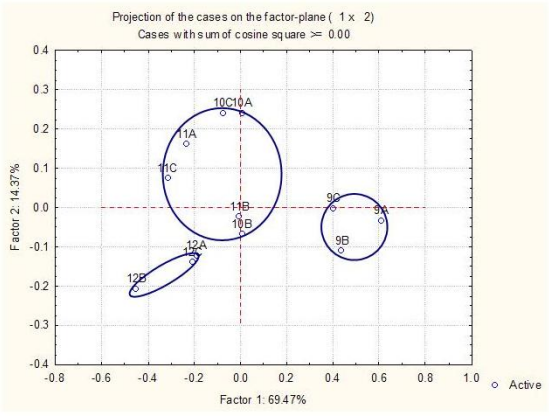

(b)

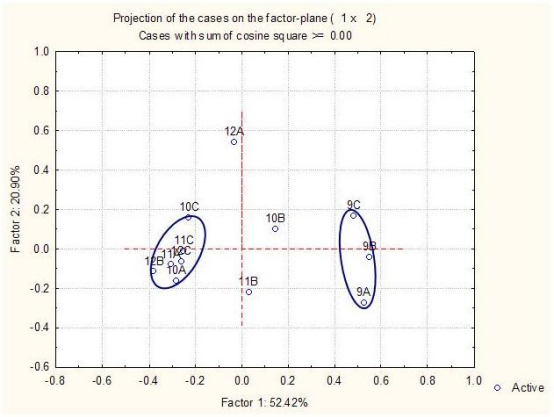

(c)

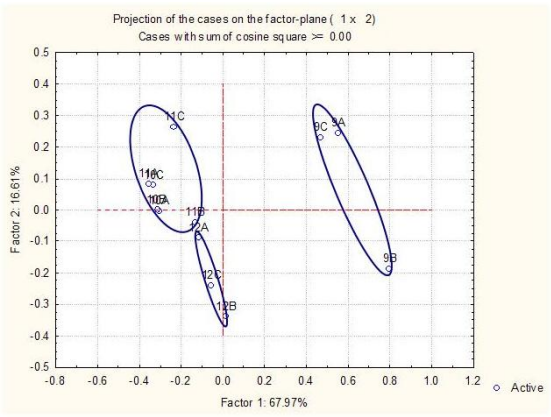

(d)

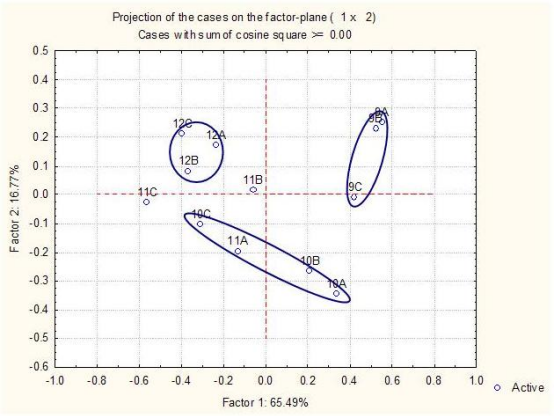

(e)

(a) = Case 7.0 - All ECOplate substrates
(b) = Case 7.1 - Carbohydrate substrates only
(c) = Case 7.2 - Carboxylic Acid substrates only
(d) = Case 7.3 - Polymer and Miscellaneous substrates only
(e) = Case 7.4 - Amine and Amino Acid substrates only

Figure 4.8.: *PCA Ordination for Cases 7.0 through 7.4 - ECOplates 9 through 12 - Glucose Dosing*

the combination of a high dose of COD equivalence in the first sodium acetate pulse and the lower operational levels observed in MFC#1. This hypothesis introduced a confounding effect linked to the lower operational limits of MFC#1 with no discernible way to assure independence of sodium acetate and glucose results. Future studies should incorporate longer intermediate times between multiple carbon source pulse tests. Table 4.8 indicates that the COD equivalency of all the glucose added to each MFC was approximately 11.4 mg COD. If a yield coefficient of 1 is used, the glucose dosing would have resulted in less than 12 mg of bacterial growth in each MFC. Similarly to sodium acetate dosing, shifts in carbon source utilization were more likely the result of a shift in microbial community activity rather than microbial community composition.

4.6. Response to Glycerol Dosing

4.6.1. Current and Power Production

Table 4.9 presents the current and power production results for MFC#1 and MFC#2 during glycerol dosing.

Table 4.9.: *Glycerol Dosing: Coulomb and Power Production*

Electrical Variable	MFC#1	MFC#2
Coulombs per day	9.21	28.10
Maximum Power (mW)	0.057	0.123
Average Power (mW)	0.032	0.098

MFC#1 operated at approximately 33% to 46% of MFC#2 levels for all three electrical variables presented in Table 4.9. Similar to the performance comparison during sodium acetate and glucose dosing, the lower current levels observed for MFC#1 were a direct result of the electron accpetor used. The measured DO concentration range in the MFC#1 catholyte during glycerol dosing was 2.9-4.2 mg/L, which was equivalent to 0.09-0.13 mM. Ferricyanide concentrations in the MFC#2 catholyte were maintained at levels approaching 40 mM. A lower electron acceptor concentration and slower electron acceptor kinetics limited MFC#1 operation during glycerol dosing.

Using the average power calculated for each MFC and the EESA and EMSA, upper and lower estimates of the average power densities for each MFC were calculated. For MFC#1, the EESA resulted in a power density of 1.14 mW/m^2 while the EMSA resulted in a power density of 45.8 mW/m^2. For MFC#2, the EESA resulted in a power density of 3.47 mW/m^2 while the EMSA resulted in a power density of 139.8 mW/m^2. With respect to current and power production in MFC#1, glycerol dosing appeared to increase the production only slightly when compared to results during glucose dosing. MFC#2 results were even closer, suggesting glycerol dosing had even less of an effect on current and power production in MFC#2.

During glycerol dosing, almost no response in current was observed. The dosing points were more easily observable for MFC#1, due to the lower operational current as compared to MFC#2. Figure 4.9 illustrates no increase in the MFC#1 current in response to glycerol dosing. It appeared that current values dropped slightly during and immediately following glycerol dosing, which is indicated with the red line. This may have been a result of small amounts of oxygen entering the anolyte and providing a short-lived, alternative electron acceptor. With no electrical response, it was difficult to determine biodegradation comparisons to the other carbon sources.

4.6.2. Wastewater Anolyte, Catholyte and Head Space Gas Analyses

Table 4.10 presents the COD results for the anolyte samples and head space gas during glycerol dosing.

The COD balance results during glycerol dosing were almost identical to those observed during glucose dosing. COD removal due to electricity production in MFC#2 was greater than that in MFC#1, while all other terms in the COD balance were similar for both MFCs. The ferricyanide catholyte results for MFC#2 were comparable to the electricity results. These results represent the accumulated totals from approximately 7 samples. The 95% confidence intervals associated with the results represents the accumulated error associated with the multiple sample analysis. Coulombic efficiencies were not calculated due to the large confidence intervals.

The pH of the feed ranged from 8.0 to 8.2, while the anolyte samples ranged from 6.7 to 7.3

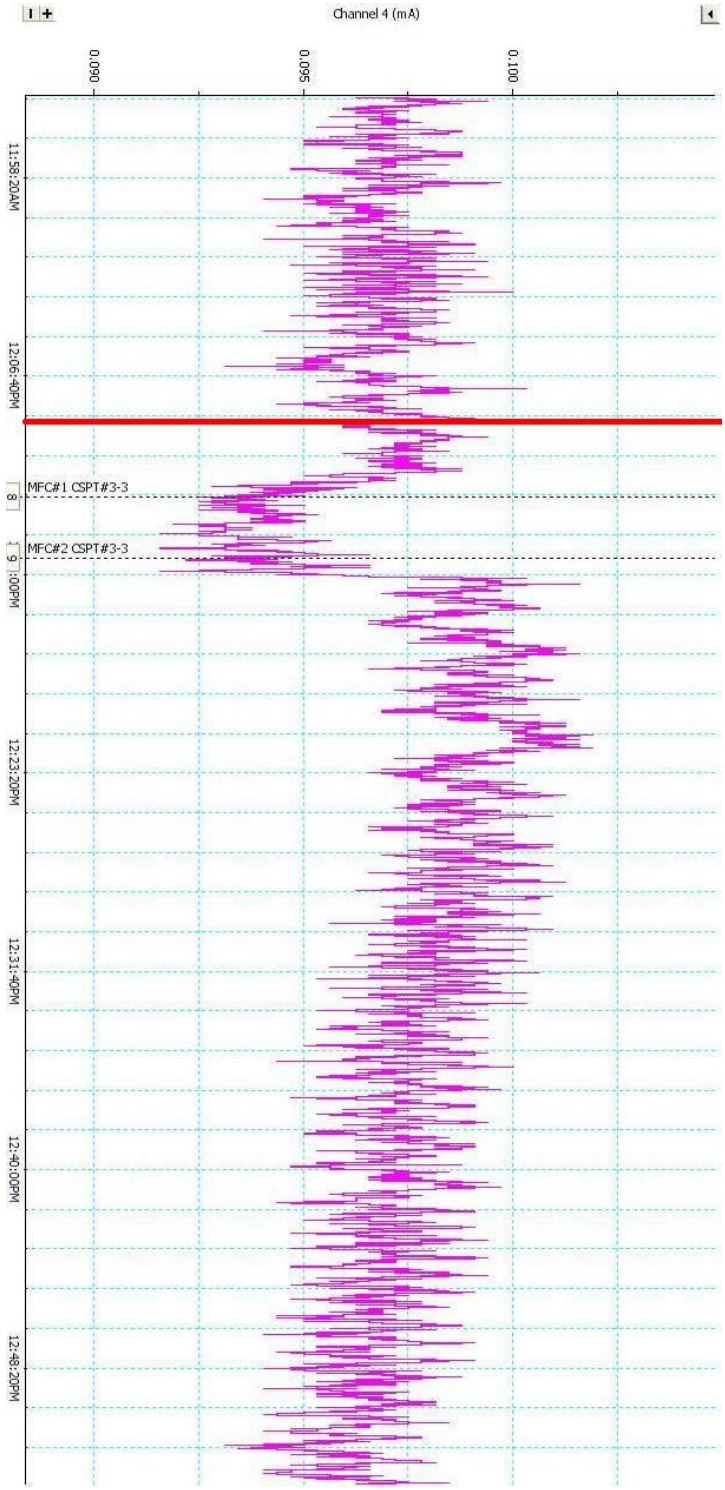

Figure 4.9.: *MFC#1 Current Response to Glycerol Pulse*

Table 4.10.: *Glycerol Dosing: Cumulative Chemical Oxygen Demand Results*

COD Variable	MFC#1 (mg)	MFC#2 (mg)
COD_{Feed}	1973∓47	1973∓47
COD_{CSP}	11.4∓0.6	11.4∓0.6
COD_{Smpl}	534∓99	669∓121
COD_{Elec}	10.7∓0.4	32.6∓6.1
COD_{Gas}	20.4∓15.2	27.9∓20.7
COD_{Acc} (calculated from Equation 2.4)	1419∓162	1254∓196
COD_{Ferri}		13.8∓135.2

and 7.0 to 7.6 for MFC#1 and MFC#2, respectively. The feed pH continued to increase when compared to pH levels during earlier operation. The anolytes showed lower pH values than the feed waste activated sludge, but the values increased during glycerol dosing as compared to the values during glucose dosing. Higher feed pH values were responsible for negating some of the pH lowering effects of volatile fatty acid (VFAs) production in the anolytes.

Figure 4.10 presents the nitrogen content results for the feed and both MFCs during glycerol dosing. Error bars were added with a 95% confidence level, and the CSPT dosage points are represented by red lines. The analytical procedures required to obtain these results are presented in Chapter 2.

nitrogen content results during glycerol dosing were similar to those observed during earlier operation:

- feed waste activated sludge nitrogen content was primarily found in the particulate matter
- NH4-N content in MFC#1 samples was 75-125 mg/L throughout glycerol dosing
- NH4-N content in MFC#2 samples was 100-175 mg/L throughout glycerol dosing
- NH4-N content in both MFC anolyte samples was approximately 60% soluble, of which most of the soluble nitrogen was free and saline ammonia (FSA)

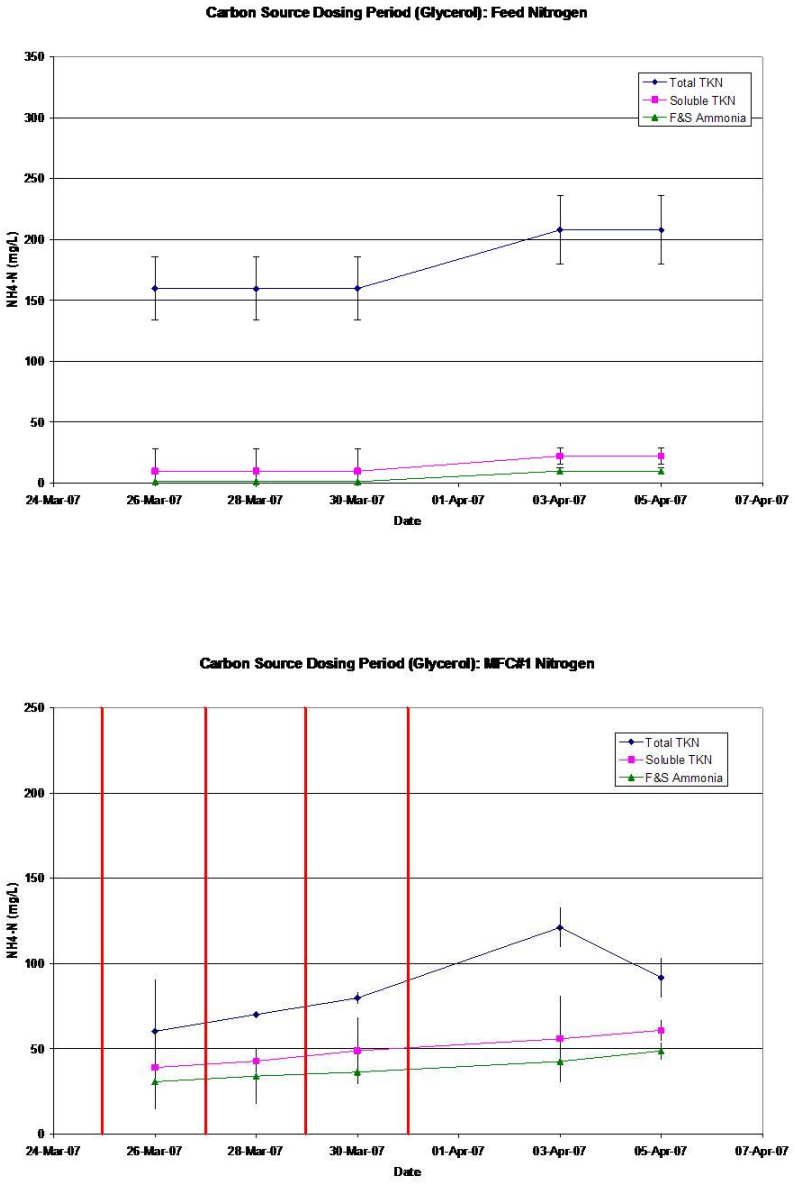

Figure 4.10.: *Nitrogen Content Results during Glycerol Dosing*

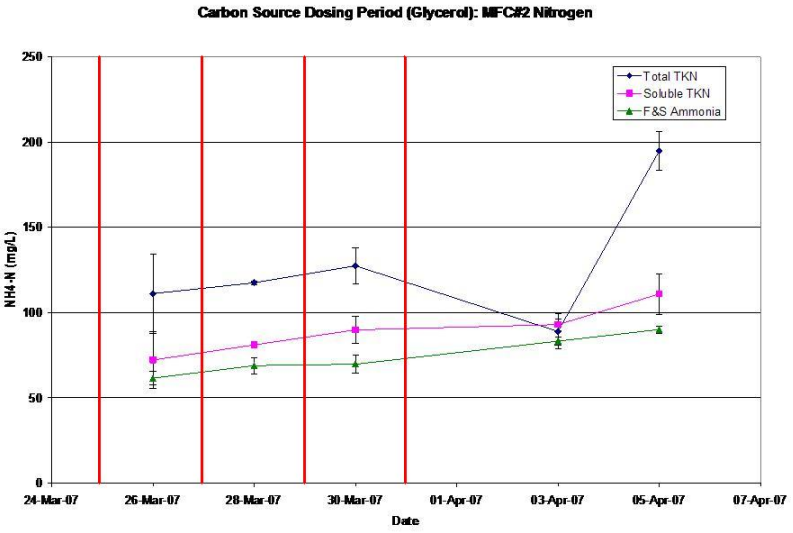

Figure 4.10.: *Cont'd*

Both MFCs behaved similarly to each other with respect to nitrogen content results. The nitrogen content results during glycerol dosing exhibited a trend in the nitrogen analysis. The total nitrogen in the anolyte samples increased with time, while the soluble nitrogen and FSA remained constant. This decreased the FSA portion of the effluent nitrogen from the MFCs. Nitrogen containing particulate was not being solubilized as quickly as it was added to the system. Particulate nitrogen components had reached an accumulation threshold, and increased levels were observed in the anolyte samples due to greater particulate nitrogen in the effluent.

4.6.3. Microbial Ecology

Figure 4.11 shows the results of the principal component analysis (PCA) performed on ECOplates 11 through 14. ECOplates 11 and 13 represent the bulk anolyte samples from MFC#1, before and after glycerol dosing, respectively. ECOplates 12 and 14 represent the bulk anolyte samples from MFC#2, before and after glycerol dosing, respectively. The first PCA ordination, Case 8.0, represents PCA performed on the dataset containing all the carbon source variables. The four following ordinations, Cases 8.1 to 8.4, represent PCA performed on datasets containing only subsets of the carbon source variables. These

subsets represented carbohydrates (Case 8.1), carboxylic acids (Case 8.2), polymers and miscellaneous (Case 8.3) and amines and amino acids (Case 8.4). The analytical procedures required to obtain these results and the carbon source classifications are presented in Chapter 3. Evaluation of PCA ordinations is discussed in Chapter 3 as well.

The purpose of this case and set of sub-cases was to compare the anolyte samples drawn from both MFCs, before and after glycerol dosing. It was hypothesized that the microbial communities of the MFCs would have converging shift responses, due to the common substrate dosing. Because glycerol was classified as a carbohydrate, it was hypothesized that the primary microbial community activity shift would be due to carbohydrate utilization.

From Case 8.0 (a), the opposite effect of what was hypothesized was observed. Glycerol dosing resulted in a divergence of the microbial community activity of the MFCs. ECOplates 11 and 12 were grouped together, indicating a common microbial community activity in the MFCs before glycerol dosing. ECOplates 13 and 14 shifted in opposite directions with respect to the first principal component. Analysis of the sub-cases indicated that responses in the carboxylic acids (Case 8.2 - c) and amines and amino acids (Case 8.4 - e) were primarily responsible for the shift in the MFC#2 microbial community activity. Responses in the carbohydrates (Case 8.1 - b) were primarily responsible for the shift in the MFC#1 microbial community activity. Responses in the polymers and miscellaneous (Case 8.3 - d) were similar to the parent case, since the second principal component represented an amount of the dataset variance nearly equal to that of the first principal component. From these results, it appeared that MFC#1 responded to the glycerol dosing with shifts in the carbohydrate utilization, while MFC#2 showed shifts in less related carbon source classifications. The shift in the carboxylic acid utilization for MFC#2 may have been in response to the presence of glycerol, due to interactions between volatile fatty acids and glycerol.

4.7. Response to Bovine Serum Albumin (BSA) Dosing

4.7.1. Current and Power Production

Table 4.11 presents the current and power production results for MFC#1 and MFC#2 during BSA dosing.

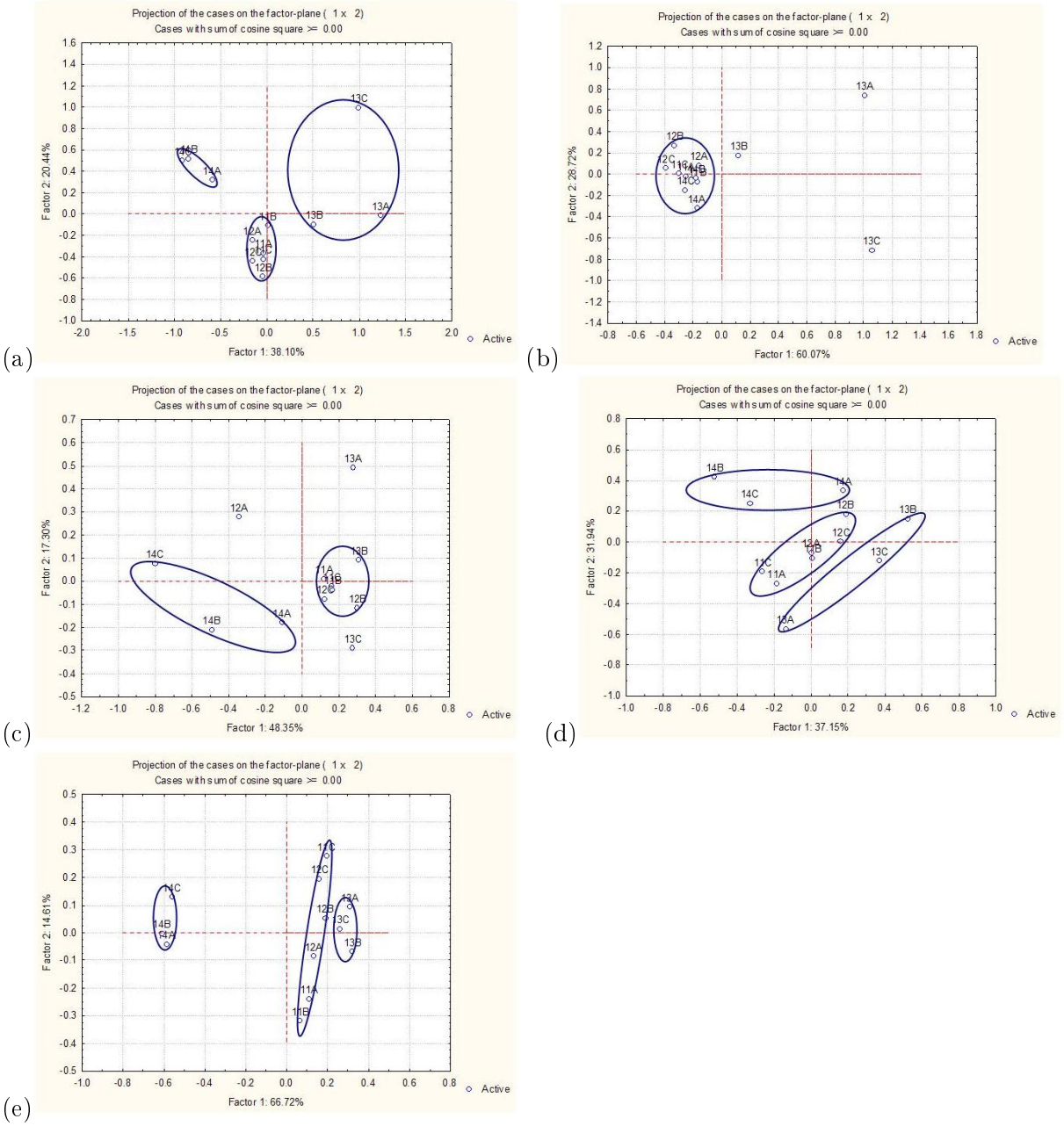

(a) = Case 8.0 - All ECOplate substrates
(b) = Case 8.1 - Carbohydrate substrates only
(c) = Case 8.2 - Carboxylic Acid substrates only
(d) = Case 8.3 - Polymer and Miscellaneous substrates only
(e) = Case 8.4 - Amine and Amino Acid substrates only

Figure 4.11.: *PCA Ordination for Cases 8.0 through 8.4 - ECOplates 11 through 14 - Glycerol Dosing*

Table 4.11.: *BSA Dosing: Coulomb and Power Production*

Electrical Variable	MFC#1	MFC#2
Coulombs per day	17.88	35.15
Maximum Power (mW)	0.154	0.316
Average Power (mW)	0.062	0.122

MFC#1 operated at approximately 50% of MFC#2 levels for all three electrical variables presented in Table 4.11. Both MFCs showed significantly increased performance when compared to all earlier observations. MFC#1 showed an increase of 100% in average power, while MFC#2 showed an increase of 25% when compared to power production levels observed during glycerol dosing. Lower current levels observed for MFC#1 were a direct result of the electron accpetor used. The measured DO concentration range in the MFC#1 catholyte during BSA dosing was 3.6-4.8 mg/L, which was equivalent to 0.11-0.15 mM. Ferricyanide concentrations in the MFC#2 catholyte were maintained at levels approaching 40 mM. A lower electron acceptor concentration and slower electron acceptor kinetics limited MFC#1 operation during BSA dosing.

Using the average power calculated for each MFC and the EESA and EMSA, upper and lower estimates of the average power densities for each MFC were calculated. For MFC#1, the EESA resulted in a power density of 2.21 mW/m^2 while the EMSA resulted in a power density of 88.9 mW/m^2. For MFC#2, the EESA resulted in a power density of 4.34 mW/m^2 while the EMSA resulted in a power density of 174.8 mW/m^2. With respect to current and power production in MFC#1, BSA dosing increased the current and power production of both MFCs by significant levels when compared to results observed during other carbon source dosings. Results for MFC#1 were particularly unexpected. Average power output during the 14 day duration of the BSA dosing was doubled when compared to glycerol dosing. There are two hypotheses posed to address these increases in current production following BSA dosing:

1. the BSA provided a nutrient or structural component that increased the biodegradation potential by electricity producing bacteria
2. electrochemical properties of BSA allowed the protein to act as an electron mediator between electricity producing bacteria in the anolyte and the anode surface

Regardless of the mechanism or interaction of BSA with the anolyte resulting in increased current production, MFC#1 showed twice the magnitude of current increase as compared to MFC#2. The lower operational state of MFC#1 was limited by the dissolved oxygen catholyte. Changes in the anolyte chemistry were able to partially overcome these limitations. MFC#2 showed similar behaviour, but to a lesser degree, due to the higher operational state with a ferricyanide catholyte.

During BSA dosing, gradual responses in current were observed, similar to the results observed during glucose dosing. These responses were more easily observable for MFC#1, due to the lower operational current as compared to MFC#2. Figure 4.12 illustrates an increase in the MFC#1 current of 0.015mA over approximately 25 min in response to BSA dosing, which is indicated with the red line. This was only 25% of the current increase response seen with sodium acetate dosing with a response time that was approximately 17 times longer. BSA was active at an electricity producing level, but was less biodegradable than sodium acetate.

4.7.2. Wastewater Anolyte, Catholyte and Head Space Gas Analyses

Table 4.12 presents the COD results for the anolyte samples and head space gas during BSA dosing.

Table 4.12.: *BSA Dosing: Cumulative Chemical Oxygen Demand Results*

COD Variable	MFC#1 (mg)	MFC#2 (mg)
COD_{Feed}	1912∓94	1912∓94
COD_{CSP}	11.4∓0.6	11.4∓0.6
COD_{Smpl}	1748∓198	1239∓118
COD_{Elec}	20.7∓0.7	40.8∓7.7
COD_{Gas}	6.0∓54.7	17.8∓7.2
COD_{Acc} (calculated from Equation 2.4)	149∓349	626∓227
COD_{Ferri}		41.1∓141.4

The COD balance results during BSA dosing were similar to those observed during the other

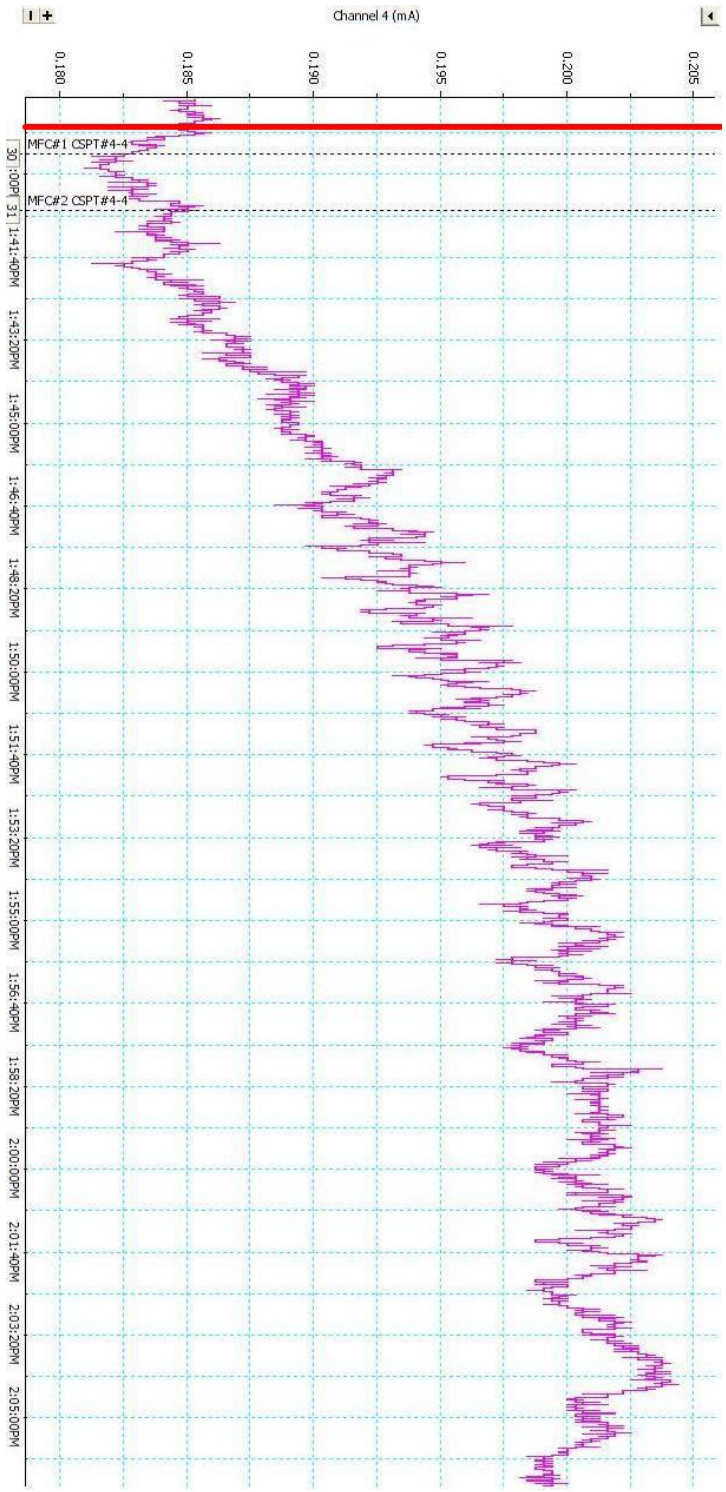

Figure 4.12.: *MFC#1 Current Response to BSA Pulse*

carbon source dosings. COD removal due to electricity production in MFC#2 was greater than that in MFC#1, while all other terms in the COD balance were similar for both MFCs. The COD removed due to electricity generation was higher during BSA dosing than during the other carbon source dosings due to the higher current production. However, this did not translate into large changes in the COD removal relative to the COD fed to the MFCs. COD removal due to anolyte sampling was significantly larger, but this was due to manual agitation of the anolyte in the anode chambers of both MFCs on April 19th, 2007, prior to sampling. The significantly higher COD values observed for anolyte samples following manual agitation provided some confirmation of COD accumulation within both MFCs. The ferricyanide catholyte results for MFC#2 were almost identical to the electricity results, though the confidence interval was significantly larger. These results represent the accumulated totals from approximately 7 samples. The 95% confidence intervals associated with the results represents the accumulated error associated with the multiple sample analysis. Coulombic efficiencies were not calculated due to the large confidence intervals.

The pH of the feed ranged from 8.0 to 8.2, while the anolyte samples ranged from 6.9 to 7.7 and 7.1 to 7.5 for MFC#1 and MFC#2, respectively. The feed pH was equal to levels observed during glycerol dosing. The anolytes showed lower pH values than the feed waste activated sludge, but the values continued to increase during BSA dosing when compared to levels observed during earlier carbon source dosing. A decrease in volatile fatty acid (VFAs) production in the anolytes would result in higher pH values and indicate less fermentation processes being active. This was in agreement with the increased current and power production observed during BSA dosing.

Figure 4.13 presents the nitrogen content results for the feed and both MFCs during BSA dosing. Error bars were added with a 95% confidence level, and the CSPT dosage points are represented by red lines.

Several conclusions can be made from Figure 4.13:

- feed waste activated sludge nitrogen content was primarily found in the particulate matter
- NH4-N content in MFC#1 samples was 125-150 mg/L throughout BSA dosing

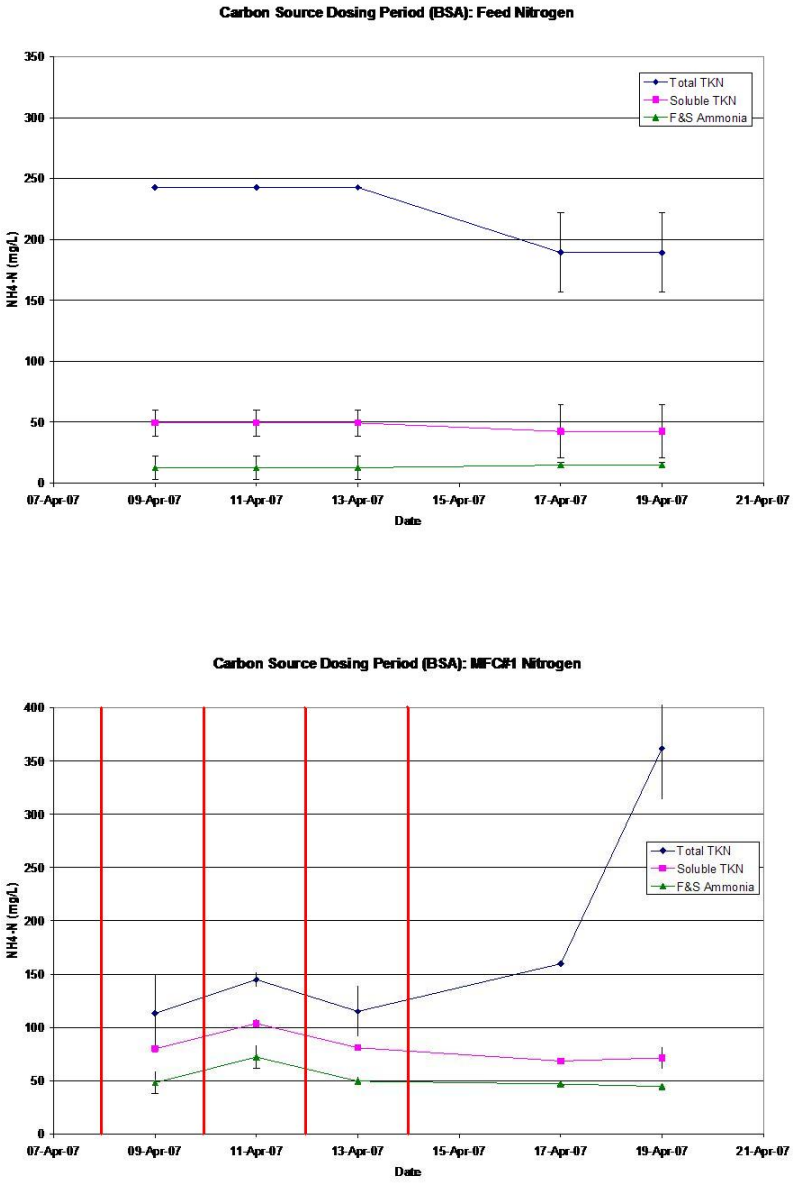

Figure 4.13.: *Nitrogen Content Results during BSA Dosing*

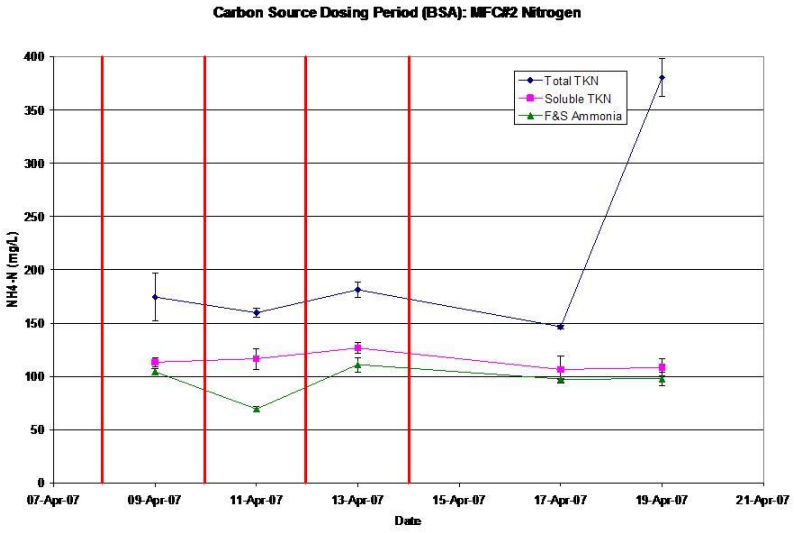

Figure 4.13.: *Cont'd*

- NH4-N content in MFC#2 samples was 150-175 mg/L throughout BSA dosing
- NH4-N content in both MFC anolyte samples was approximately 60% soluble, of which most of the soluble nitrogen was free and saline ammonia (FSA)
- the final nitrogen sample on April 19th, 2007 showed nitrogen levels in excess of 350 mg NH4-N/L, primarily particulate in nature

Both MFCs behaved similarly to each other with respect to nitrogen content results. The nitrogen content results observed during BSA dosing showed further increases in particulate nitrogen in the anolyte samples. This was in agreement with the identified trend of increased nitrogen in the anolyte samples due to accumulated particulate nitrogen in the MFCs. BSA contains nitrogen, so increases in the soluble nitrogen levels in the anolyte samples were expected and observed. These trends were more pronounced in the MFC#1 results, which was in agreement with the greater electricity production response due to BSA dosing observed in MFC#1. The high levels of particulate nitrogen observed in the April 19th, 2007 anolyte samples were a direct result of manual agitation of the anolyte prior to sampling. These results confirmed nitrogen accumulation observations from earlier observations and provided further evidence of particulate accumulation in the MFCs.

4.7.3. Microbial Ecology

Figure 4.14 shows the results of the principal component analysis (PCA) performed on ECOplates 13 through 16. ECOplates 13 and 15 represent the bulk anolyte samples from MFC#1, before and after BSA dosing, respectively. ECOplates 14 and 16 represent the bulk anolyte samples from MFC#2, before and after BSA dosing, respectively. The first PCA ordination, Case 9.0, represents PCA performed on the dataset containing all the carbon source variables. The four following ordinations, Cases 9.1 to 9.4, represent PCA performed on datasets containing only subsets of the carbon source variables. These subsets represented carbohydrates (Case 9.1), carboxylic acids (Case 9.2), polymers and miscellaneous (Case 9.3) and amines and amino acids (Case 9.4).

The purpose of this case and set of sub-cases was to compare the anolyte samples drawn from both MFCs, before and after BSA dosing. It was hypothesized that the microbial communities of the MFCs would have converging shift responses, due to the common substrate dosing. Because BSA was classified as a protein, it was hypothesized that the primary microbial community activity shift would be due to amine and amino acid utilization.

From Case 9.0 (a), no convergence of the MFC microbial communities was observed. MFC#1 showed a definitive shift in microbial community activity, while MFC#2 showed no response to BSA dosing. From the carbohydrates sub-case (Case 9.1 - b), convergence was observed for the MFC microbial communities, however, this was a result of a shift for MFC#1 alone. MFC#2 showed no response in carbohydrate utilization as a result of BSA dosing. There was no response to carboxylic acid utilization (Case 9.2 - c) for either MFC. MFC#2 showed a slight shift in polymer and miscellaneous carbon source utilization (Case 9.3 - d) with respect to the second principal component, while MFC#1 showed a larger shift toward convergence of the MFC microbial communities. MFC#2 showed no response in amine and amino acid utilization (Case 9.4 - e). MFC#1 showed no shift in amine and amino acid utilization, but showed a much larger variance in amine and amino acid utilization. BSA dosing had no effect on the microbial community activity in MFC#2, while moderate responses in carbohydrate, polymer, miscellaneous, amine and amino acid utilization for MFC#1 summed to a defined overall response. These results are in agreement with the two hypotheses posed earlier with respect to increased electricity production. If BSA provided a nutrient or structural component that increased microbial community activity for electricity production, this is in

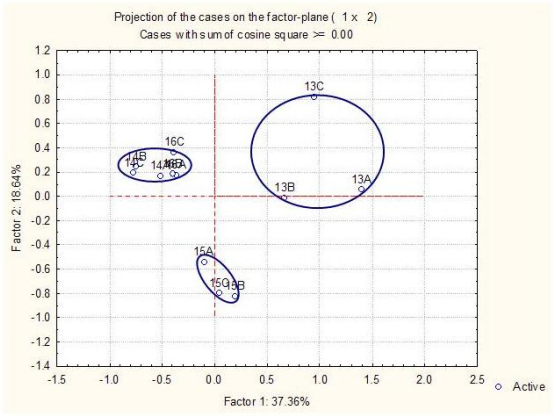

(a)

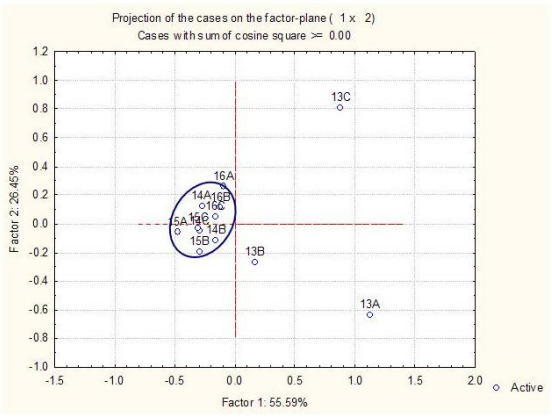

(b)

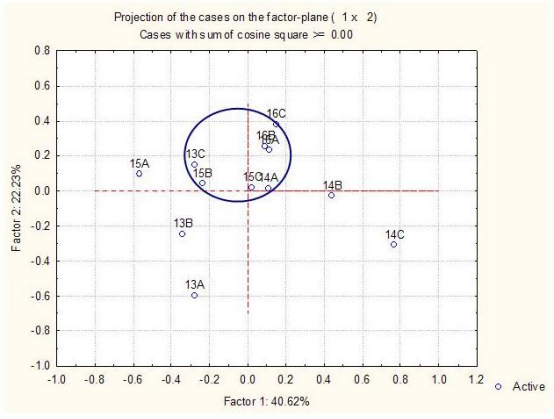

(c)

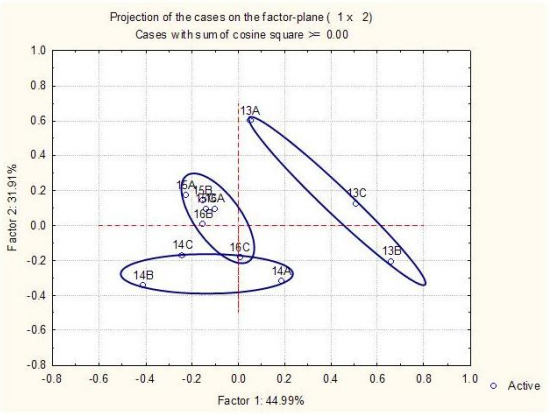

(d)

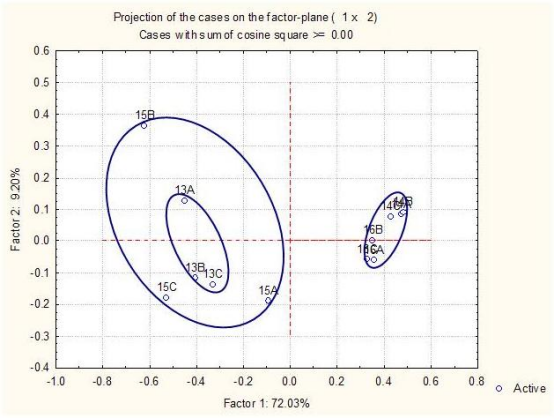

(e)

(a) = Case 9.0 - All ECOplate substrates
(b) = Case 9.1 - Carbohydrate substrates only
(c) = Case 9.2 - Carboxylic Acid substrates only
(d) = Case 9.3 - Polymer and Miscellaneous substrates only
(e) = Case 9.4 - Amine and Amino Acid substrates only

Figure 4.14.: *PCA Ordination for Cases 9.0 through 9.4 - ECOplates 13 through 16 - BSA Dosing*

agreement with the microbial community activity shifts observed for MFC#1. If BSA was acting as an electron mediator, delivering a greater number of electrons to the anode surface without interacting with the microbial community at a substrate level, this is in agreement with the lack of microbial community activity shifts observed for MFC#2.

4.8. Electricity Generation and COD Removal Due to CSPTs

Figure 4.15 summarizes the COD removal results for the CSPTs for comparison to each other. They are presented as percentages, where the value is equal to the ratio of the COD mass equivalence removed as visible current production responses to the COD mass equivalence added in the form of each CSPT.

Both MFCs responded similarly. The first dose of sodium acetate had a COD mass equivalence of 50 mg, and the current response translated to less than 4% of this COD mass. The COD mass equivalence of the remaining CSPTs were all approximately 2.857 mg. Current responses to the remaining sodium acetate doses were less than 0.5% of the dosage COD mass equivalence. Current responses to glucose dosing reached almost 1% of the fed COD mass equivalence for the first and fourth doses. The second and third glucose doses responded similarly to the last three sodium acetate doses. Glycerol dosing showed no discernible response in current, thus 0% of the dosage COD mass equivalence was removed via current response to glycerol dosing. The bovine serum albumin (BSA) dosing showed current responses similar to the second through fourth sodium acetate doses and the second and third glucose doses, with less than 0.5% of the dosage COD mass equivalence.

When the COD mass equivalence of the CSPTs were the same, sodium acetate, glucose and BSA showed similar COD removal percentages due to current response, despite the differences in response magnitude and duration. However, glycerol doses showed no response in current production, and thus, no response in COD removal due to current response. Glycerol dosing had no impact on electricity production as a whole. Anolyte quality during glycerol dosing was similar to previously observed values, however, the microbial community activity showed a diverging shift response to glycerol dosing. Glycerol had little impact on the operational variables in this study, but illustrated the opposite microbial community activity shift response as compared to the other three carbon source dosed during the CSPTs.

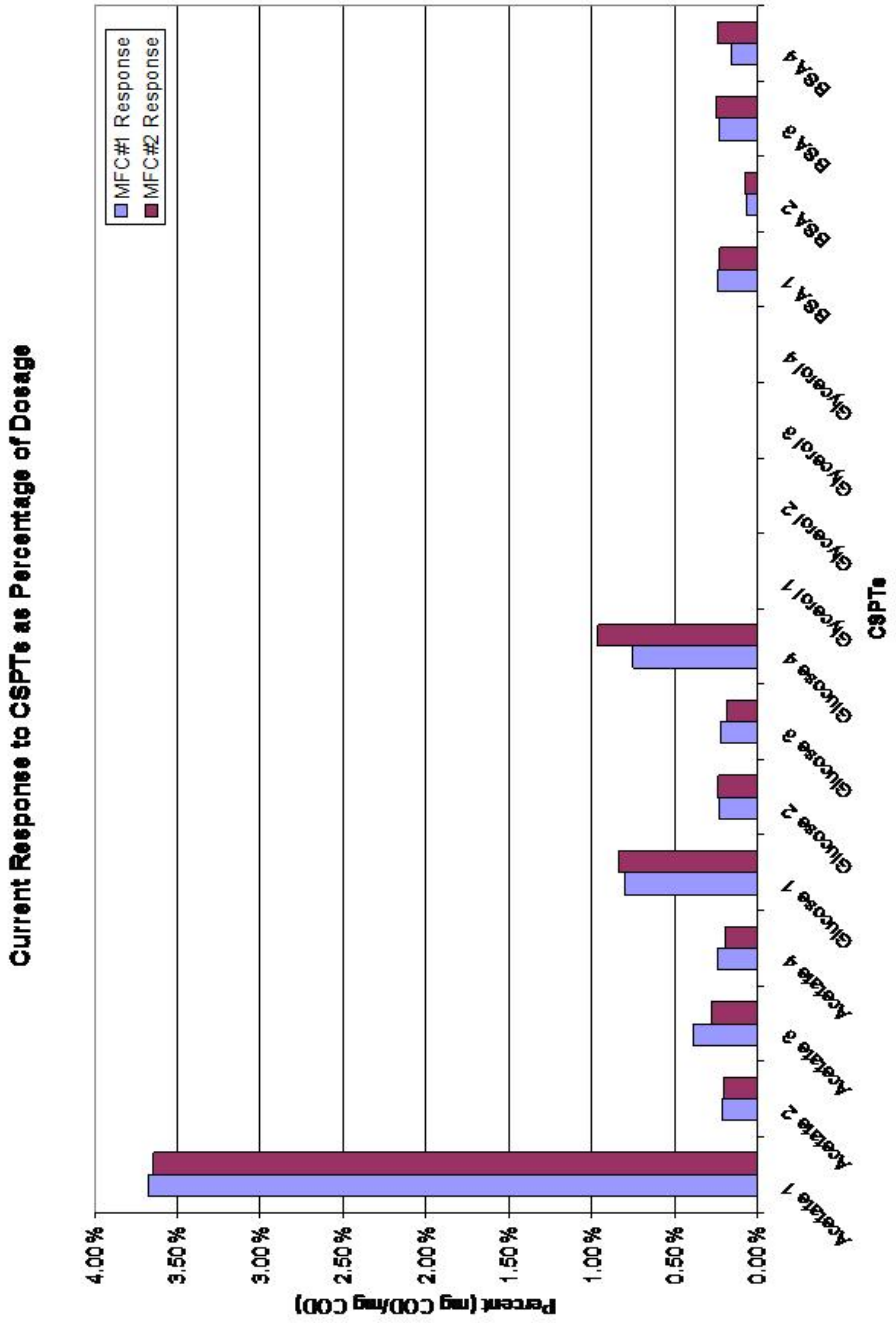

Figure 4.15.: *COD Removed by Electricity Generation as Percentage of COD Added by CSPT*

4.9. Functional Diversity

Zak *et al* (1994) defined functional diversity as the "numbers, types, activities, and rates at which a suite of substrates are utilized by the bacterial community". Each ECOplate was evaluated for the functional diversity indices: substrate diversity, substrate richness and substrate evenness. Definitions of these indicies and their analytical methods are presented in Chapter 3. Figure 4.16 contains normalized results from ECOplates 6, 7, 9, 11, 13 and 15, prepared from MFC #1 and the initial waste activated sludge. Figure 4.17 contains normalized results from ECOplates 6, 8, 10, 12, 14 and 16, prepared from MFC#2 and the initial waste activated.

From Figures 4.16 and 4.17, the functional diversity was compared for wastewater anolyte samples taken before, between, and after the carbon source pulse tests (CSPTs). In addition, points at the beginning and end of the acclimation period were also compared. From the results, it appeared that both MFCs behaved in the same manner throughout the experiment, though the impact on MFC#1 appeared to be slightly greater than that on MFC#2. The addition of the carbon sources during the CSPTs had little effect on the substrate evenness. The substrate diversity dropped to 85% to 90% of the substrate diversity of the initial waste activated sludge after the first three CSPTs, but increased to about 92% of the substrate diversity of the initial waste activated sludge following bovine serum albumin (BSA) addition. The substrate richness showed a similar trend to that of the substrate diversity, but magnified such that values were as low as 73% of the substrate richness of the initial waste activated sludge.

Two key conclusions were made from the functional diversity results:

- all three indices showed little to no difference before and after the acclimation period of approximately 2.5 months in experiment #2
- MFC#1 and MFC#2 showed the same trends in functional diversity throughout operation and CSPTs in experiment #2

From these results and those in Chapter 3, it was concluded that the functional diversity of a microbial community in the anolyte decreased during the acclimation period, but subsequently recovered to nearly the same levels as those seen in the initial waste activated

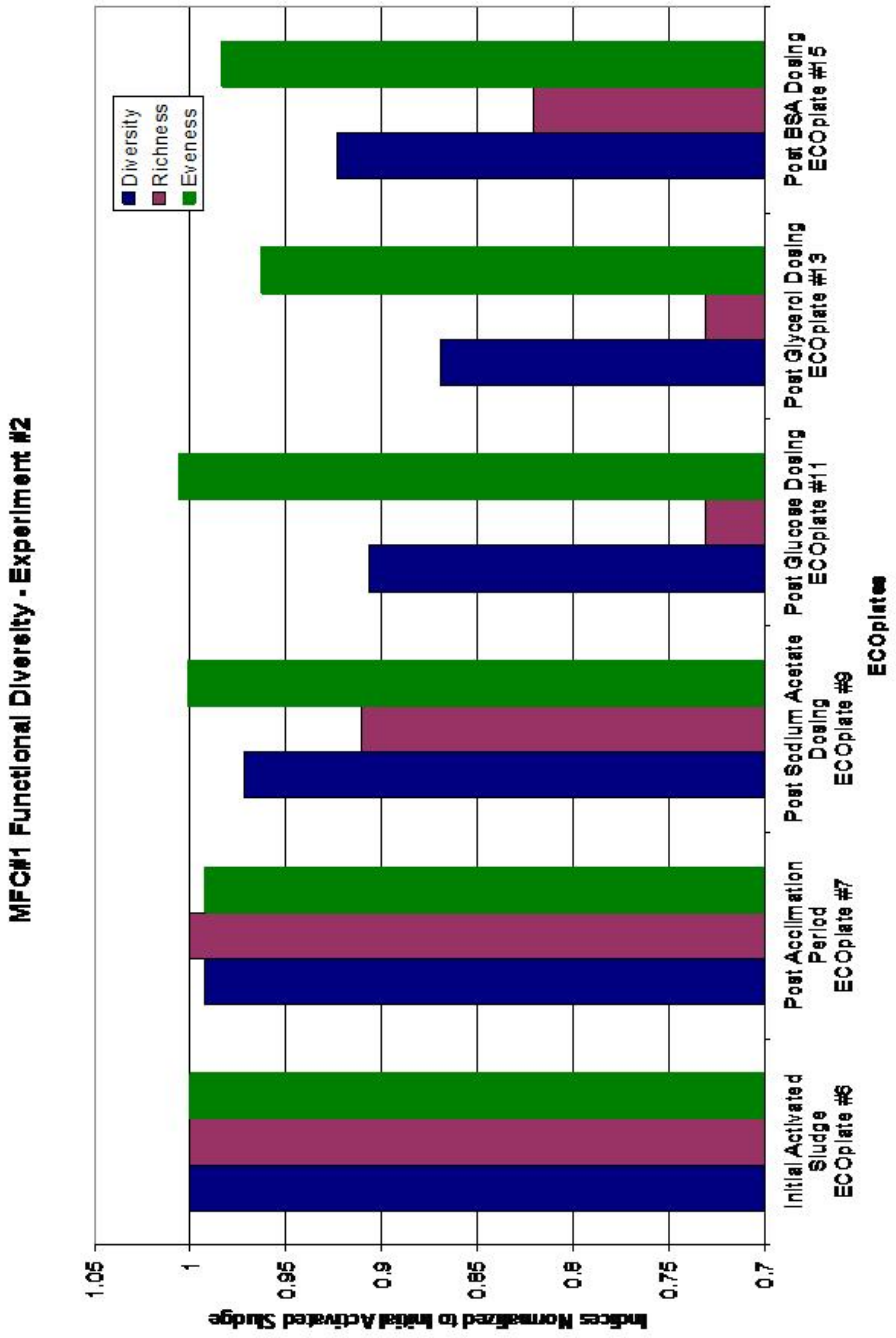

Figure 4.16.: *Functional Diversity Indices for Experiment #2 - MFC#1*

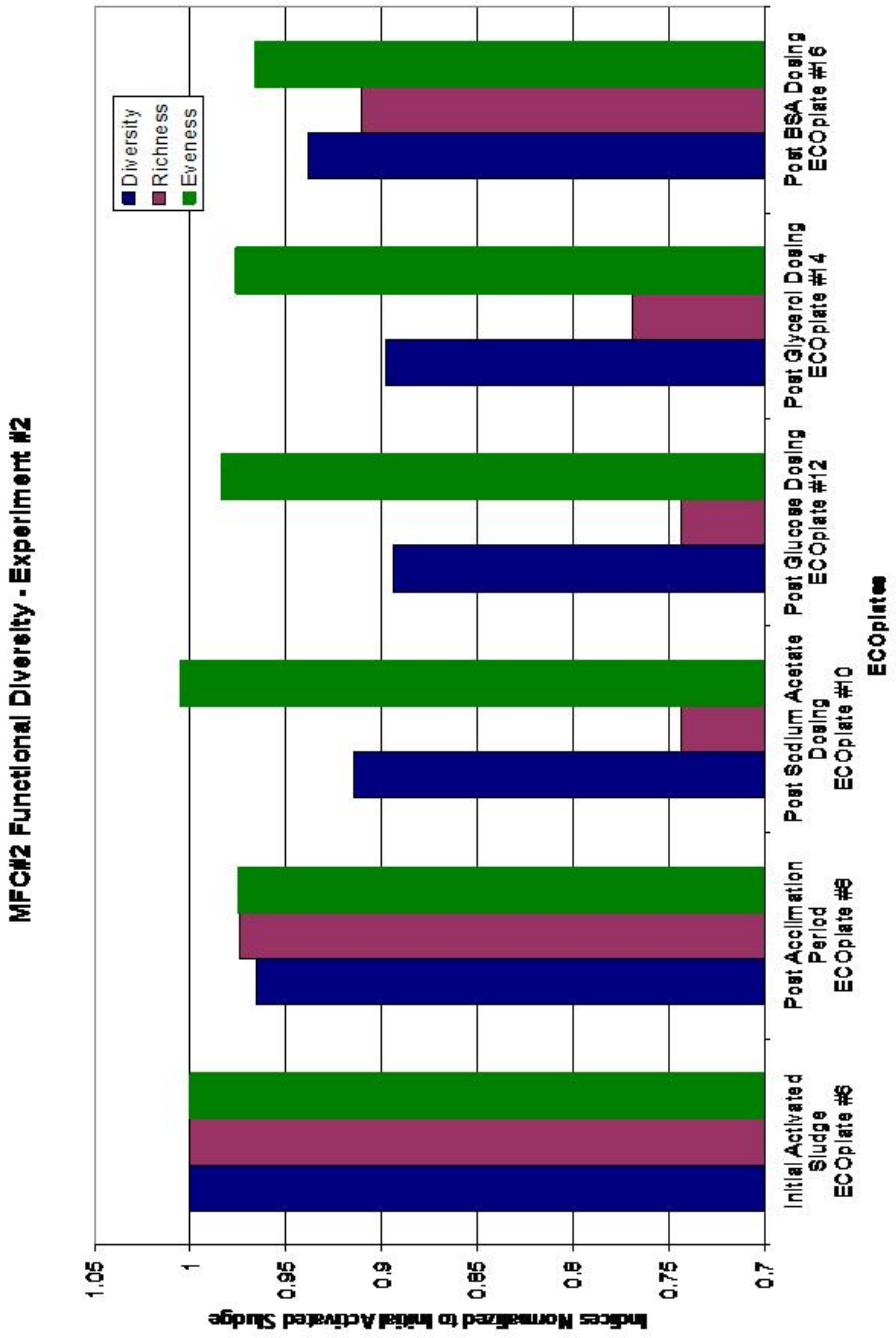

Figure 4.17.: *Functional Diversity Indices for Experiment #2 - MFC#2*

sludge. This is further support for the existence of and need to accommodate an acclimation period during MFC system start up. The addition of specific carbon sources during operation decreased the functional diversity of the microbial community in the anolyte slightly, though the addition of BSA appeared to negate some of the decreased functional diversity. The hypothesized impacts of BSA on microbial community activity may have been partially responsible for the increased functional diversity. Electrochemical properties or particular nutrients or structural components could have allowed greater diversity in the microbial community activity. Finally, the specific MFC and catholyte choice had no effect on the trends in functional diversity, indicating that these system variables did not influence the diversity of the microbial community activity.

4.10. Conclusions

The surface area of the proton exchange membrane (PEM) as compared to the surface area of the electrodes is known to have a significant effect on electricity production in MFCs (Oh & Logan, 2006). Due to the significantly smaller PEM surface area when compared to the electrodes used in this study, an uncertainty in the actual effective surface area arose. This made it difficult to report with confidence, power densities for comparison to other studies.

From the acclimation period, average power productions of 0.020 mW and 0.093 mW were observed for MFC#1 and MFC#2, respectively. When normalized by the effective membrane surface area (EMSA) of 7 cm^2, power densities of 29.3 mW/m^2 and 139.5 mW/m^2 were observed. These values were comparable to values reported in the literature (Oh & Logan, 2006). Approximately 79% of the COD fed to the MFCs during the acclimation period was calculated to accumulate within the MFCs, primarily as particulate. 96% of the COD removed from the MFCs was found in the anolyte samples, while the remaining 4% was found in electricity and methane production. In addition to COD accumulation, nitrogen was calculated to accumulate in the MFCs as well. MFC#1 and MFC#2 were found to diverge in microbial community activity after the acclimation period. The only exception was carboxylic acid utilization, which remained generally unchanged after the acclimation period. This was attributed to a continued anaerobic environment and fermentive processes resulting in the same volatile fatty acids (VFAs) being present throughout the acclimation period.

During sodium acetate dosing, average power productions of 0.024 mW and 0.095 mW were observed for MFC#1 and MFC#2, respectively. These values were nearly identical to those observed during the acclimation period. Current production responses to sodium acetate dosing were found to be immediate and significantly larger than responses to the other carbon sources. Approximately 75% of the COD fed to the MFCs during sodium acetate dosing was calculated to accumulate within the MFCs, primarily as particulate. 92% of the COD removed from the MFCs was found in the anolyte samples, while the remaining 8% was found in electricity and methane production. In addition to COD accumulation, nitrogen was calculated to accumulate in the MFCs as well. The microbial community activity of MFC#1 only responded to sodium acetate dosing in the carboxylic acid utilization, while MFC#2 responded with respect to all the carbon source classifications. The microbial community activity in MFC#1 appeared to be converging to a similar point as the community in MFC#2 after lagging behind during the acclimation period.

During glucose dosing, average power productions of 0.027 mW and 0.096 mW were observed for MFC#1 and MFC#2, respectively. These values were nearly identical to those observed during the acclimation period and sodium acetate dosing. Current production responses to glucose dosing were found to be gradual with a magnitude several times lower than the response to sodium acetate. Approximately 71% of the COD fed to the MFCs during glucose dosing was calculated to accumulate within the MFCs, primarily as particulate. 92% of the COD removed from the MFCs was found in the anolyte samples, while the remaining 8% was found in electricity and methane production. In addition to COD accumulation, nitrogen was calculated to accumulate in the MFCs as well. The results of glucose dosing showed further evidence that the microbial community activity of MFC#1 was converging to a similar point as the community in MFC#2 after lagging behind during previous operation. The response of the microbial community activity in MFC#1 to the glucose dosing was more pronounced than the response observed for MFC#2.

During glycerol dosing, average power productions of 0.032 mW and 0.098 mW were observed for MFC#1 and MFC#2, respectively. These values were nearly identical to those observed previously. No current production responses to glycerol dosing were observed. This was attributed to a lower biodegradability or competing interactions with volatile fatty acids in the anolyte. Approximately 67% of the COD fed to the MFCs during glycerol dosing

was calculated to accumulate within the MFCs, primarily as particulate. 94% of the COD removed from the MFCs was found in the anolyte samples, while the remaining 6% was found in electricity and methane production. In addition to COD accumulation, nitrogen was calculated to accumulate in the MFCs as well, though increasing amounts of particulate nitrogen were observed in the anolyte samples. MFC#1 and MFC#2 were found to diverge in microbial community activity after glycerol dosing. Following converging behaviour seen following sodium acetate and glucose dosing, glycerol caused a divergent behavoiur, indicating differing responses to glycerol. The response of the microbial community activity in MFC#1 to the glycerol dosing was most evident in the carbohydrate utilization. MFC#2 responses were observed in carboxylic acid and amine and amino acid utilization. Glycerol was expected to impact the carbohydrate utilization most, though impacts on carboxylic acid utilization may have been due to interactions between glycerol and volatile fatty acids.

During bovine serum albumin (BSA) dosing, average power productions of 0.062 mW and 0.122 mW were observed for MFC#1 and MFC#2, respectively. These values were significantly greater than those observed during previous operation. Current production responses to BSA dosing were similar to the responses seen with glucose dosing. Two hypotheses were proposed to address the greater current levels following BSA dosing. Increased current may have been due to interactions of a particular nutrient or structural component on the electricity producing bacteria activity. The increased current may also have been due to electrochemical properties of BSA allowing the molecule to act as an electron mediator between electricity producing bacteria and the anode surface. Approximately 20% of the COD fed to the MFCs during BSA dosing was calculated to accumulate within the MFCs, primarily as particulate. 97% of the COD removed from the MFCs was found in the anolyte samples, while the remaining 3% was found in electricity and methane production. The significant increase in COD removal due to anolyte sampling was attributed to higher concentrations of COD in the anolyte samples after a manual agitation of the anolytes on April 19th, 2007. In addition to COD accumulation, nitrogen was calculated to accumulate in the MFCs as well. Nitrogen as particulate was seen to rise significantly following the manual agitation of the anolytes on April 19th, 2007, confirming earlier observations of nitrogen accumulation in the MFCs. MFC#2 showed almost no response in microbial community activity following BSA dosing. In contrast, MFC#1 showed significant shifts in microbial community activity. BSA enabled MFC#1 to approach the microbial community activity of MFC#2 except in

amine and amino acid utilization. This highlighted the differing responses between the two MFCS, which may be attributed to the two hypotheses proposed earlier. Each hypothesized activity may have been prevalent in one MFC and not the other.

The functional diversity of the microbial communities of each ECOplate were calculated and compared to identify any further ecological trends. The indices used to evaluate the functional diversity were the substrate diversity, substrate evenness and substrate richness. All three indices were observed to decrease during the acclimation period of the MFC operation. However, given enough acclimation time, the functional diversity of the microbial communities in the wastewater anolyte were found to approach the same levels as those in the initial waste activated sludge. The addition of several carbon sources during MFC operation had little effect on the substrate evenness, but resulted in drops of approximately 15% in substrate diversity as compared to the initial waste activated sludge. The only exception was the addition of bovine serum albumin, which was observed to increase the substrate diversity to approximately 92% of the initial waste activated sludge values. Substrate richness was found to behave in the same manner as substrate diversity. Finally, the functional diversity trends were found to be independent of the specific MFC and catholyte used.

References

References marked with an asterisk indicate studies included in the meta-analysis.

Aelterman, P., Rabaey, K., Clauwaert, P., & Verstraete, W. (2006). Microbial fuel cells for wastewater treatment. *Water Science & Technology*, *54*(8), 9-15.

Bond, D. R., & Lovley, D. R. (2003). Electricity production by *Geobacter sulfurreducens* attached to electrodes. *Applied and Environmental Microbiology*, *69*, 1548-1555.

*Franklin, R. B., Garland, J. L., Bolster, C. H., & Mills, A. L. (2001). Impact of dilution on microbial community structure and functional potential: comparison of numerical simulations and batch culture experiments. *Applied and Environmental Microbiology*, *67*(2), 702-712.

*Garland, J. L. (1996). Analytical approaches to the characterization of samples of microbial communities using patterns of potential c source utilization. *Soil Biology & Biochemistry*, *28*(2), 213-221.

*Garland, J. L., & Mills, A. L. (1991). Classification and characterization of heterotrophic microbial communities on the basis of patterns of community-level sole-carbon-source utilization. *Applied and Environmental Microbiology*, *57*(8), 2351-2359.

*Garland, J. L., Mills, A. L., & Young, J. S. (2001). Relative effectiveness of kinetic analysis vs single point readings for classifying environmental samples based on community-level physiological profiles (clpp). *Soil Biology & Biochemistry*, *33*, 1059-1066.

Gil, G. C., Chang, I. S., Kim, B. H., Kim, M., Jang, J. K., Park, H. S., et al. (2003). Operational parameters affecting the performance of a mediator-less microbial fuel cell. *Biosensors and Bioelectronics*, *18*, 327-334.

*Grove, J. A., Kautola, H., Javadpour, S., Moo-Young, M., & Anderson, W. A. (2004). Assessment of changes in the microorganism community in a biofilter. *Biochemical Engineering Journal*, *18*, 111-114.

He, Z., Minteer, S. D., & Angenent, L. T. (2005). Electricity generation from artificial wastewater using an upflow microbial fuel cell. *Environmental Science and Technology*, *39*, 5262-5267.

Kim, N., Choi, Y., Jung, S., & Kim, S. (2000). Effect of initial carbon sources on the performance of microbial fuel cells containing *Proteus vularis*. *Biotechnology and Bioengineering*, *70*(1), 109-114.

Min, B., Kim, J. R., Oh, S. E., Regan, J. M., & Logan, B. E. (2005). Electricity generation from swine wastewater using microbial fuel cells. *Water Research*, *39*, 4961-4968.

Moon, H., Chang, I. S., & Kim, B. H. (2006). Continuous electricity production from artificial wastewater using a mediator-less microbial fuel cell. *Bioresource Technology*, *97*, 621-627.

Muller, A. W., Wentzel, M. C., & Ekama, G. A. (2004). Experimental determination of the heterotroph anoxic yield in anoxic-aerobic activated sludge systems treating municipal wastewater. *Water SA*, *30*(5), 7-12.

Oh, S.-E., & Logan, B. E. (2006). Proton exchange membrane and electrode surface areas as factors that affect power generation in microbial fuel cells. *Applied Microbiology and Biotechnology*, *70*(2), 162-169.

Ringeisen, B. R., Ray, R., & Little, B. (2007). A miniature microbial fuel cell operating with an aerobic anode chamber. *Journal of Power Sources*, *165*, 591-597.

*Weber, K. P. (2006). *Investigation of the mechanisms and fundamental variables affecting acid mine drainage treatment in wetland mesocosms.* Unpublished master's thesis, University of Waterloo, Ontario, Canada.

You, S. J., Zhao, Q. L., Jiang, J. Q., & Zhang, J. N. (2006). Treatment of domestic wastewater with simultaneous electricity generation in microbial fuel cell under continuous operation. *Chemical and Biochemical Engineering Q.*, *20*(4), 407-412.

Zak, J. C., Willig, M. R., Moorhead, D. L., & Wildman, H. G. (1994). Functional diversity of microbial communities: a quantitative approach. *Soil Biology & Biochemistry*, *26*, 1101-1108.

5. Conclusions and Recommendations

5.1. Principal Conclusions

Several conclusions were drawn from this research and are presented in this section. Microbial fuel cell (MFC) design and operation is addressed first, followed by a summary of the anolyte wastewater quality observed during this study. The choice of catholyte is presented with discussion of the constraints involved with each of the catholytes used in this study. Electricity production impacts of the carbon source pulse tests are presented and compared. Finally the use of data transformations and principal component analysis (PCA) on ecological data and the microbial ecology results from this study are summarized.

5.1.1. Microbial Fuel Cell (MFC) Design and Operation

Consistent power production levels of 0.03 mW and 0.10 mW were attained from MFCs operating with a dissolved oxygen (DO) and ferricyanide catholyte, respectively. Power densities were difficult to determine due to an uncertainty in the true effective surface area. The power densities were recorded relative to the cathode surface area, also called the effective electrode surface area (EESA) and the PEM surface area, also called the effective membrane surface area (EMSA). Power densities calculated with the EMSA were consistently observed at 46 mW/m^2 and 140 mW/m^2 for MFC#1 and MFC#2, respectively. These were in agreement with values reported in the literature (Oh & Logan, 2006)

5.1.2. Anolyte Wastewater Quality

A COD mass balance was performed for both MFCs. The COD removal due to electricity generation and measured methane production was almost negligible relative to COD loading, with the following approximate values expressed as percentages of the total COD feed:

- COD removal due to sampling - 23.5%

- COD removal due to electricity production - 1.0%
- COD removal due to methane off-gas - 0.5%
- calculated COD accumulation in the MFCs - 75%
- measured COD accumulation in the MFCs - 30%

Considering the low percentage of COD removal due to electricity production, the COD mass balance results of both MFCs were nearly identical. Due to the particulate nature of the COD added to the MFCs, solubilization and substrate utilization rates likely limited the electricity production. Design impacts, such as the relatively small size of the proton exchange membrane, also limited the electricity production in both MFCs. COD that passed through the MFCs was measured in the anolyte samples drawn from the MFCs. The lack of closure in the COD mass balance was attributed to unmeasured methane off-gas, which would have resulted in a lower measured COD accumulation than what was calculated. The seals of both MFCs were suspected of allowing constant, low-flow gas leakage. During the second experiment of approximately 6 months, only 25 mL/day of methane gas leakage from each MFC would be required to account for the discrepancy in COD accumulation values.

Nitrogen results based on the TKN analysis showed particulate nitrogen accumulation in the MFCs, supporting the observation of COD accumulation. The prevalence of nitrogen as free and saline ammonia (FSA) in the anolyte samples indicated that some of the particulate nitrogen fed to the MFCs was solubilized. Nitrogen analyses provided insight into protein hydrolysis processes active in the waste activated sludge in the anode chambers of the MFCs. TKN analyses required a large amount of resources and time. Future studies should invest the time and resources into TKN analyses when protein-based investigations are required.

The pH of the anolytes was measured throughout the study. The pH of the feed waste activated sludge ranged from 7.4 to 8.2, while the anolytes ranged from 6.4 to 7.6. Anolyte pH was always lower than the feed waste activated sludge. This was attributed to the accumulation of volatile fatty acids (VFAs) from fermentation processes active in the anolyte. Other literature has suggested that the acclimation time for MFCs operating on a wastewater anolyte could be decreased with acidification/anaerobic pretreatment (Rodrigo et al., 2007).

5.1.3. Dissolved Oxygen (DO) versus Ferricyanide as the Electron Acceptor (EA)

Two electron acceptors (EAs) were used in this study. The first MFC, MFC#1, operated with a dissolved oxygen (DO) catholyte, while the second MFC, MFC#2, operated with a ferricyanide catholyte. MFC#2 operated at electricity production rates of 2-5 times higher than those observed for MFC#1. COD removal rates were comparable, considering the minimal nature that electricity generation had on COD removal. The increased performance in the ferricyanide catholyte was attributed to increased electron acceptor reaction rates. This was due the relatively high ferricyanide concentrations as compared to the DO concentrations. Ferricyanide concentrations were maintained at approximately 40mM, while DO concentrations were below the maximum threshold of 0.22mM as permitted by solubility limitations.

While ferricyanide increased MFC performance, it did not constitute a viable catholyte option for future MFC scale-up. Scale-up designs would need to operate with large amounts of ferricyanide, which is inadvisable from both a health and safety and design budget standpoint. Oxygen is a safer and more readily available alternative, but it is limited by solubility, which limits the overall reaction rate. Other studies have used an air cathode system, exploiting the relatively high concentration of oxygen in air. Mass transfer of oxygen to the cathode under liquid phase conditions continues to be a design challenge.

5.1.4. Carbon Source Pulse Tests (CSPTs)

The dosing levels on a COD mass basis were negligible in comparison to the COD mass equivalence of the feed waste activated sludge. Sodium acetate, glucose and bovine serum albumin (BSA) showed current production responses following dosing, with sodium acetate showing the largest effects. Only BSA showed a significant, long-term effect on power production, increasing it by 100% and 25% for MFC#1 and MFC#2, respectively. This was attributed to either or both of the following factors:

- BSA was readily hydrolyzed and provided a nutrient or structural component that increased the activity of electricity-producing microorganisms
- BSA acted as an electron mediator, moving electrons from active bacteria in the anolyte to the anode surface

Effects on the wastewater variables and and full-scale COD mass balance were negligible due to the low COD mass equivalence of the CSPTs. When compared to each other, sodium acetate, glucose and BSA all displayed similar amounts of COD mass equivalence in the current response to dosing. The COD removal due to the electricity production of the responses was typically less than 0.5% of the CSPT COD mass equivalence introduced in the doses. Glycerol dosing did not show an electrical response. This did not indicate that glycerol was not utilized, but any current resulting from glycerol utilization was concealed by the background electricity production from waste activated sludge components in the anolytes. Microbial ecology effects are presented in Section 5.1.7

5.1.5. Data Transformations and Principal Component Analysis (PCA) of Ecological Data

Principal component analysis (PCA) was utilized to perform community level physiological profiling (CLPP) of the microbial communities in the MFC anolytes. Several statistical constraints on the datasets, including homoscedasticity, dataset normality and linear correlation between variables, must be optimized before PCA can be applied. Taylor power law and natural logarithm data transforms were evaluated against untransformed data, and both transforms were found to improve the dataset compliance to the statistical constraints. The natural logarithm transformed datasets were used for PCA in this study because of increased statistical constraint compliance in earlier case studies and consistency between all cases studied.

5.1.6. Microbial Ecology in MFCs

Results from the CLPP performed via PCA on the transformed ECOplate datasets:

- microbial community activity differed between samples obtained from the MFCs during two separate experiments, which ran for 28 days and 182 days, respectively
- differences in the microbial community activity were observed after acclimation periods of 28 days and 77 days
- anode and anolyte samples from the same MFC at the same approximate time were similar with respect to the microbial community profile
- waste activated sludge samples showed very similar microbial community profiles

- the microbial community profile of MFC#1 appeared to lag behind the microbial community profile observed from MFC#2, which may be related to the lower operational state of MFC#1
- dosing of sodium acetate and glucose appeared to result in a convergence of the microbial community profiles of the two MFCs, indicating a similar response in each MFC
- glycerol dosing and MFC acclimation periods appeared to result in a divergence of the microbial community profiles of the two MFCs, indicating distinct responses in each MFC
- BSA dosing resulted in little to no effect on the microbial community profiles in the two MFCs
- the acclimation period initially decreased functional diversity in the MFCs, though longer periods saw functional diversity levels return to those observed in the waste activated sludge samples
- carbon source dosing decreased functional diversity levels in the MFCs, though BSA addition resulted in a partial return to waste activated sludge levels, indicating that BSA was increasing the microbial communities' capability to utilize a greater range of carbon sources

5.2. Recommendations

5.2.1. Microbial Fuel Cell (MFC) Design and Operation

Improvements in MFC design in the following areas are recommended for the reasons indicated:

MFC Size/Configuration:

The relatively small COD removal due to electricity production and the lack of mass balance closure on the COD results suggest that the liquid anolyte volume used in the MFCs was greater than required. Waste activated sludge feed volumes should be reduced, resulting in

the need for a smaller volumetric MFC. Smaller COD feed values would increase the probability of closing future COD mass balances performed on the MFCs. The use of a single chamber MFC configuration as described in the literature should be considered in future designs (Liu & Logan, 2004; Liu, Ramnarayanan, & Logan, 2004; Cheng, Liu, & Logan, 2006b, 2006a).

Effective Surface Area:

In this study, the surface area of the anode, cathode and proton exchange membrane (PEM) all differed significantly. The surface area of the PEM was less than 2.5% and 1.8% of the cathode and anode surface areas, respectively. A relatively small PEM surface area creates large internal resistance within the MFC, impeding electricity production. In addition, confident reporting of power and current densities was difficult due to the uncertainty introduced in the effective surface area of each MFC. With MFC redesign and possible scale-down, the electrode surface areas should be reduced to similar levels as the surface area of the PEM.

Materials:

The MFCs were primarily constructed from acrylic glass, that was bolted together. During operation, damage to the floor of the anode chamber was observed, due to the magnetic stir bar rotation. With longer operation, system failure was likely. Repairs were carried out before the onset of the second experiment in this study, however, the insertion of a teflon disc only served to slow the bottom plate deterioration. Investigation into alternative construction materials or alternative materials for the floor plate of the anode chamber is recommended. If a plug flow design were pursued in future studies, mixing within the anode chamber may not be required.

Uniform Anolyte Mixing and Plug Flow Design:

Throughout this study, obtaining uniform, representative samples of the MFC anolytes was difficult. Redesign of the MFC size and configuration should take anolyte mixing into account. In addition, a plug flow system should be investigated to minimize the necessity of anolyte mixing within the anode chamber. With a relatively small size compared to current

prototypes, a single sampling point would still be representative of the anolyte chemistry within the MFC.

MFC Seal:

The lack of COD mass balance closure was attributed to a poor seal on the MFCs, allowing methane in the head space to leak out to the atmosphere, unmeasured. A relatively small volume of approximately 25 mL/day of methane was required in each MFC to account for the COD discrepancy. Future designs should incorporate a more reliable seal, capable of withstanding pressure changes associated with the sampling and feeding of the MFCs.

5.2.2. Waste Activated Sludge as the Anolyte

The use of waste activated sludge in MFCs provided a widely assorted seed culture for MFC start up. In addition, the COD equivalence of the particulate in the waste activated sludge contains several times more potential energy than soluble components. Overcoming slow solubilization and biodegredation rates is a continuing challenge, but the use of waste activated sludge as a seed culture, anolyte and biodegradable substrate is recommended. Other studies have shown that pretreatment of sludge anolytes decreased the necessary acclimation time and increased MFC performance, thus it is recommended that sludge pretreatment methods be investigated in future research (Rodrigo et al., 2007).

5.2.3. BIOLOG® ECOplates and Microbial Ecology of MFCs

The use of BIOLOG® ECOplates in this study provided a successful means of gathering ecological data from an anaerobic system and culture. Data transforms and PCA applied to the ecological datasets provided sound analytical results. The classification of the carbon sources in the ECOplate resulted in several sub-case studies, further elaborating on the microbial community activity within the MFC anolytes. These results provide a starting point for better understanding the microbial community profiles in a waste activated sludge MFC and how they respond during acclimation and with regard to specific carbon sources. Replicate studies are recommended to confirm repeatability. Future studies on the microbial ecology within MFCs should focus on microbial community stability in response to disturbances administered after steady MFC operation is attained.

5.2.4. Related Studies

Alternative anolytes/substrates should be further investigated, with a bias toward the less investigated particulates or solids, since these represent further high energy substances for electricity production potential. A recent study has illustrated the use of manure in MFCs (Scott, Murano, & Rimbu, 2007). The sensitive electrical responses to relatively low COD dosages of soluble substrates suggests the use of MFCs as a readily biodegradable oxygen demand (rBOD) biosensor. Another recent study has designed a biosensor prototype of this nature and investigated some possibilities (Kumlanghan, Liu, Thavarungkul, Kanatharana, & Mattiasson, 2007)

References

Cheng, S., Liu, H., & Logan, B. E. (2006a). Increased performance of single-chamber microbial fuel cells using an improved cathode structure. *Electrochemistry Communications*, *8*, 489-494.

Cheng, S., Liu, H., & Logan, B. E. (2006b). Power densities using different cathode catalysts (pt and cotmpp) and polymer binders (nafion and ptfe) in single chamber microbial fuel cells. *Environmental Science and Technology*, *40*(1), 364-369.

Kumlanghan, A., Liu, J., Thavarungkul, P., Kanatharana, P., & Mattiasson, B. (2007). Microbial fuel cell-based biosensor for fast analysis of biodegradable organic matter. *Biosensors and Bioelectronics*, *22*, 2939-2944.

Liu, H., & Logan, B. E. (2004). Electricity generation using an air-cathode single chamber microbial fuel cell in the presence and absence of a proton exchange membrane. *Environmental Science & Technology*, *38*(14), 4040-4046.

Liu, H., Ramnarayanan, R., & Logan, B. E. (2004). Production of electricity during wastewater treatment using a single chamber microbial fuel cell. *Environmental Science and Technology*, *38*, 2281-2285.

Oh, S.-E., & Logan, B. E. (2006). Proton exchange membrane and electrode surface areas as factors that affect power generation in microbial fuel cells. *Applied Microbiology and Biotechnology*, *70*(2), 162-169.

Rodrigo, M. A., Cañizares, P., Lobato, J., Paz, R., Sáez, C., & Linares, J. J. (2007). Production of electricity from the treatment of urban waste water using a microbial fuel cell. *Journal of Power Sources*, *169*, 198-204.

Scott, K., Murano, C., & Rimbu, G. (2007). A tubular microbial fuel cell. *Journal of Applied Electrochemistry*, *37*, 1063-1068.

A. Abbreviations

Table A.1.: *Abbreviations*

AWCD	Average Well Colour Development
BSA	Bovine Serum Albumin
COD	Chemical Oxygen Demand
CSPT	Carbon Source Pulse Test
DO	Dissolved Oxygen
EESA	Effective Electrode Surface Area
EMSA	Effective Membrane Surface Area
FSA	Free and Saline Ammonia
GC	Gas Chromatography
MFC	Microbial Fuel Cell
NPT	National Pipe Thread Taper
OCP	Open Circuit Potential
OD	Optical Density
TKN	Total Kjeldahl Nitrogen

B. Sample/Feed and Anaerobic Sampling Procedure

Associated Reagents:

- Wastewater is picked up on the first sample/feed day of the week (either Monday or Tuesday), kept in small refrigerator, warmed in a pail of hot water before withdrawn and fed to the microbial fuel cells
- Ferricyanide - mixed in 1L beaker:
  - Weigh out 16.48g of potassium ferricyanide and put it in the 1L beaker
  - Weigh out 13.69g of potassium phosphate monobasic and put it in the 1L beaker
  - Add 750mL of DI water and stir until crystals are dissolved
  - Add 200mL of DI water and stir again
  - If not prepared, make a concentrated sodium hydroxide solution by adding 15 pellets to about 50mL of DI water in a 100mL beaker, stir until completely dissolved, add 10-20mL more of DI water if necessary
  - Pour 5-10mL of the concentrated sodium hydroxide solution into the ferricyanide mixture and stir, use pH paper to test pH
    - If pH 7, fill 1L beaker to the 1L mark, stir, and put Parafilm over the top of the beaker
    - If pH is still <7, add 5mL of sodium hydroxide solution again, stir, and test pH, stop adding sodium hydroxide at pH 7 and top up 1L beaker to 1L mark with DI water, stir, and put Parafilm over the top
  - Ensure that the concentrated sodium hydroxide solution has Parafilm over it
- Phosphate-buffered Saline Solution - mixed in 500mL flask:

  - Weigh out 1.70113g of potassium phosphate monobasic and put it in 500mL flask
  - Weigh out 2.17725g of potassium phosphate dibasic and put it in 500mL flask
  - Weigh out 2.922g of sodium chloride and put it in 500mL flask
  - Add 400mL of DI water and stir until crystals are dissolved
  - Add 75mL of DI water and stir again
  - If not prepared, make a concentrated sodium hydroxide solution by adding 15 pellets to about 50mL of DI water in a 100mL beaker, stir until completely dissolved, add 10-20mL more of DI water if necessary
  - Pour 5mL of the concentrated sodium hydroxide solution into the saline solution and stir, use pH paper to test pH
    * If pH 7, fill 500mL flask to the 500mL mark, stir, and put Parafilm over the top of the flask
    * If pH is still $<$7, add 5mL of sodium hydroxide solution again, stir, and test pH, stop adding sodium hydroxide at pH 7 and top up 500mL flask to 500mL mark with DI water, stir, and put Parafilm over the top
  - Ensure that the concentrated sodium hydroxide solution has Parafilm over it

- Phosphate-buffered Saline and Sodium Sulphite Solution - mixed in 500mL flask:
  - Weigh out 0.5g of sodium sulphite and put it in 500mL flask
  - Weigh out 0.17g of potassium phosphate monobasic and put it in 500mL flask
  - Weigh out 0.605g of potassium phosphate dibasic and put it in 500mL flask
  - Weigh out 4.0g of sodium chloride and put it in 500mL flask
  - Add 400mL of DI water and stir until crystals are dissolved
  - Add 100mL of DI water and stir, place fabric plug into flask mouth loosely and wrap the top of the flask in tin foil loosely
  - Autoclave the 500mL flask and solution at 120°C, let cool to handling temperature
  - Ensure the fabric plug is pushed into the flask mouth tightly, tighten tin foil around top of flask, let cool to room temperature and store

Procedures:

Head Space Gas (DWE 2524)

- Remove one of the 1mL syringes with no red mark on the plunger from the rubber stopper and ensure that it is empty
- Pierce the rubber port plug at the top of the anode chamber on MFC#1 with the needle and withdraw 1mL of head space gas. Do not insert the needle very far in order to prevent withdrawing wastewater anolyte
- Remove the needle from MFC#1 and insert the tip of the needle back into the rubber stopper to prevent head space gas leakage during sample transport
- Repeat this procedure to obtain a duplicate sample from MFC#1
- Take two samples in the same manner from MFC#2 using the syringes with red marks on the plunger
- Record the time the gas samples were taken in the MFC logbook

Ferricyanide Sample/Feed (DWE 2524)

- Remove the rubber stopper from the cathode section of the lid on MFC#2
- Using a 20mL syringe with tubing attached to it, remove 100mL of ferricyanide solution from the cathode chamber (5x20mL) and put it in a 100mL beaker
- Pour fresh ferricyanide reagent from the 1L beaker into another 100mL beaker to match the amount removed (100mL)
- Pour the 100mL of fresh ferricyanide reagent into the cathode chamber of MFC#2 and place the rubber stopper back into the hole
- Pour 1.0mL of the ferricyanide solution removed earlier into a 1.5mL sample vial - repeat this process to get a duplicate sample of the ferricyanide solution
- If the ferricyanide reagent is a new batch, pour 1.0mL of the fresh ferricyanide reagent into one of the 1.5mL sample vials with 'Feed' written on it - repeat this process to get a duplicate sample of the fresh ferricyanide reagent

- Empty the remaining ferricyanide solution into the waste bucket and rinse the 100mL beakers, 20mL syringe and tubing
- Record the time the ferricyanide sampling and feed took place in the MFC logbook

Dissolved Oxygen (DWE 2524)

- Turn off the air feed to the right hand side of the cathode chamber of MFC#1 by closing the clamp on the tubing at the side port
- Remove the DO probe tip from the storage bottle with DI water in it
- Insert the probe into the cathode chamber through the open access port in the cathode side of MFC#1's lid
- Secure the DO probe with the arm of the stand used to hold the probe upright
- Ensure that the DO probe is submerged in the catholyte such that the silver circle is just below the surface
- Turn on the DO meter on the bench to the right of the incubator and MFC setup by pressing the power button
- Allow the DO meter to warm up and steady its readings for about 1 minute
- Use the up and down arrow keys on the DO meter to select between 'mg/L' and '%Sat' reading options
- Record the 'mg/L', '%Sat', and temperature readings at three different points over approximately 5 minutes time in the MFC logbook, record the time the readings were taken as well
- Turn off the DO meter on the bench by holding the power key down until the display shuts off
- Remove the DO probe from the cathode chamber of MFC#1 and rinse it well with DI water
- Push the DO probe tip back into the storage bottle with DI water in it - be sure that the tip does not touch the bottom of the storage bottle

- Hang the DO probe back in the arm of the stand
- Turn on the air feed to the right hand side of the cathode chamber of MFC#1 by opening the clamp on the tubing at the side port

Wastewater Sample/Feed (DWE 2524)

- Warm the feed sludge by removing it from the refrigerator the night before a sample/feed event and/or by giving it 30-60min in a pail of hot
- To help ensure a uniform and representative sample, move the MFCs around on the stir plates, the stir bars will rattle and bounce around within the chambers, continue for 1-2min until anode chamber fluid is not transparent, stir bars should be centred again by turning off the stir plate for 5-10sec, then back on to the original speed setting
- Set the controlled voltage on the potentiostat to 0.25V by turning the small, black dial on channel 'B' counter-clockwise until the numbers say '247', make a comment 'Control V set to 0.25V for S/F' on the Chart software on the computer by typing the comment into the comment box and pressing enter, save the file after making the comment, record the controlled voltage setting change and associated time in the MFC logbook
- Turn MFC#1 clockwise about 45 degrees to make the right side sample/feed port of the anode chamber more accessible
- Take the 60mL syringe marked 'Sample' and insert it into the tubing on the right side of the anode chamber of MFC#1
- Open the clamp on the tubing and withdraw a 50mL sample, there will be a little air in the syringe, use this to push sample fluid back out of the tubing
- Close the clamp on the tubing and remove the syringe
- Expel the sample into the 50mL sample vial marked 'MFC 1-1'
- Repeat the last four steps expelling the second 50mL sample into the 50mL sample vial marked 'MFC 1-2', this makes a 100mL sample in total
- Attach the 1.5 inch piece of thick-walled tubing to the 60mL syringe marked 'Feed'

B. Sample/Feed and Anaerobic Sampling Procedure

- Remove the feed sludge container from the hot water and dry it off
- Shake the feed sludge up and pour 120mL into a 200mL beaker
- Swirl the feed sludge around in the 200mL beaker, withdraw 50mL of feed sludge using the 'Feed' syringe, draw about 5mL of excess air and remove the thick-walled tubing
- Insert the 'Feed' syringe into the tubing on the right side of the anode chamber of MFC#1
- Open the clamp on the tubing and withdraw the air from the tube, invert the syringe so it is pointing downwards, inject the 50mL of feed sludge and enough air to push it all out of the tubing
- Close the clamp on the tubing and remove the syringe, expel the excess air into the 200mL beaker for feed sludge
- Repeat the last four steps ensuring no air is injected into the anode chamber itself, this makes a 100mL feed in total, return any unused feed sludge from the 200mL beaker to the original container
- Turn MFC#1 counter-clockwise about 45 degrees to return it to its original position with the cathode chamber facing directly forwards, record the times the sampling and feeding took place in the MFC logbook
- Repeat the same sample/feed procedure used for MFC#1 for MFC#2, noting the following differences
  - The 'Sample' syringe should be rinsed out with tap water three times and have air drawn in and expelled three times before using it to take samples from MFC#2
  - The 1.5 inch, thick-walled tubing will be required in both the 'Sample' and 'Feed' syringes when attaching to the tubing on the right side of the anode chamber of MFC#2, this is due to the larger inner diameter of the tubing used for the side ports on MFC#2
  - The 50mL sample vials are labelled 'MFC 2-1' and 'MFC 2-2' for the samples withdrawn from MFC#2

- If the feed is new (just retrieved from the Waterloo WWTP that morning), shake the feed sludge in the container and pour 30mL into each of two 50mL sample vials marked 'Feed Sample'
- Wash the thick-walled bits of tubing and the 200mL beaker using dish soap, rinse out the 60mL syringes with tap water three times and draw in air and push it out three times
- About 2-3 hours after the sample/feed routine, set the controlled voltage on the potentiostat to 0.3V again by turning the small, black dial on channel 'B' counter-clockwise until the numbers say '297', make a comment 'Control V set to 0.3V again' on the Chart software on the computer by typing the comment into the comment box and pressing enter, save the file after making the comment, record the controlled voltage setting change and associated time in the MFC logbook

Sludge Preservation and pH Procedure (CPH 1324)

- Label four (six if feed samples were taken) 125mL sample bottles with the sample date, MFC # or feed, sampler initials and sample type (Total or Soluble), for ease and standardization, follow the format below:
  - Month Day/Yr i.e.) Jan 1/07
  - MFC # or Feed i.e.) MFC#1
  - Initials and Sample Type i.e.) VB Total
- Pour 25mL of each of 'MFC 1-1' and 'MFC 1-2' samples into the bottle labelled for MFC#1 Total samples
- Pour 25mL of each of 'MFC 2-1' and 'MFC 2-2' samples into the bottle labelled for MFC#2 Total samples
- If applicable, pour 15mL of each of the 'Feed Sludge' samples into the bottle labelled for Feed Total samples
- Put the lids back on all the Total samples and place them in the sample refrigerator
- Take the remaining samples in the 50mL sample vials (with caps securely fastened again) and place them in the centrifuge unit, ensure symmetry so the centrifuge will

stay balanced, maximize each of the settings (braking and RPM), turn the timer dial to 30min, close and lock the lid and press the start button

- Once the centrifuge is finished and the braking has completed (red light indicator is on), unlock and open the lid, remove the samples and shut the lid again
- Retrieve the filter apparatus (dome, filter tube, funnel, clamp, and filter paper), piece it together, take the bottle labelled for MFC#1 Soluble samples, remove the cap and place it on the large rubber plug on the vacuum pump apparatus
- Place the filter apparatus over the sample bottle so the filter tube is pointing into the sample bottle, ensure the dome is securely placed around the rubber o-ring and the clamp is tightly pinching the filter paper between the funnel and the filter tube
- Turn on the vacuum pump and empty the remaining liquid from 'MFC 1-1' and 'MFC 1-2' onto the filter paper, allow the pump to run for 10 seconds after the liquid has passed through the filter, shut off the pump, remove the MFC#1 Sample bottle and put the cap back on
- Remove and dispose of the filter paper, rinse the filter tube and funnel thoroughly, place another filter paper in the apparatus and reassemble and secure it
- Repeat the same procedure for MFC#2 Soluble samples with 'MFC 2-1' and 'MFC 2-2' as well as the Feed Soluble samples with both 'Feed Sludge' vials if applicable
- Take the Soluble samples and use the pH probe and meter on the inside bench to take pH readings of each sample, rinse the probe before and after each sample, place the probe back in the pH 7 buffer once finished, readings will take a few minutes to stabilize
- Put one drop of concentrated sulphuric acid in each Soluble sample bottle, put the cap back on, shake it, and put the samples in the sample refrigerator
- Wash and rinse the filter apparatus, rinsing containers and 50mL sample vials, take the 50mL sample vials back to the MFC apparatus

Anaerobic Sampling Procedure for BIOLOG® ECOplates (DWE 2524)

- Ensure that Glove Bag™, Model X−37−27 from I2R, is attached to nitrogen cylinder, use 5% bleach solution and disposable towels to wipe clean before use
- Place the 500mL flask containing phosphate-buffered saline and sodium sulphite solution on hot plate, loosen fabric and foil on the flask opening, bring solution to a boil
- Turn off hot plate, remove 500mL flask CAREFULLY, push the fabric plug in and re-wrap the foil around the flask opening, allow solution to cool for approximately 1 hour
- Gather the following equipment:
  - metal stirring rod
  - 3mL syringe with 6 inch tubing attached
  - 55mL Potter Elvehejm Homogenizer
  - 2 glass cuvettes with rack, ensure surface cleanliness, fill one cuvette half full of DI water
  - 50mL graduated cylinder
  - 8-lane pipetter (10−100μL) with pipette tips attached
  - microplate lid or similar container
  - portable lab-bench spectrophotometer, set wavelength to 590nm
  - BIOLOG® ECOplate, leave sealed
  - Scotch™ tape
- place gathered equipment into Glove Bag along with cooled down phosphate-buffered saline and sodium sulphite solution
- unhook MFC of interest and place in Glove Bag
- close Glove Bag and inflate with nitrogen, open Glove Bag and push out gas, repeat twice
- close and seal Glove Bag, inflate with nitrogen to functional volume

B. Sample/Feed and Anaerobic Sampling Procedure

- remove rubber cap from multi-purpose port in MFC lid, stir wastewater anolyte with metal stirring rod for 1 minute
- draw 3mL sample of wastewater anolyte, remove plunger from homogenizer, add wastewater anolyte sample to homogenizer, place rubber cap back in multi-purpose port in MFC lid
- add 15ml of phosphate-buffered saline and sodium sulphite solution to homogenizer using graduated cylinder
- use plunger to homogenize wastewater anolyte and phosphate-buffered saline and sodium sulphite solution
- half fill second glass cuvette with homogenized solution
- use DI water cuvette to set blank on spectrophotometer
- measure OD of homogenized solution
  - If OD at 590nm is greater than 0.35, pour homogenized solution from cuvette back into homogenizer, swirl, add phosphate-buffered saline and sodium sulphite solution to homogenizer, homogenize again, and take another OD reading, ensure over-dilution does not occur, homogenizer maximum volume is 55mL
  - If OD at 590nm is less than 0.25, pour homogenized solution from cuvette back into homogenizer, swirl, open MFC, stir wastewater anolyte again, remove 0.5mL of wastewater anolyte and add to homogenizer solution, homogenize again, and take another OD reading, more dilution is necessary if OD rises above 0.35
- With OD at 590nm less than 0.35 (but greater than 0.25), pour homogenized solution from cuvette back into homogenizer, swirl, pour 15−30mL of homogenized solution into microplate lid
- open the BIOLOG® ECOplate and remove the ECOplate lid
- use the 8-lane pipetter to draw eight 100μL samples at the same time, inoculate the first column and repeat 11 times in order to inoculate all ECOplate wells
- place ECOplate lid back on inoculated ECOplate, seal lid around the sides of the plate with Scotch™ tape, ensure that ECOplate wells remain facing upwards

- open Glove Bag and remove contents, hook MFC back up to system apparatus, ensure fabric and tin foil are tightly placed in and around phosphate-buffered saline and sodium sulphate solution flask mouth
- take ECOplate to plate reader and follow analysis procedure
- wash, rinse and dry labware that came into contact with wastewater anolyte or phosphate-buffered saline and sodium sulphite solution, discard used pipette tips, use 5% bleach solution and disposable towels to wipe clean interior and exterior of Glove Bag

C. Analysis Techniques and Reagent/Solution Chemistry

Head Gas Analysis (CPH 1324)

Procedure:

- Turn on the computer beside the gas chromatography (GC) unit and let Windows boot up
- Turn the helium feed to the GC unit on by turning the main valve counter-clockwise a quarter turn followed by the line-feed valve counter-clockwise a quarter turn
- Turn the GC unit on (switch on bottom left side)
- Lift the cover on the unit up again and find the current switch with settings 'high', 'off', and 'low', the switch should be set to the middle (off), set it to 'low'
- Ensure the helium is reaching the GC unit by using the small bottle of DI water inside the machine (take cap off DI water and put small metal tube sticking out of the unit into the DI water, watch for bubbles, recap DI water when done), close the cover on the GC unit
- Open the 'PeakSimple' software on the computer and wait for it to load
- Go to File -> Open Control File and select test2.con from the list, let this control file load
- Right-click and select 'postrun' from the dropdown list
- Change the file and run names to: YrMnDyMFC_air_00.CHR and YrMnDyMFC.LOG (i.e. 070101MFC_air_00.CHR and 070101MFC.LOG are for January 1st 2007)

- Once the 'Run' button on the GC unit is lit up (green), use the empty syringe beside the unit to draw 1mL of air and inject it into the unit, wait 2-3 seconds and push the lit up, green, 'Run' button, let the unit run for the 2 minutes required for analysis
- Repeat this last step 2 more times
- Right-click and select 'postrun' from the dropdown list
- Change the run name to: YrMnDyMFC_1_gas_00.CHR
- Once the 'Run' button is lit up, inject the first of two 1mL gas samples from MFC#1 into the unit and push the 'Run' button, let the unit run for 2 minutes for analysis
- Repeat the last step once for the second MFC#1 gas sample
- Right-click and select 'postrun' from the dropdown list
- Change the run name to YrMnDyMFC_2_gas_00.CHR
- One the 'Run' button is lit up, inject the first of two 1mL gas samples from MFC#2 into the unit and push the 'Run' button, let the unit run for 2 minutes for analysis
- Repeat the last step once for the second MFC#2 gas sample
- Close the 'PeakSimple' software and select 'Save all' when prompted to save before exiting
- Open the 'Peak329' folder (shortcut on desktop) and select the YrMnDyMFC.LOG file associated with the samples just run, copy it and paste it into the appropriate folder (desktop as well)
- Hibernate the computer, turn the current switch on the GC unit to 'off' (centre setting), turn off the GC unit, and shut off the helium feed by turning the main then the line-feed valves clockwise until snug

Ferricyanide Analysis (DWE 1524)

Procedure:

- Turn on the Spectrophotometer and let the machine warm up
- Take the four glass test tubes on the drying rack at the sink used for ferricyanide and place them in the circular carrying rack
- If ferricyanide feed is being tested (new feed mixture made after last sample/feed), take an extra four glass test tubes from the drying rack
- At the bench, use a 1mL pipette with appropriate tips to extract 0.5mL of the first ferricyanide sample and put it in one of the test tubes, using the same pipette tip extract 0.5mL of the second ferricyanide sample and put it in another test tube
- If ferricyanide feed is being tested, repeat the last step for the feed ferricyanide samples (use a different pipette tip for these samples as compared to the non-feed related samples)
- Add 4.5mL of DI water from the DI water bottle with plunger pump to each of the test tubes with 0.5mL of ferricyanide solution in it
- Mix the samples using the vortex mixer (set the dial on the mixer to 3)
- At the bench, use the 1mL pipette with appropriate tips to extract 0.5mL from the test tube with the 10x diluted first ferricyanide sample and expel it into another clean test tube, repeat this using the same pipette tip for the test tube with the 10x diluted second ferricyanide sample in it
- If ferricyanide feed is being tested, repeat the last step for the 10x diluted feed ferricyanide samples (use a different pipette tip for these samples as compared to the non-feed related samples)
- Add 4.5mL of DI water from the DI water bottle with plunger pump to each of the test tubes with 0.5mL of 10x diluted ferricyanide solution in it
- Mix the samples using the vortex mixer (set the dial on the mixer to 3)

- Select option 1 on the spectrophotometer and press enter, if the wavelength indicated on the machine is not 420nm press the 'Go to WL' button, type in 420 on the keypad, and press the enter button
- Take an empty cuvette from the cuvette rack and fill it with DI water from the DI water bottle with plunger pump, wipe the faces of the cuvette with a Kim wipe
- Open the spectrophotometer lid and place the DI water sample in the first cuvette bay such that the 'window' faces are facing left and right, close the lid
- Repeat the last two steps with the 100x diluted ferricyanide samples instead of DI water, place the samples in the cuvette bays directly behind the DI water sample
- Using the up and down arrow keys on the keypad of the spectrophotometer, select the DI water sample and press the 'zero' button (not the number zero) to set the DI water sample as a zero point to measure the ferricyanide samples from
- Using the up and down arrow keys, navigate through the rest of the ferricyanide samples and record the values for the samples in the logbook
- Turn the spectrophotometer off once finished, dump all of the ferricyanide waste into the 50mL sample vial marked for ferricyanide waste, rinse out the test tubes and cuvettes with DI water and place them in their drying racks, empty the ferricyanide waste in the waste bucket and rinse the 50mL waste vial and 1.5mL ferricyanide sample vials out with tap water and let dry in rack

Total Solids and Volatile Solids Analysis (CPH 1324, DWE 3506)

Empty Weights Procedure:

- Take empty tins and label them with the following identifiers as appropriate to the samples they will be used for:
  - Sample Date
  - Initials
  - MFC # or 'Feed'
- Place the tins in the furnaces for 10 minutes
- Remove the tins and place them in a dessicator to cool for 5 minutes
- Weigh each of the tins and record the weights as 'Empty Weights', this can be done on a loose piece of paper and the values are recorded in the logbook when samples are run
- Put the tins back in the dessicator for transport
- Store the tins in the 105 °C oven

Dried Weights Procedure:

- Remove the appropriate tins from the oven
- Using the Total samples for the dates to be analyzed, shake the samples to distribute the particulate matter evenly and remove 5mL from each
- Put 5mL of each sample into the appropriate tins
- Place the tins in the oven, leave them for at least 12 hours (24+ preferred)
- Take the remaining amount of each Total sample and pour each into a clean Nalgene cup
- Homogenize each Total sample for 1min at a speed of 55-60, rinse the homogenizer before and after each sample is homogenized

- Rinse the Total sample bottle out with DI water, pour the homogenized Total sample back into the appropriate storage bottle
- Put the Total samples back in the refrigerator, discard the diluted remaining TS/VS samples in the drain, wash and rinse the Nalgene cups
- Remove tins from oven after the designated drying time, place in dessicator for transport
- Weigh each of the tins and record the weights as 'Dried Weights' in the logbook

Flamed Weights Procedure:

- After 'Dried Weights' are recorded, place the tins in the furnaces in for 1 hour
- Remove the tins and place them in the dessicator to cool for 5-10 minutes
- Weigh each of the tins and record the weights as 'Flamed Weights' in the logbook
- Dispose of the tins in the appropriate waste bin
- Perform the Empty Weights procedure for the next weeks samples

Total Kjeldahl Nitrogen Digestion (CPH 1324)

Associated Reagents and Standards:

TKN Digestive Reagent

- Empty and rinse out the TKN Digestive Reagent bottle with DI water into the appropriate waste container
- Weigh out 40g of potassium sulphate and put it in the TKN Digestive Reagent bottle
- Add 2mL of selenium oxychloride to the bottle, perform transfer under fume hood
- Add 250mL of DI water and swirl until crystals are dissolved
- Add 250mL of sulphuric acid and swirl to mix well, CAUTION - bottle will become very hot
- Cap the bottle and swirl the mixture for 30 seconds, store on shelves below the fume hood

1000mg/L Ammonia Standard

- Empty any remaining 1000 Ammonia Standard
- Weigh out 4.717g of Ammonium Sulphate and put it in the 1000 Ammonia Standard bottle
- Add 1L of DI water, cap the bottle, shake mixture for 2-4min and put in standards refrigerator

500mg/L Glutamic Acid Standard

- Empty any remaining 500 Glutamic Standard and rinse flask with DI water
- Remove the magnetic stir bar and rinse with DI water
- Weigh out 5.252g of Glutamic Acid and put it in the 500 Glutamic Standard 1L flask
- Fill the flask to the 1L mark with DI water, place the magnetic stir bar back in the flask and put the flask on a stir plate

- Turn the stir plate on to full speed and stir until no flakes are apparent
- Use the glass stopper to cap the flask and put it in the standards refrigerator

Procedure:

- Get the 500 Glutamic Acid Standard out of the standards refrigerator and set it on a magnetic stir plate, turn on the plate and stir at max speed while carrying out the next four steps
- Retrieve the Total and Soluble samples from the sludge sample refrigerator (TS/VS should be done first if needed, thus Total samples are assumed to be homogenized at this point)
- Get out enough TKN digestion vials for all the samples and standards (# of samples being run +7), label the vials with labelling tape
  - For standards write the standard type and strength i.e.) NH4-1000 or Glut-500
  - For samples, write the sample code, MFC# or 'F', and 'T' or 'S' for sample type i.e.) J1-1-T is January 1st, MFC#1, Total sample
- Make Ammonia standards for digestion by serial dilution
  - 2mL 1000 standard + 2mL DI water = 500 standard
  - 2mL 500 standard + 2mL DI water = 250 standard
  - 2mL 250 standard + 2mL DI water = 125 standard
  - Also need the 1000 Ammonia standard and a blank (DI water) for digestion use Nalgene cups, return 1000 Ammonia standard to the standards refrigerator when finished
- Make a 125 Glutamic standard by adding 3mL of DI water to 1mL of the 500 Glutamic standard, also need the 500 Glutamic standard for digestion, use Nalgene cups, return 500 Glutamic standard to the standards refrigerator when finished
- Use the 1mL pipette to transfer 1mL of each of the Ammonia standards (5 counting the blank), Glutamic standards (2), and samples (Total and Soluble samples) into the appropriate TKN digestion vials

- Use the 5mL pipette to transfer 3mL of TKN Digestive Reagent into each vial, perform transfer under the fume hood by pouring just enough reagent from the bottle into a glass beaker and using pipette to transfer from beaker to vials
- Put two glass boiling beads (found in beaker under fume hood) in each vial using tweezers
- Place the vials in the TKN digestion block heater under the fume hood, turn on, set the temperature to 200 °C and let it run for 1.5 hours, empty any diluted samples and standards and wash the Nalgene cups and glass beaker used
- Turn the operating temperature on the TKN digestion block heater up to 380 °C after 1.5 hours has passed, let it run for 3.5 hours
- After the full digestion of 5 hours is up, turn off the TKN digestion block heater, carefully remove the vials and let them cool in the vial blocks beside the block heater for 10-15min, then move vials to workbench
- Retrieve the same number of 100mL flasks as TKN digestion vials, rinse each vial into a flask by adding 15mL of DI water and dumping it into the flask, repeat this rinse twice for a total of three rinses for each vial, transfer the vial label to the appropriate 100mL flask
- Fill each 100mL flask to the 100mL mark with DI water, use Parafilm squares to seal the top of each flask, shake each flask 10-20 times, put the 100mL flasks in the standards refrigerator
- Wash, sonicate, and rinse all the TKN digestion vials and dry in a rack, clean up workspace and discard of any wastes appropriately

Chemical Oxygen Demand Digestion and Optical Density Analysis (CPH 1324, DWE 3506)

Associated Reagents and Standards:

COD Sulphuric Reagent

- Empty the COD Sulphuric Reagent bottle into the appropriate waste container
- Weigh out 10.12g of silver sulphate and put it in the COD Sulphuric Reagent bottle
- Add 1L (1.84kg) of sulphuric acid to the bottle - add 600mL first, cap the bottle and shake dissolve salts, add remaining 400mL, cap the bottle and shake well for up to 5min
- Allow up to 48 hours for the salts to dissolve before use
- Store on shelves below the fume hood

COD Digestive Chromate Reagent

- Empty the COD Digestive Chromate Reagent bottle into the appropriate waste container and rinse with DI water
- Weigh out 10.216g of potassium dichromate and put it in the COD Digestive Chromate Reagent bottle
- Weigh out 33.3g of mercuric sulphate and put it in the COD Digestive Chromate Reagent bottle
- Add 500mL of DI water, cap the bottle, swirl the mixture to dissolve the salts, if needed, use a metal or plastic stirring rod to break up salt chunks, DO NOT shake since bottle is not well sealed
- Add 167mL of sulphuric acid, cap the bottle, swirl the mixture to mix well, CAUTION - bottle will become very hot
- Add 333mL of DI water, cap the bottle, swirl the mixture to mix well
- Store on shelves below the fume hood

1000mg/L COD Standard

- Empty any remaining 1000 COD Standard
- Weigh out 850mg of potassium hydrogen phthalate ('KHP') and put it in the 1000 COD Standard bottle
- Add 1L of DI water, cap the bottle, shake mixture for 2-4min and put in standards refrigerator

Procedure:

- Retrieve the Total and Soluble samples from the sludge sample refrigerator (TS/VS should be done first if needed, thus Total samples are assumed to be homogenized at this point)
- Dilute each Total sample with DI water (1mL sample + 9mL DI water), use Nalgene cups, [1:10 dilution]
- Get out enough COD digestion vials for all the samples and standards (# of samples being run times 3 plus 2 or 10), label the vials with labelling tape
  - For standards write the strength i.e.) 1000 for the 1000 COD standard or Blank for the DI water
  - For samples, write the sample code, MFC# or 'F', 'T' or 'S' for sample type, and 1, 2, or 3 to denote which replicate i.e.) J1-1-T1 is January 1st, MFC#1, Total sample, replicate 1
- If either COD reagent has been remixed or the 1000 standard has been remixed since the last digestion, prepare the following COD standards dilution series:
  - 1000, 800, 600, 400, 300, 200, 100, 50, 25, Blank (DI water)
  - Use DI water and the 1000 COD standard to prepare other standard strengths with a total volume of 10mL, use the table below:
  - Use Nalgene cups, return 1000 COD standard to the standards refrigerator when finished
- If reagents and standards are unchanged since the last digestion, prepare only the 1000 COD standard and a blank (DI water) for digestion, use Nalgene cups

Table C.1.: *Chemical Oxygen Demand Standards Preparation*

Standard	Use XmL of 1000 COD Standard	Use XmL of DI water
1000	10	0
800	8	2
600	6	4
400	4	6
300	3	7
200	2	8
100	1	9
50	0.5	9.5
25	0.25	9.75
Blank	0	10

- Use the 5mL pipette to transfer 2.5mL of each of the COD standards (2 or 10 counting the blank) and samples into the appropriate COD digestion vials
- Use the 5mL pipette to transfer 3.5mL of COD Sulphuric Reagent into each vial, perform transfer under the fume hood by pouring just enough reagent from the bottle into a glass beaker and using pipette to transfer from beaker to vials
- Use the 5mL pipette to transfer 1.5mL of COD Digestive Chromate Reagent into each vial, perform transfer under the fume hood by pouring just enough reagent from the bottle into a glass beaker and using pipette to transfer from beaker to vials
- Cap each of the COD digestion vials with a clean cap, shake the vials 3-5 times
- Place the vials in a test tube rack
- Place the vials in the COD digestion block heater, turn on with the temperature at 150 °C and let it run for 3 hours, empty any diluted samples and standards and wash the Nalgene cups and glass beakers used
- After the full digestion of 3 hours is up, turn off the COD digestion block heater, carefully remove the vials and let them cool in the test tube rack for 20-30min, then

move vials to workbench

- Use ethanol and Kimwipes to clean the outside of each of the COD digestion vials
- Use the spectrophotometer to get optical density (OD) readings for each COD sample and standard
  - Turn on the spectrophotometer, press zero and enter when prompted for the program
  - Using the COD blank, zero the machine by placing it in the vial port, covering it with the black tube cover and pressing the 'Set zero' button
  - Read each COD optical density value by placing it in the vial port and covering it with the black tube cover, digital readout will be given
  - Record all the COD values in the MFC logbook
- Once COD values are obtained, place the COD digestion vials with samples and standards in them in the storage test tube racks with older samples

TKN Analysis Procedure (CPH 1324)

Associated Reagents and Standards:

Alkaline Phenate Reagent

- Empty the Alkaline Phenate Reagent bottle into the appropriate waste container and rinse with DI water
- Weigh out 14g of liquefied phenol poured directly into the Alkaline Phenate Reagent bottle, be careful not to add too much
- Weigh out 6.5g of sodium hydroxide (pellets) and put it in the Alkaline Phenate Reagent bottle
- Add 500mL of DI water, cap the bottle, swirl the mixture to dissolve the salts, DO NOT shake up and down since bottle is not well sealed
- Store in front of Ammonia Analyser apparatus

Buffer Reagent

- Empty the Buffer Reagent bottle into the appropriate waste container and rinse with DI water
- Weigh out 40g of sodium citrate and put it in the Buffer Reagent bottle
- Weigh out 0.3g of sodium nitroprusside (nitroferricyanide) and put it in the Buffer Reagent bottle
- Add 600mL of DI water, cap the bottle, shake the mixture to dissolve the salts
- Add 400mL of DI water and 1mL of Brij-35, cap the bottle, shake and swirl to mix well
- Store in front of Ammonia Analyser apparatus

Sodium Hypochlorite Reagent

- Empty the Sodium Hypochlorite Reagent bottle into the appropriate waste container and rinse with DI water

- Pour 60mL of sodium hypochlorite solution (bleach) into a graduated cylinder, add 40mL of DI water, pour the resulting 100mL into the Sodium

Hypochlorite Reagent bottle

- Add 100mL of DI water, cap the bottle, shake and swirl to mix well
- Store in front of Ammonia Analyser apparatus

30,10,5,1,0.5mg/L Ammonia Standards

- Prepared in 125mL sample bottles from dilutions of the 1000 Ammonia Standard, 30 will need to be prepared more often, only prepare if they are low, discard remainder before mixing new standard, to mix the standards follow the table below:

Table C.2.: *Ammonia Analyzer Standards*

Standard	Use XmL of 1000 Amm Standard	Use XmL of DI water
30	3	97
10	1	99
5	0.5	99.5
1	0.1	99.9
0.5	0.05	99.95

- Once appropriate amounts of 1000 Ammonia Standard and DI water are in the standards bottles, cap them and shake for 20-30sec to ensure the standards are well mixed
- Store in standards refrigerator

Sample Wash

- Prepared in 1L bottle, only prepare if old solution is used up
- Add 3mL of Brij-35 to 1L of DI water in Sample Wash bottle, cap and shake the bottle to mix the wash solution well
- Store on shelves above the Ammonia Analyser apparatus

Procedure:

- Retrieve Soluble samples matching sample dates from the digested TKN samples to be analyzed, add 25mL of DI water to 1mL of each Soluble sample, use Nalgene cups, these are free and saline ammonia samples
- Retrieve 30,10,5,1,0.5 Ammonia Standards and digested TKN samples, place them on the workspace countertop
- Ammonia Analyzer apparatus has 4 components - computer, analysis unit, dialysis unit, sample wheel unit
- Turn on computer, assemble the dialysis unit (between other two units) by securing the tubing and clamping the plate portion down on top of the tubes, turn on the dialysis unit
- Set dialysis unit to 'Run' and the speed to 'Fast' with all feed tubes in the DI water bottle, let this rinse run for 5-10min
- While the dialysis unit is rinsing, go to the computer, open AAce software, go to Setup -> Analysis, in resulting window, double click the folder 'Ammonia 1-40', new list of files will appear, select appropriate previous MFC run file and click the 'Copy Run' button, repeat for each analysis run required (2 analysis runs required per digestion, use old MFC runs of a similar nature to minimize setup changes needed)
- In resultant window, ensure that the filename is of the form: YrMtDyMFCsRun#, use the analysis date not the digestion date, filename auto format will often set the default filename as YrMtDy with the letter 'A' appended
  - i.e. 070101MFCsRun1 for January 1st, 2007, first analysis run
- Go to the second tab in the window and ensure the sample order is correct, see below for order:
  - For the first analysis run:
- 30, 30, 30, BLANK, BLANK, 30, 10, 5, 1, 0.5, BLANK for settings and Ammonia Standards calibration curve (8 cups used)
- Triplicates of digested Ammonia Standards from Blank to 1000 (totals 15 cups with a BLANK in the middle and afterward)

- Duplicates of Glutamic 500 and 125 followed by BLANK (4 cups used)
- Duplicates of free and saline ammonia samples for appropriate dates with a BLANK in the middle and afterward (8-10 cups depending on number of samples digested)
- One 30 Ammonia Standard followed by an End point
  - For the second analysis run:
- 30, 30, 30, BLANK, BLANK, 30, 10, 5, 1, 0.5, BLANK for settings and Ammonia Standards calibration curve (8 cups used)
- Duplicates of digested Ammonia Standards from Blank to 1000 (totals 10 cups with a BLANK in the middle and two afterward)
- Duplicates of each digested TKN sample with the appropriate dates with a few BLANKS in the middle and afterward (16-20 cups depending on number of samples digested)
- One 30 Ammonia Standard followed by an End point
- Click the 'Ok' button once the analyses are set up
- Switch the dialysis unit to 'Stop' and 'Normal', turn on the analysis unit and sample wheel unit, switch the dialysis unit back to 'Run' but leave it on 'Normal' speed, put the dialysis unit tubing from DI water bottle in appropriate reagent bottles (Alkaline Phenate, Buffer, and Hypochlorite), drape DI water tubes on sample wheel unit, empty DI water bottle and rinse with DI three times, fill DI water bottle to at least 2/3 full of DI water, put back in front of dialysis unit and put DI water tubing back in DI water bottle, this only has to be done before the first analysis run
- On the computer, press the 'Charting' button in the top, left hand corner of the window that opened with the analysis software, Click 'Ok' in resulting window, Click 'No' for downloads prompt, allow charting to begin, then right click within the charting grid and select 'Set Base' from the drop-down list, DO NOT click 'Set Gain' as this will cause analysis problems unless returned to normal, charting will have to be run between the first and second analysis run as well
- Allow the apparatus to chart for 15-20min while the sample wheel is prepared, retrieve sample wheel from sample wheel unit, get the sample cups out of the workspace cupboard, follow the directions below:

– For the first analysis run, follow the sample cup order listed in the table below, be sure to shake all standards and samples before pouring them into the sample cups, also rinse each sample cup by filling it with the appropriate standard or sample once and emptying it into a Nalgene cup before filling it up with the appropriate standard or sample again, free and saline ammonia samples should be loaded chronologically then by MFC # or feed (MFC#1 first, then #2, then feed if applicable) all in duplicate

Table C.3.: *First Ammonia Analysis Run Layout*

Wheel Spot	Contents
1−4	30 Ammonia Standard
5	10 Ammonia Standard
6	5 Ammonia Standard
7	1 Ammonia Standard
8	0.5 Ammonia Standard
9−11	Digested Blank Standard
12−14	Digested 125 Ammonia Standard
15−17	Digested 250 Ammonia Standard
18−20	Digested 500 Ammonia Standard
21−23	Digested 1000 Ammonia Standard
24−25	Digested 500 Glutamic Acid Standard
26−27	Digested 125 Glutamic Acid Standard
28−35 or 37	Free and Saline Ammonia Samples
36 or 38	30 Ammonia Standard

– For the second analysis run, follow the sample cup order listed in the table below, samples and standards are shaken and cups are rinsed in the same manner as for the first analysis run, samples that are the same as the first run can be left in the wheel for the second run (i.e. digestion Ammonia Standards), digested TKN samples should be loaded chronologically then by MFC # or feed (MFC#1 first, then #2, then feed if applicable) then by Total followed by Soluble samples all in duplicate

Table C.4.: *Second Ammonia Analysis Run Layout*

Wheel Spot	Contents
1–4	30 Ammonia Standard
5	10 Ammonia Standard
6	5 Ammonia Standard
7	1 Ammonia Standard
8	0.5 Ammonia Standard
9–10	Digested Blank Standard
11–12	Digested 125 Ammonia Standard
13–14	Digested 250 Ammonia Standard
15–16	Digested 500 Ammonia Standard
17–18	Digested 1000 Ammonia Standard
19–34 or 38	Digested TKN Samples
35 or 39	30 Ammonia Standard

- On the computer, right click within the charting grid and select 'Set Base' from the drop-down list several times throughout and at the end of the charting period, the signal should be relatively stead at 5%
- Load the filled sample wheel onto the sample wheel unit, with charting for 15-20min done and a steady 5% signal, go to Start -> Run in the software and from the resultant window select the appropriate analysis run setup earlier, when prompted select 'Ok' to start, fill in the operator name and any notes in the next window and press 'Ok', analysis will take 60-90min
- Charting will need to be done between the two analysis runs, before second run is started, check to ensure that the results from the first run are good by going to Results -> View Chart and select the first analysis file, make sure the peak values make sense with respect to what was expected with standards and previous runs
- Once the second analysis is complete, check to ensure the results are good, then close the analysis software and shut down the computer, turn off the analysis unit and the sample wheel unit, the dialysis unit will start to run, switch it to 'Stop' move all the tubing in the reagent bottles into the 'Sample Wash' bottle, switch the dialysis unit to 'Run' and 'Fast', run this wash cycle for 10min, switch dialysis unit to 'Stop', move the tubing from the 'Sample Wash' bottle to the DI water bottle with the DI water tubing, switch dialysis unit back to 'Fast' for 10-15min, then turn off the dialysis unit and disassemble it by unclamping the tubes with the plate section and unhooking the tension bar
- While dialysis unit is washing/rinsing, ensure that all samples and standards are returned to the appropriate refrigerators, empty all the Nalgene cups and 100mL flasks in the appropriate containers, wash and rinse the Nalgene cups and 100mL flasks, put on racks to dry, wash and rinse the analysis sample wheel cups and lay out to dry

BIOLOG® ECOplate OD Measurement Procedure (DWE 3505)

Procedure:

- turn on lab computer and microplate reader (VERSAmax tunable microplate reader)
- ensure that the ECOplate is sealed well and no marks or smudges are on the lid
- eject microplate reader tray and place microplate in tray, orient well A1 in the top-left corner, insert microplate reader tray
- start SOFTmax PRO 3.1.1 software on lab computer
- click the temperature button and turn on temperature controller for microplate reader, set temperature to 37°C
  - if this is first ECOplate analysis, start new analysis file and enter Experiment 1 settings:
    - choose kinetic experimental settings
    - set wavelength to 590nm for OD or absorbance readings
    - set length of experiment to 42hrs, set measurement interval to every 1hr
    - turn on microplate shaking before OD readings, set shake time to 15s
  - if this is not first ECOplate analysis, open existing analysis file and start new experiment within analysis file, ensure that all settings from previous experiments in analysis file are applied to new experiment settings
- ensure that preferences are set such that an appropriate output file type, name and location are specified, use the textfile type, an identifiable name, and a consistent and personal location on lab computer
- once microplate reader controlled temperature is greater than 30°C, start analysis, wait 44−48hrs for completion
- ensure that analysis is complete, check saved textfile and copy to floppy disk for transfer to computer for data analysis, save SOFTmax analysis file and close SOFTmax PRO 3.1.1 software

- eject microplate reader tray and remove ECOplate, insert empty microplate reader tray, shut down lab computer and microplate reader, store used ECOplate

D. Experimental Data and Analytical Files

Appendix D contains all of the experimental data and analytical files provided on CD-ROM (attached to back cover). The data has been organized by variables and can be viewed using Microsoft Word, Excel, and PowerPoint (version 97 or later). Various pictures taken throughout the project are included as well.

Note: This is not available with the electronic version of this thesis.

E. Collected Literature to Date

Appendix E contains a collection of the associated literature to date (October 24, 2007), provided on CD-ROM (attached to back cover). The papers have been left in the original sorting order used during bibliography generation and can be viewed using Adobe Acrobat Reader (version 7.0 or later).

Note: This is not available with the electronic version of this thesis.